A Framework for Statistical Characterization of Epidemic Cycles: COVID-19 Case Study

Eduardo Atem De Carvalho, Rogerio Atem De Carvalho

Submitted to: JMIRx Med
on: July 19, 2020

Table of Contents

A Framework for Statistical Characterization of Epidemic Cycles: COVID-19 Case Study

Eduardo Atem De Carvalho[1*] PhD, MSc, BSc; Rogerio Atem De Carvalho[2*] DSC, MSc, BSc

[1]Universidade Estadual do Norte Fluminense; Campos BR
[2]Instituto Federal Fluminense Campos BR
[*]these authors contributed equally

Corresponding Author:
Rogerio Atem De Carvalho DSC, MSc, BSc
Instituto Federal Fluminense
R. Cel Walter Kramer, 357, Campos/RJ
Campos
BR

Abstract

Background: Since the beginning of the COVID-19 pandemic, researchers and health services have been looking for patterns in the series of deaths caused by the virus, in order to try to predict the future course of the epidemic in different locations or to find relationships between the deaths and the different measures taken in infection control and treatment of infected people.

Objective: This article presents several cycles practically closed and compares them with others that are in progress in order to show how it is possible to use similarity patterns to make predictions.

Methods: Virtually closed cycles are compared with cycles in progress from other locations with similar patterns. In order to be able to compare populations of different sizes at different times, the cycles are normalized by known and simple methods. Three normalization methods are presented and discussed.

Results: Several practically closed cycles are used to show their similarity to cycles in progress. The case of the city of Rio de Janeiro, Brazil, is analyzed in detail and its prediction is shown with high precision.

Conclusions: It is evident that there is a practically universal pattern among the studied cycles, which takes a triangular shape. This repeated shape can be used to make predictions on cycles duration.

(JMIR Preprints 19/07/2020:22617)
DOI: https://doi.org/10.2196/preprints.22617

Original Manuscript

A Framework for Statistical Characterization of Epidemic Cycles: COVID-19 Case Study

Eduardo Atem de Carvalho[1] and Rogerio Atem de Carvalho[2]
[1]B.Sc., M.Sc., PhD in Mechanical Engineering, Advanced Materials Laboratory, Universidade Estadual do Norte Fluminense, Brazil, eatem@uenf.br

[2]B.Sc. in Computer Science, M.Sc., D.Sc. in Production Engineering, Innovation Hub, Instituto Federal Fluminense, Brazil, ratem@iff.edu.br

ABSTRACT

Background: Since the beginning of the COVID-19 pandemic, researchers and health authorities have sought to identify the different parameters that drive its local transmission cycles, in order to be able to make better decisions regarding prevention and control measures. Different modeling approaches have been proposed in an attempt to predict the behavior of these local cycles.

Objective: This article presents a framework to characterize the different variables that drives the local, or epidemic, cycles of the COVID-19 pandemic, in order to provide a set of relatively simple, yet efficient, statistical tools to be used by local health authorities to support their decision making.

Methods: Virtually closed cycles are compared to cycles in progress from different locations that present similar patterns in the figures that describe them. Aiming at comparing populations of different sizes at different periods of time and locations, the cycles are normalized, allowing an analysis based on the core behavior of the numerical series. A model for the Reproduction Number is derived from the experimental data, and its performance is presented, including the effect of sub notification. A variation of the Logistic Model is used together with an innovative inventory model to calculate the actual number of infected persons, to analyze the incubation period, and to determine the actual onset of local epidemic cycles.

Results: The similarities among cycles is demonstrated. A pattern between the cycles studied, which takes on a triangular shape, is identified and used to make predictions about the duration of future cycles. Analyses on R_t and sub-notification effects for Germany, Italy, and Sweden are presented to show the performance of the framework here introduced. After comparing data from the three countries, it is possible to determine the actual probable dates of the actual onset of the epidemic cycles for each country, the typical duration of the incubation period for the disease, as well as the total number of infected persons during each cycle.

Conclusions: It is demonstrated that, with relatively simple mathematical tools, it is possible to obtain reliable understanding on the behavior of COVID-19 local epidemic cycles, by introducing an integrated framework for identifying cycle patterns and calculating the variables that drive it, namely: the effective reproduction number, the sub-notification effects on estimations, the most probable actual cycles start dates, the total number of infected, and the most likely incubation period for Sars-CoV-2.

KEYWORDS

COVID-19; Pandemics; Infection Control; Models, Experimental; Longitudinal Studies; Statistical Modeling; Epidemic Cycles;

Introduction

The analysis of the life cycles of any epidemic involves the analysis of a series of quantitative parameters that govern these cycles and which, given the inherent uncertainty of these events, are generally treated by statistical models. For a number of practical reasons, the registration of deaths and of infections are inevitably imprecise, although these numbers can be corrected over time. Therefore, with the COVID-19 pandemic, a subject that immediately became the center of debates and different studies was the characterization of the different local epidemic cycles and their corresponding variables. Local cycles are those that have occurred or occur in specific countries, regions or cities, and not the pandemic cycle as a whole, as the virus does not spread instantly across the continents. Thus, it can be seen that some countries were in more advanced epidemic stages than others whose first infections were detected later. In other words, as expected, different "infection windows" co-exist in parallel in different locations, with some locations at a more advanced stage, while others present more “delayed” cycles. Thus, analyzing numerically the behavior of the early cycles was the measure taken by a series of researchers.

Although it is not the only one, as will be seen in this paper, the Reproduction Number (R_0) is considered the central variable in the analysis of epidemic cycles. In order to determine R_0, different categories of models have been proposed: Artificial Neural Networks [1], Poisson [2, 3], Exponential [4], Markov Chain [5], Gaussian [6, 7], Weibull [8], Logistic-S [9], and Moving Averages [10]. Most of the papers try to frame the local epidemic cycles into Gaussian and/or Weibull behaviors, creating complex models that still led to errors in predictions, as we now know. More importantly, [11] shows that the initial models, most based on the Gaussian Distribution and its derivatives, failed to make their predictions. After observing these findings, we could see that there was room to propose a framework that would provide an efficient and more comprehensive analysis of the epidemic cycles, going beyond the calculation of R_0 and that, moreover, it would be both easy to understand and to compute, since local authorities, especially in low income countries, do not always have statistical experts at their disposal to propose, calibrate and analyze the results of complex models. Thus, based on experimental and publicly available data, the authors produced a series of studies that initially dealt with the identification of patterns in epidemic cycles and their use for predicting deaths [12], time-dependent Effective Reproduction Number and sub-notification effect estimation modeling [13] and finally, estimation of the actual onset of local epidemic cycles, determination of the total number of infected, and the duration of the incubation period [14]. In this article, these findings are integrated and summarized in a coherent framework, presented in the next topics.

Methods

Based on experimental data, the framework here proposed is divided into four parts: (a) applying the Moving Averages method and identifying the parameters of the epidemic cycle patterns, which are used to predict the number of future deaths in local epidemics, (b) modeling the Effective Reproduction Number (R_t), (c) the effects of sub-notification, and (d) applying the Logistic Model associated to a novel inventory model to obtain the final count for the total infected, the daily infection rate and the lag time, and the incubation period.

Epidemic Cycles Patterns

Our method begins with the observation of several cycles of western countries in which the pandemic hit earlier, especially in Europe. From there, patterns are identified and predictions are applied. The attempt to describe the different epidemic cycles that make up the current pandemic often comes up against the quality of the data that is made public. Most data made public are based on “date of recording”, which is different of “day of death”,

meaning that the date that a given set of deaths are recorded in the public health statistics systems is not necessarily the same that they occurred, given the usual bureaucratic procedures, which delay the recording.

The fact is that the distribution of fatalities suffers a distortion that generates a “saw” appearance in the graphs, such that on weekends there is a clear absence of death records, followed by an explosion of values at the beginning of the weeks. A simple technique that softens this effect is to apply the so-called Moving Average Method (MAM), in which the daily value of deaths is replaced by the sum of the previous six days with the current day, divided by seven, in other words, the average of the week ended in the current day. In particular, MAMI, or MAM with Initial Position, will be used here, which means assigning the average of the seven days to the first day of the week (Sunday).

In the period in which the data were obtained and analyzed (first week of July, 2020), several cities, regions, states and countries have already completed what will be called here as the Most Lethal Cycle of the Epidemic (MLCE), which is when the number of deaths increases daily, on average, until it reaches a peak and then begins to decrease continuously until it reaches a minimum value. After this period, the occurrence of deaths continues intermittently, but relatively small and oscillating, decreasing to certain levels of daily deaths, where it then becomes apparently chronic and presents relatively low values, but greater than zero.

In order to show numerical cases of the application of the proposed model, the data from three European countries with different cycles are analyzed: Germany, a country that was reported as exemplary in terms of application of Non-Pharmaceutical Interventions (NPIs); Italy, which stayed at the center of the initial crisis; and Sweden, which didn’t apply strong NPIs in general. The data for this part of the study was obtained from the Worldometer’s COVID-19 portal (https://www.worldometers.info/coronavirus/) as of 09th of July, 2020, and is presented, together with the calculations, in Appendix 2.

Germany

Described from the beginning of the pandemic as a country that managed the crisis in an exemplary way, testing significant portions of its population and controlling and releasing the public movement based on well-known numbers and percentages of cases. Figure 1 shows the evolution of deaths in Germany. This framework points to the existence of the so-called False Peaks. These are local maximums that were recorded during the cycle of rising or falling in the trend of deaths, but they are not inflection points. In order for a point to be considered as a (real) Peak, it is necessary to register a tendency of a dropping in the number of deaths. This fall will not be linear, but there is an obvious, numerical and visual trend that indicates such trend.

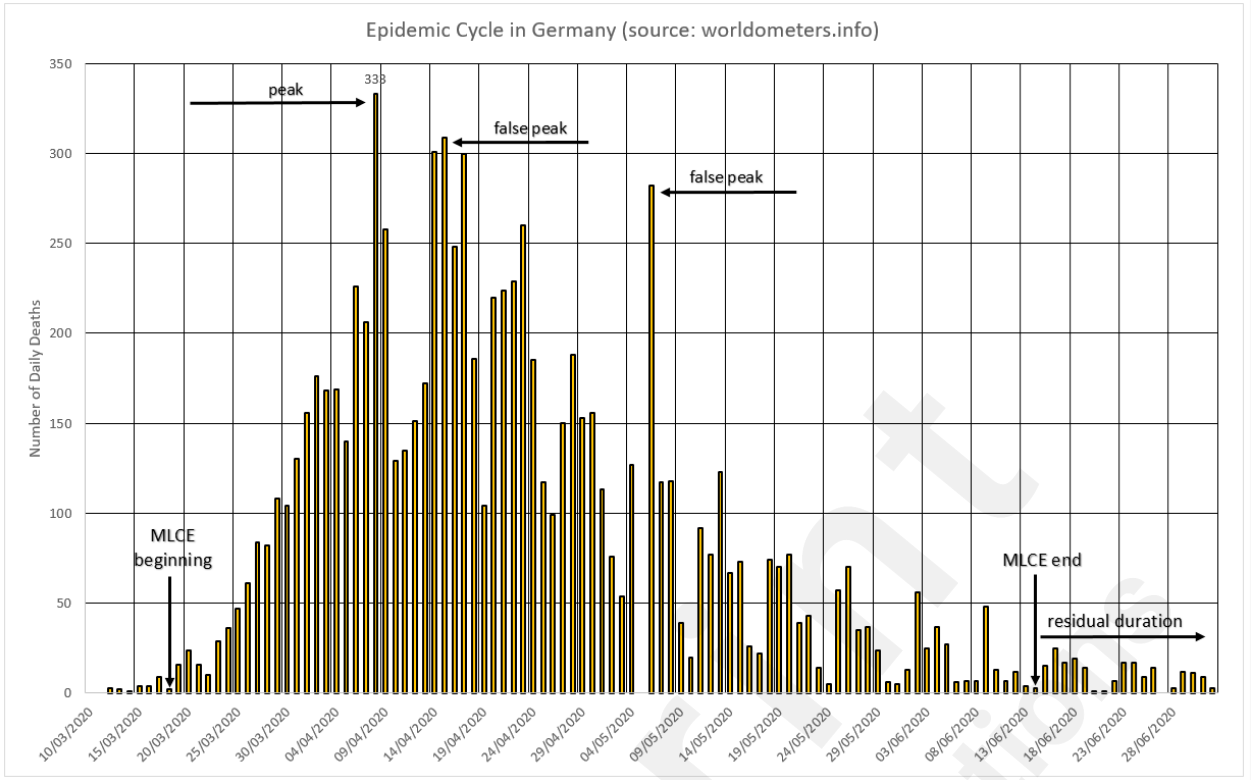

Figure 1 – The German cycle.

Italy

A country that was at the European epicenter of the crisis, it has an evolution in the number of deaths (Figure 2) that indicates the overcoming of the MLCE.

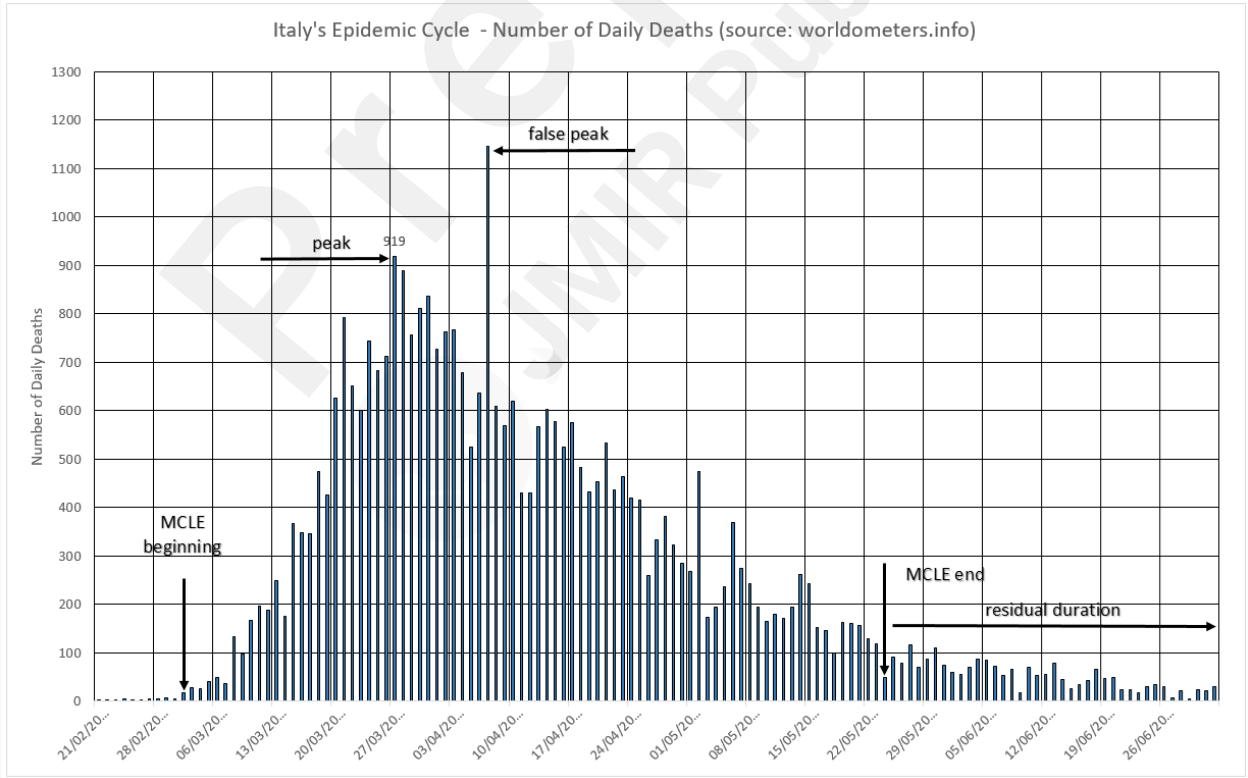

Figure 2 – The Italian cycle.

Sweden

An European country that has not adopted the practices of radical social isolation as its

neighbors, has a cycle of aspect not unlike that of all other European countries. Figure 3 shows the values of deaths that have already been corrected for the dates on which they actually occurred and not the date of registration.

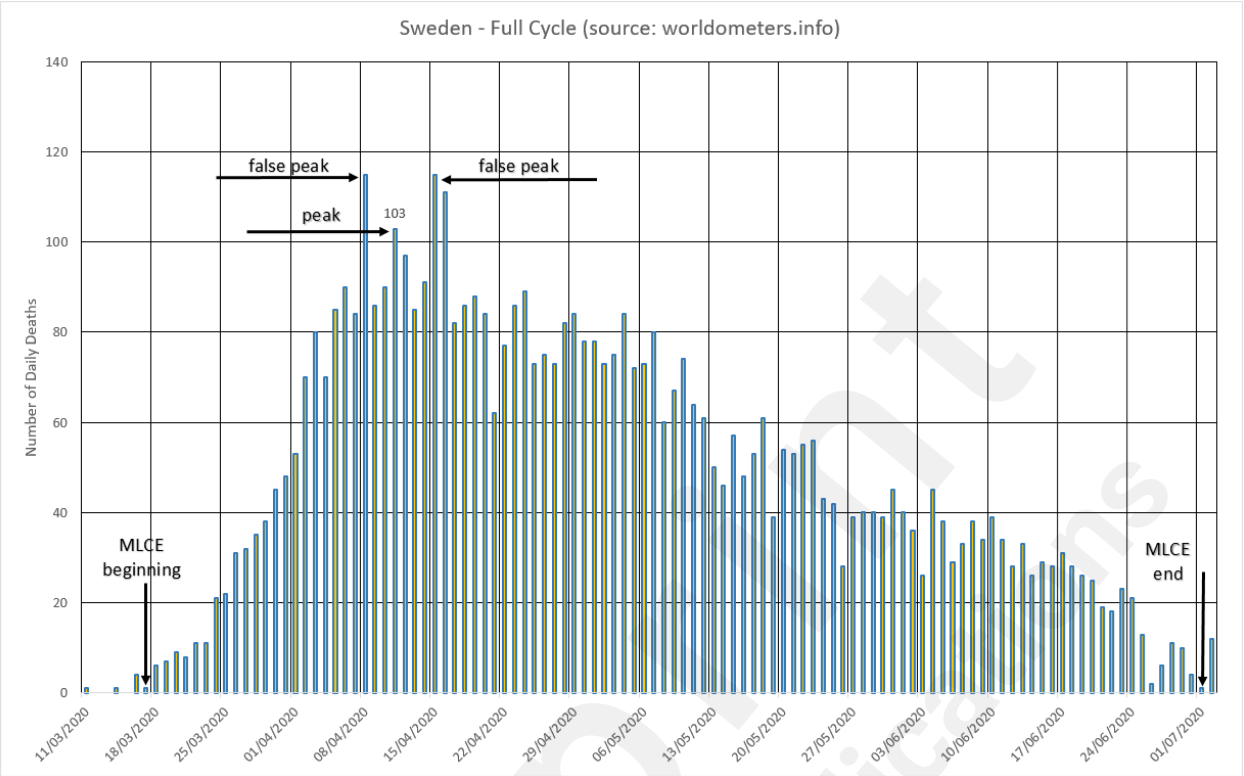

Figure 3 – The Swedish Cycle.

Non-dimensional Characteristics of Epidemic Cycles

In general, the epidemic cycles described here have some common geometric characteristics, the main one being a triangular aspect (Figure 4), where a smaller side is formed, which corresponds to an average daily increase in the number of deaths until a peak is reached. This peak can be easily identifiable or requires extrapolation of a line, because the values oscillate naturally and some spurious points (false peaks) may appear. After the peak, a period is formed where the number of deaths occurring daily tends to decrease on average. This period, for the observed cases, is longer than the previous one. According to [15], the Triangular Distribution is used when there is no exact idea on what the distribution is, however, there is an idea of the minimum and maximum values for the variable. Therefore, this distribution was chosen given its particular nature and use in situations where the description of a given population is uncertain, as is in this case. This distribution is based on the minimum and maximum estimates. Hence, Table 1 gathers values of the so-called triangular cycles presented earlier

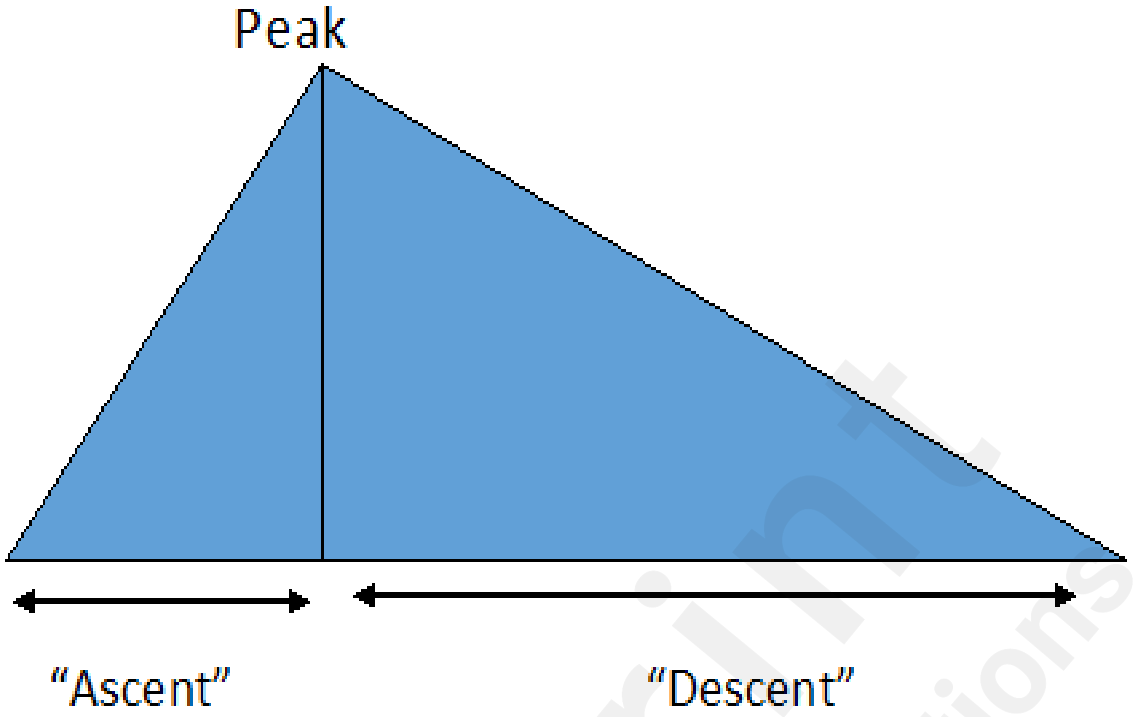

Figure 4 –COVID-19 lethal cycles generic shape.

Table 1 - Proportions between the time of ascent until the peak of deaths and descent until the end of the most severe cycle of the disease.

Country	Start	Peak	End	Days to the Peak	Days to the End	Proportion between ascent and descent
Italy	03/07	03/27	05/24	20	57	2,9
Sweden	03/17	04/11	07/01	25	81	3,2
Germany	03/18	04/08	06/14	21	69	3,3

The values listed in Table 1 indicate that the period of rise of the disease, in countries of relatively small sizes or in big cities, is about 21 days, in a range that goes from 19 to 25 days until reaching the so-called peak. From then until the end of this critical period, about 60 days pass, in a range from 45 to 81 days, the ratio between the two periods oscillates between 2.1 and 3.3, with an average of 2.8. Table 2 shows the values of the number of deaths in the periods described above.

Table 2 – Proportions between the number of deaths associated with the cycle of rising to the peak and of descending to the end of the most severe cycle of the disease.

Place	Start	Peak	End	Deaths to the Peak	Deaths to the End	Proportion between ascent and descent
Italy	07/03	27/03	24/05	8937	24082	2,7
Sweden	17/03	11/04	01/07	1255	4141	3,3
Germany	18/03	08/04	14/06	2323	6521	2,8

The values listed in Table 2 indicate that the number of deaths during the period of ascent of the disease, in countries of relatively small sizes or cities, is about 5791 deaths, in a

range that goes from 1255 to 10293 deaths until reaching the peak. From then until the end of this critical period, about 12673 deaths occur, in a range from 4141 to 24082 deaths. The ratio of death figures ranges from 1.6 to 3.3, with an average of 2.4.

Therefore, it is possible to identify that once the scale effects are removed, what remains is a spectrum of proportions of the epidemic cycle. Then, when submitting the data to the Moving Average Method with Initial value (MAMI), there is a minimization of the effect of seasonality in the registration of deaths, caused by weekends, holidays and other local peculiarities. After dividing all the values previously transformed by the peak of the series (peak now determined by MAMI), the values start to be dimensionless and fall between 0 and 1. In this way, the epidemic cycles can be compared with each other, since what remains are the proportions between the ascent, the peak, and the descent of the cycle. The time period does not change. One clear limitation of this method is the necessity of identifying the real peak. Then, an hypothesis arises that different locations may, under different behavioral rules, present the same behavior.

Algorithm for Cycle Predictions

After identifying the triangular pattern and through the successful application in several cases, a prediction algorithm was developed, described by the following steps.

a. MAMI is calculated for the daily figures on the number of deaths.
b. The set of values is normalized and MAMI is also applied on it.
c. A continuous curve is generated on a graph with the x-axis as the number of consecutive days of the epidemic cycle and the y-axis, the dimensionless range from 0 to 1, generally (some points, the false peaks, can go beyond this).
d. Among countries or localities, we seek those that have already ended their critical epidemic cycle (MLCE) and that is visually similar to the curve obtained in (c), although obviously on a different scale, becoming the locality of reference.
e. MAMI is applied to the locality of reference.
f. Data of the locality of reference is normalized.
g. Repeat (c) for the data of the locality of reference.
h. Considering that the cycle of the locality of reference is finished, it will be positioned previously on the graph, in relation to the place where it is desired to estimate the probable end date of the critical cycle. One should then numerically superimpose the peak of the case under study with the reference.
i. Once the superposition is made, always moving the reference case, an extrapolation can be made using the reference case as a guide to the value to be determined. As the scale of the case studied has not been changed, it is enough to consult what day it would be in the future to know the probable date.
j. If there is no similar case, you can eliminate the last days, as discussed above, and extrapolate directly from the values obtained in the public databases.

Effective Reproduction Number (Rt)

After identifying the similarities between cycles, the next step is to calculate the effective reproduction number, which is done on the experimental behavior of the curve. First, however, it is necessary to understand the effect of MAMI on R.

MAMI Effect Over Reproduction Numbers

The impact of MAMI applied to registered numbers can be better understood by analyzing Figure 5, where MAMI bears greatest effect at the very beginning of the epidemic cycle, however, after a brief period, the average and actual data tend to yield to the same value as the cycles progress. It will be shown along this paper that the Reproduction Number varies most at the early stages and the use of MAMI is plainly justified to avoid numbers that are

registered in batches and not into a smooth, daily, fashion. Daily figures for total cases collected from the John Hopkins University's website (https://coronavirus.jhu.edu/map.html) on the 22sd of July, 2020, together with the calculations, are presented in Appendix 3. The analysis of the Rt for the three European countries are represented in Figures 6, 7, and 8.

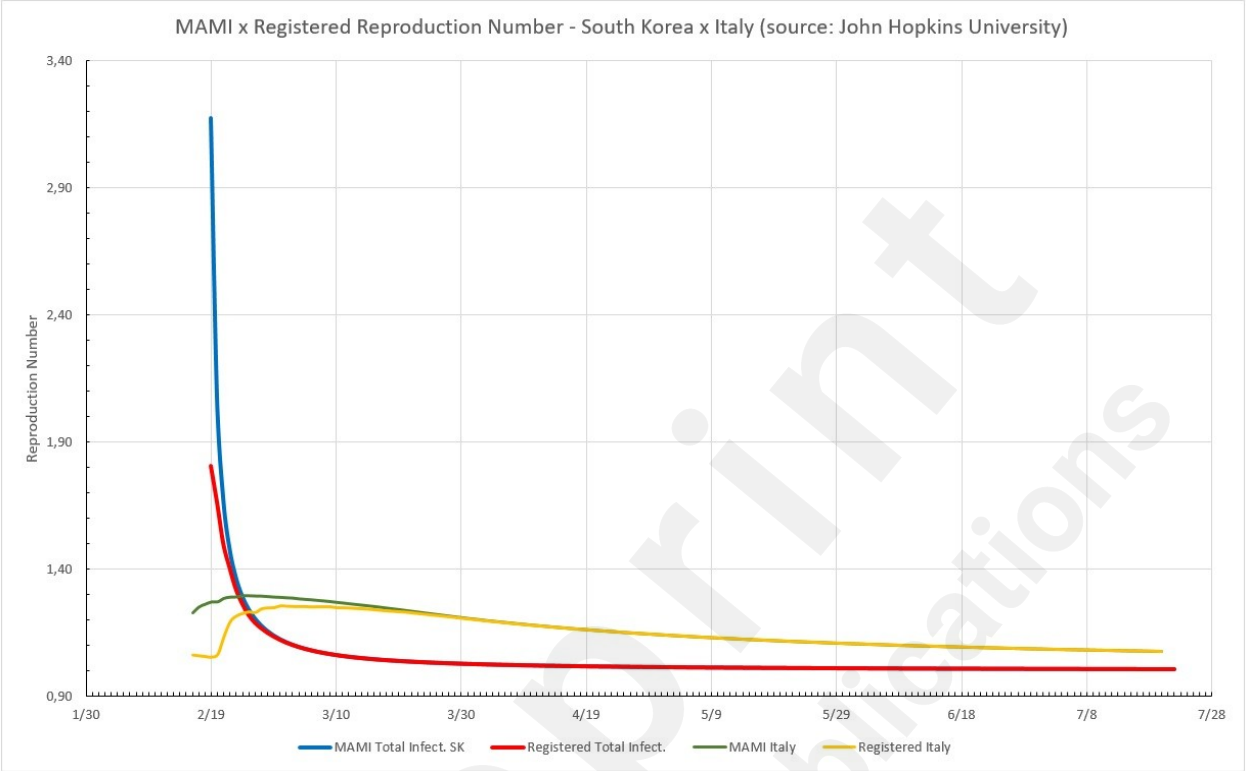

Figure 5 – MAMI effect over Reproduction Numbers expressed for two different countries, South Korea and Italy. South Korea: the blue line is R_t obtained from MAMI applied to registered data, the red line is R_t determined for registered data. For Italy: the yellow line is R_t for registered data and the green line for MAMI applied to registered data.

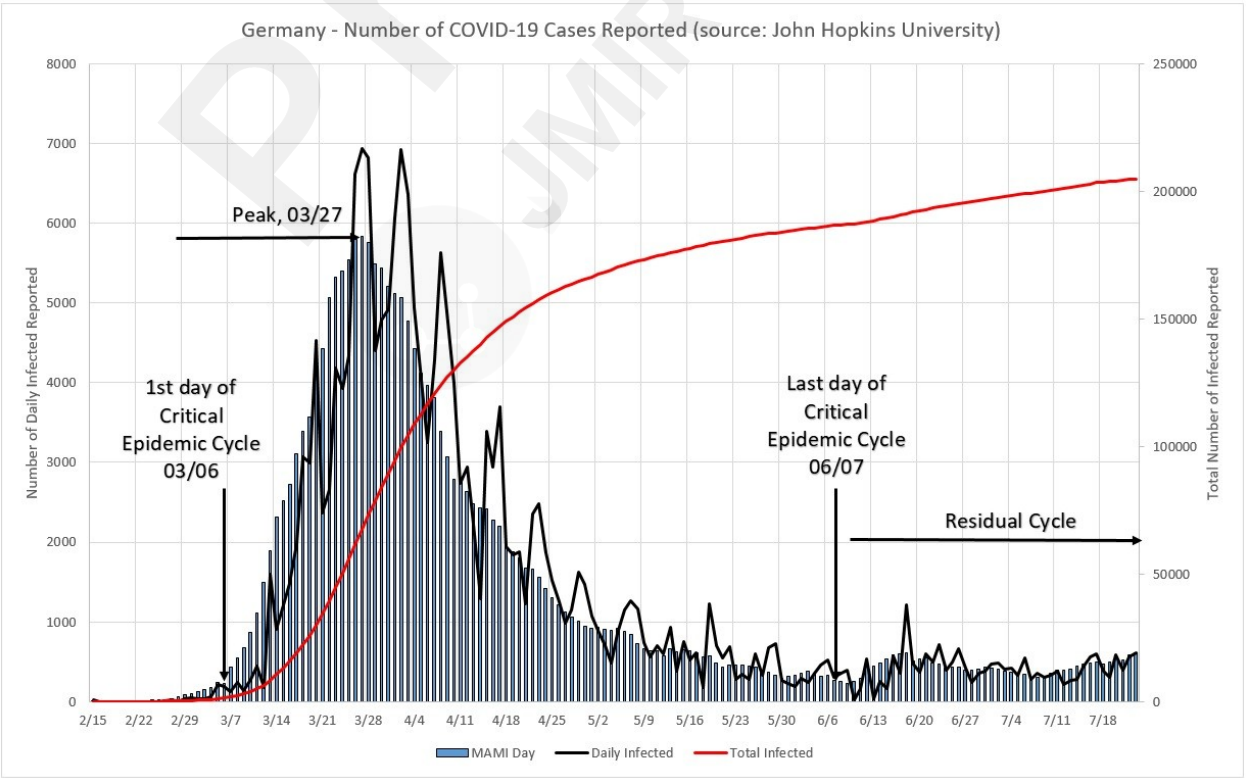

Figure 6 – Number of COVID-19 cases reported for Germany. The black line represents the daily reported numbers, blue bars their MAMI, and the red line the total cases to date and uses the right hand axis as reference.

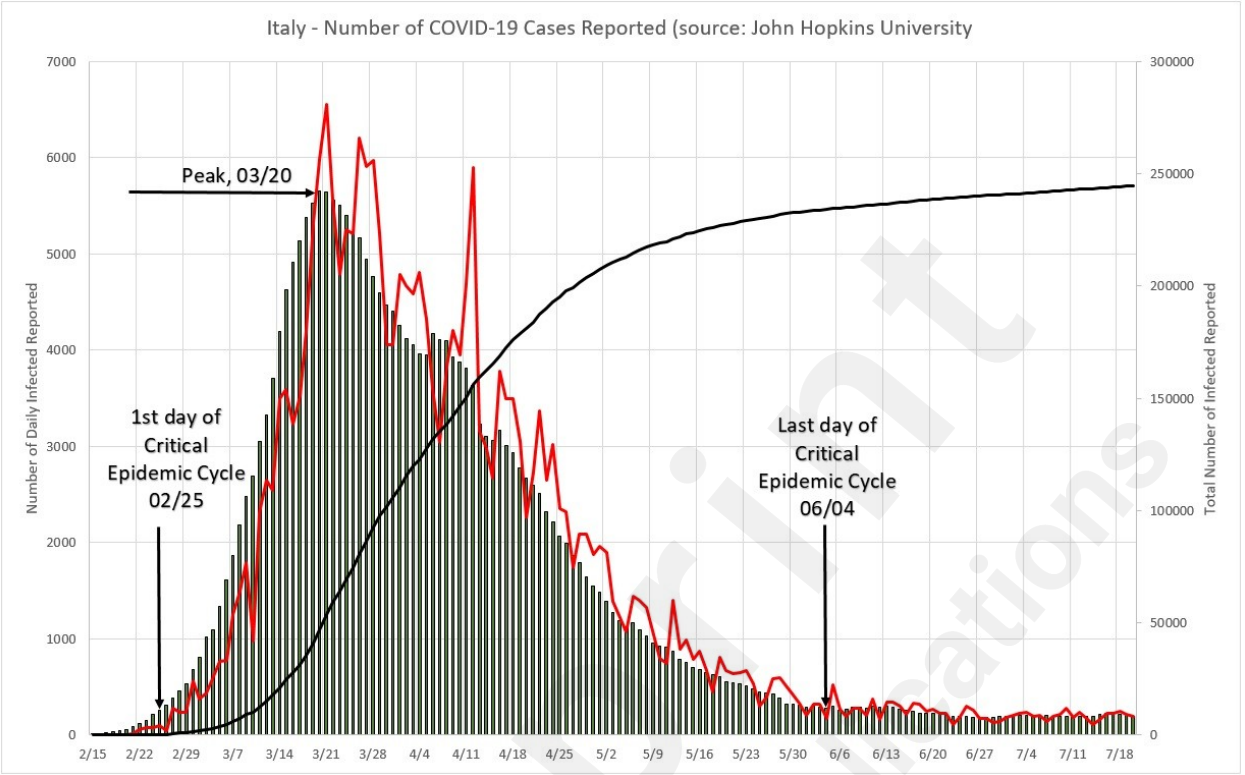

Figure 7 – Number of COVID-19 cases reported for Italy. The black line represents the daily reported numbers, blue bars their MAMI, and red line the total cases to date and uses the right hand axis as reference.

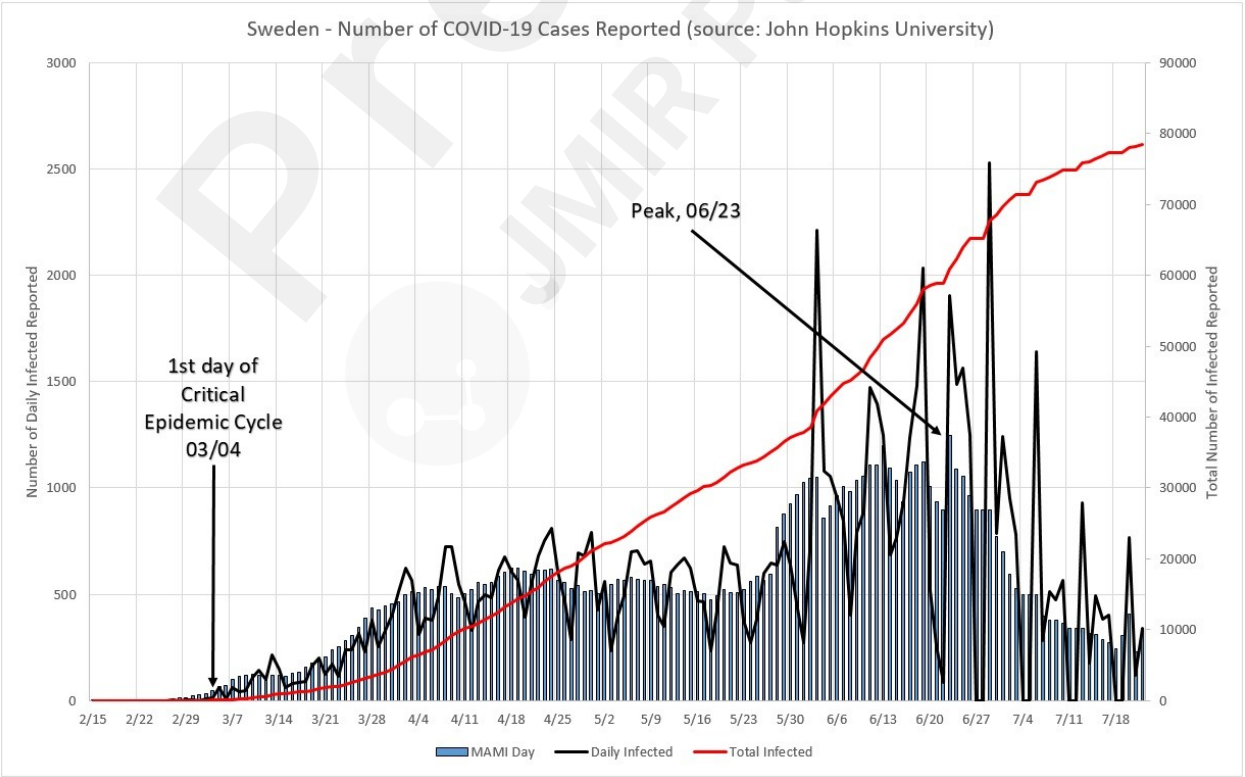

Figure 8 – Number of COVID-19 cases reported for Sweden. The black line represents the daily reported numbers, blue bars their MAMI, and red line the total cases to date and uses

the right hand axis as reference.

Deriving the Effective Reproduction Number

With the effect of moving averages measured, it is possible to proceed to an experimental method for calculating the daily number of infected and then an effective, time-varying Reproduction Number, calculating its value by means of experimental data as follows.

The total number of infected daily (I_d), during a period of time t, can be described as a function of the daily increase rate factor (1 + b) multiplied by a scale factor, as described in Formula (1):

$$I_d = a(1+b)^t \quad (1)$$

In Formula (1), “a” is the scale factor and “b” is the absolute daily increase rate, or instantaneous rate and is defined as:

$$b = \frac{I_{d,n+1}}{I_{d,n}} - 1 \quad (2)$$

Where $I_{d,n+1}$ is the current day and $I_{d,n}$ the previous day.

Formula (1) can be written as:

$$I_d = C^t \quad (3)$$

Where C is the the Time-Dependent Effective Reproduction Number, $R_e(t)$, or R_t for short, which is obtained from experimental data. For the Reproduction Number determination, it is necessary to determine the scale factor “a”. Therefore, “a” takes the following form:

$$a = \frac{I_d}{(1+b)^t} \quad (4)$$

Finally, from Formulas (3) and (4):

$$R_t = e^{\left[\frac{\ln(a)+t.\ln(1+b)}{t}\right]} \quad (5)$$

In order to map the interpretation proposed from Formulas (1) to (5) to the classical mathematical interpretation for the Reproduction Number, R_0, an equivalence transformation will be described as follows.

From the classical definition of R_0, let:

$$R_0 = \beta * \tau \quad (6)$$

Where β is infection-producing contacts per unit time (instantaneous rate), with a mean infectious period of τ. Formula (6) can be transformed into:

$$R_0 = e^{k\tau} \quad (7)$$

From Formulas (5) and (7):

$$e^{k\tau} = e^{\left[\frac{\ln(a)+t.\ln(1+b)}{t}\right]} \quad (8)$$

In (8), all dimensional units are compatible, therefore our transformations to obtain R_t in Formula (5) are valid. Formula (5) was obtained from experimental data, and it is at the core of the model here proposed. From this point onward, R_t must be interpreted as $R_e(t)$ as explained before, in the interpretation of Formula (3).

During the data analysis, we noted that the daily increase rate factor, (1 + b), is not enough to describe the number of contaminated cases registered at one given day, because it simply informs the absolute increase ratio occurred from one day to the next. The Reproduction Number coefficient needs more numerical information in order to be able to express correctly the magnitude of daily numbers. It needs the scale factor “a” to bring more information on the phenomenon. As an example of this finding, Figure 9 shows that while the (1 + b) factor varies rapidly, Rt drops steadily, changing slowly as the exponential time grows. The same behavior is displayed by the total daily registered number of deaths,

which keeps growing smoothly. This is the numerical evidence that the factor (1+b) alone cannot describe the total number of deaths.

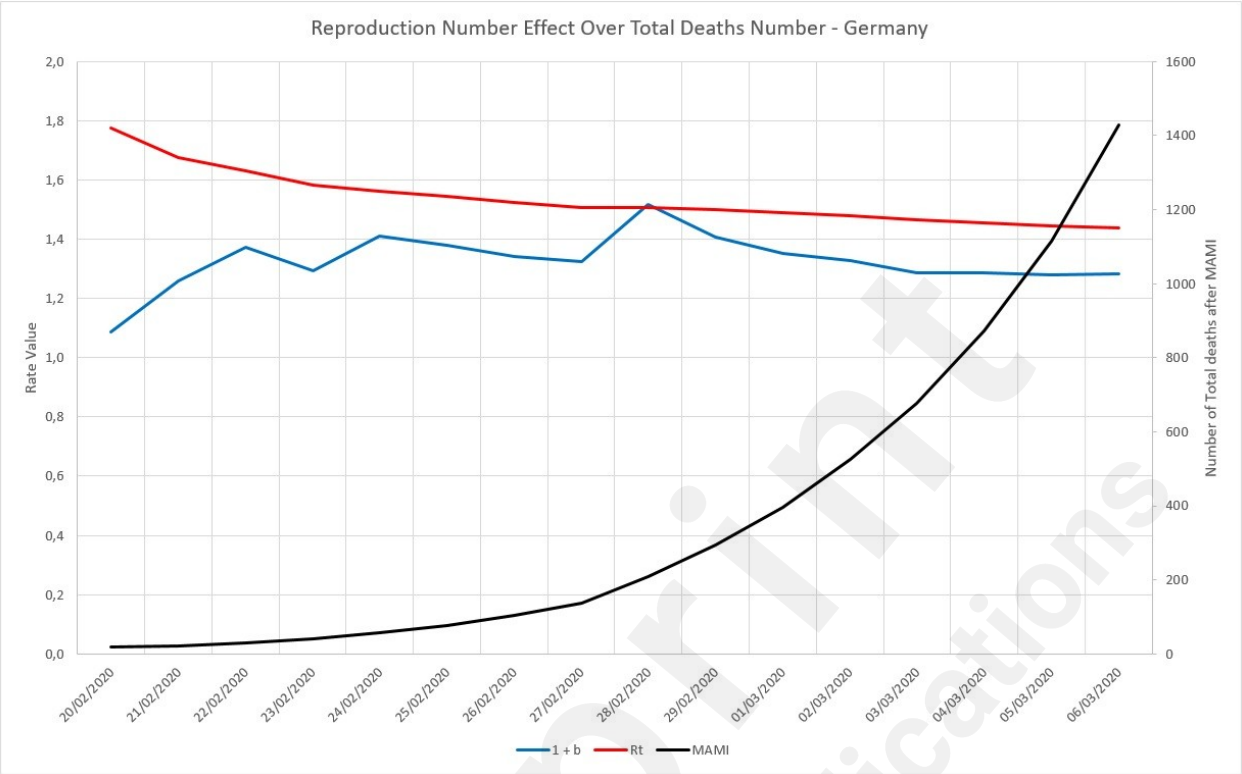

Figure 9 – Behaviors of (1 + b) and R_t factors, for the first 20 days in the German epidemic cycle.

Sub Notification Effect on the Reproduction Number

When it comes to analyze the number of cases of infection in the COVID-19 epidemic, an issue that always arises is underreporting or sub-notification and its importance in predicting the behavior of the epidemic cycle. Thus, the third part of the framework is dedicated to the study of sub-notification and its effects on prediction. Sub-notification is understood as the fact that actual figures on infected persons are only estimated by public health authorities. Given that many people exposed to the virus do not display any sign of infection or the symptoms are very mild, therefore going unnoticed and unregistered by local bureaus of health statistics, the development of evaluation tools of the impact of these non notified cases is necessary. If it is assumed that sub notification is a constant factor (eg. 10 times the registered number of cases) during the whole epidemic cycle, it does not change the absolute daily increase rate “b” or the (1 + b) factor. However, in fact it does affect the scale factor “a”, therefore changing the reproduction number (R_t).

Sub Notification Impact Estimation Method

The impact of sub-notification over R_t may be estimated by initially assuming that the actual registered figures for daily infected persons are no longer their actual values, but “real” ones multiplied by a factor, the sub notification factor. After that, the scale factor “a” is calculated. The term (1 + b) remains constant, once the ratio (Formula 3) remains constant. Then “a” and (1 + b) are applied to Formula 5, thus recalculating R_t, now reflecting the effect of the imposed sub-notification factor. This new R_t value would have been the correct one, in case all sub notified cases were suddenly registered. The percentage difference between this new, recalculated R_t and the actual one provides an estimate for the impact of sub notification over the reproduction number for a given population. Therefore, multiplying

the values for registered cases by a factor of 10, will not cause a tenfold increase in R_t. The true impact must be, therefore, calculated as described. It is also observed that sub notification affects mostly at the very beginning of the critical cycle. After a certain amount of time, error drops to insignificant values, below 5%.

Total Number of Infected, Daily Infection Rate, Lag Time, and Incubation Period

The fourth component of the framework is the application of the Logistic Model to estimate three parameters: the final count for the total of infected, and the daily infection rate, the lag, which defines when the cycle really started. An innovative model, based on the concept of inventory formation, is used to determine a fourth parameter: the most likely incubation period for the virus.

Considered by many authors as a good fit for modeling epidemic episodes [16, 17, 18], the Logistic Model describes three typical phases for this type of episode: the slow start, the steady growth, and finally the asymptotically behavior of its end. There are several ways to implement this function and this work will use the so-called Richard Growth Model to describe the accumulated number of infection cases. The generalized logistic function has the following form:

$$N(t)=\frac{x_1}{\left[1+x_4.e^{\left[-x_2(t-x_3)\right]}\right]^{\frac{1}{x_4}}} \quad (9)$$

By selecting the highest r^2 among several variations of (9), through curve-fitting, a particular form for (9) is found such as:

$$N(t)=\frac{a}{\left[1+e^{\left[-b(t-c)\right]}\right]^{\frac{1}{d}}} \quad (10)$$

Where N(t) is the number of infected persons at a given period of time t, a is the final count for the total infected, b is the daily infection rate, c is the lag phase and d is a positive real number. It can be shown that:

$$\begin{aligned} x_1&=a \\ x_2&=c \\ x_3&=b/c \end{aligned} \quad (11)$$

The constants a, b, c, and d will be used to estimate x_1, the maximum number of infected people in a given location. X_2 is the daily Infection Rate, or the average absolute daily increase in the number of infected, which can be used to determine the Reproduction Number (and to estimate the Incubation Period). Finally, x_3 is used to estimate the Lag Time, or the actual moment when the first case happened.

Incubation Period Estimation

Although there is a series of studies on the incubation period for Sars-CoV-2, in order to maintain consistency within the framework, we seek to develop a model that could also estimate what would be the best incubation period estimation method to consider when modeling epidemic cycles. For that, we defined a model of inventory of infected people similar to the one used in productive systems, as shown in Formula (12).

$$I_t=I_{t-1}+D_t-D_{t-n} \quad (12)$$

Where:

I_t: Inventory of people infected in day t, or the total of infected in day t;
I_{t-1}: Inventory of people infected in the previous day;
D_t: Number of people detected with the disease in day t;
D_{t-n}: Number of people detected with the disease n days before t;

The equation described in (12) should be interpreted as follows: the number of people who

are infectious on a given day is equal to the number of people who were infectious the day before, plus the number of infected detected on the same day, minus the number of people who have left the N-day incubation period. This reasoning therefore assumes that as soon as a person finds out he/she is infected, that is, when this person leaves the incubation period, assumes perfect isolation and stops infecting. Although this assumption is not totally realistic, since it depends not only on individual responsibility, but also on the implementation of efficient isolation measures, at the same time it must also be considered that not every infected person effectively infects others, since, knowing that the isolation is not the only way to avoid contamination by viruses, there are cases, for example, you may have people in your social life immunized in some way. Thus, we consider this assumption to be reasonable to be applied statistically.

Other basic assumptions is that of all people susceptible (not vaccinated, exposed enough to the pathogen, etc) not all of them will exposed or develop the disease in a form severe enough to be noticed. Accordingly, the recorded number of daily cases does not reflect the total number of infected, but those who seek medical attention and therefore were diagnosed as contaminated. Therefore, this is the number of infected in a given day, or the “inventory” of people that can infect other people in a given day. With the formulation defined in (12) and the assumptions described previously, we followed with the analysis and simulations for the three countries.

Results

The epidemic cycles observed were subjected to the numerical methods present in the framework and described in the previous section. The first data transformation was the application of the Moving Average Method with Initial value. The second transformation is normalization, where all the values are divided by cycle peak value, causing most of the values to fit between 0 and 1, except for the false peaks. These two consecutive transformations allow a comparison of behaviors among cycles, as well as proves that several epidemic cycles, within the pandemic, have similarities. With these first steps it is possible to estimate the duration and general behavior of a local episode, even though this, in absolute terms, does not present the same number of deaths or duration as its similar cycle. What remains approximately constant are the proportions of the similar cycles. An example of the application of this technique with great success is the performance prediction of professional athletes and teams [19].

By the time the analyses was done, the three countries considered in this paper presented more advanced cycles, so no predictions were made for them, instead, their cycles were used to perform analysis on other countries, regions and cities. For instance, Figure 10 presents the similarity of the USA’s and the Swedish cycles. A complete set of predictions for Brazil, the state of Rio de Janeiro, and the city of Rio de Janeiro, as welll as a measurement of the performance of the model, are presented in Appendix 1. Also, in [12] it is possible to find many others comparisons and predictions between cities, regions, and countries using this method.

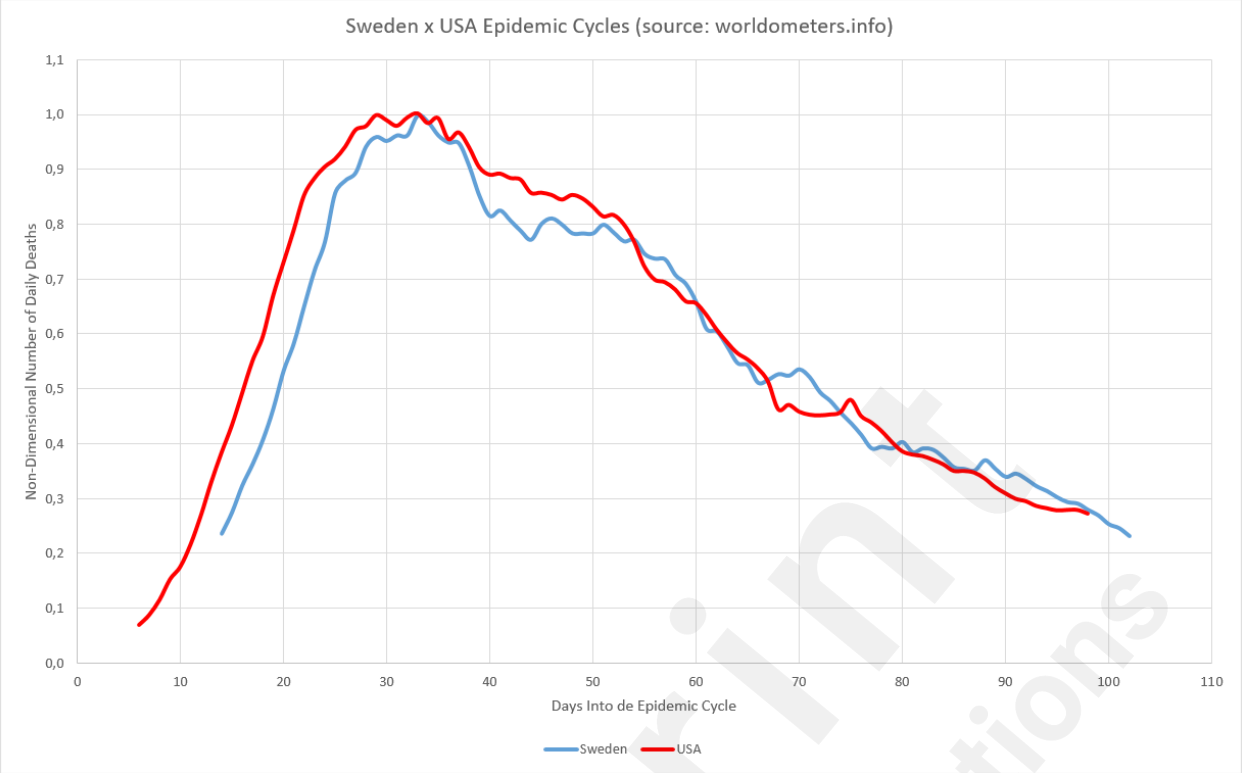

Figure 10 – Sweden's and USA's epidemic cycles compared.

The analyses of the other variables considered in the framework for Germany, Italy and Sweden are presented in the next topics. The data for this part of the study was also collected from the John Hopkins University's website on the declared dates.

The expressions developed in Formulas (1) to (5) do not explicitly take into account the incubation period, with the instantaneous rate of change, or daily increase in number of registered infected individuals, calculated as defined in Formula (5). For the sake of thoroughness, three simulations were performed, for a incubation period of 5, 10 and 15 days. This was achieved by redefining the expression (1+b) for a new set of parameters, basically dividing the total number of reported cases for a given day by the values registered in 5, 10 and 15 days before. In that way, the term (1 + b) now would reflect the incubation period over R_t. All simulations yielded zero (0%) change, to the fourth significant figure. Therefore, it is assumed that the described method is inherently insensitive to incubation period variations or influence, reinforcing its simplicity and robustness. The data and calculations are in Appendix 4.

Germany

Reproduction Numbers

In Figure 11, three distinct zones are formed. Zone "a" is in the very beginning of the cycle and the Reproduction Number varies from 1.10 to 1.48 from one day to the next, this probably is just the reflection of large initial variation in numbers, but only if we limit this zone to no more than 5% of the MAMI peak value. It is easy to notice that the figures bear small influence in the overall disease behavior. Zone "b" describes the transmission during the critical disease cycle (from March, the 6th to June the 7th), where a rapid increase in daily cases stops only around the peak than drops steadily towards the end. This is the most lethal period of the epidemic cycle and it is considered over once a 5% peak level is reached again. The remaining time, Zone "c", is the residual cycle that appears in all countries and places facing the COVID-19 crisis. In absolute values the Reproduction

Number for the critical period starts with a 1.30 value and drops continuously towards 1.00, although never quite reaches it (as for the time of this paper was written).

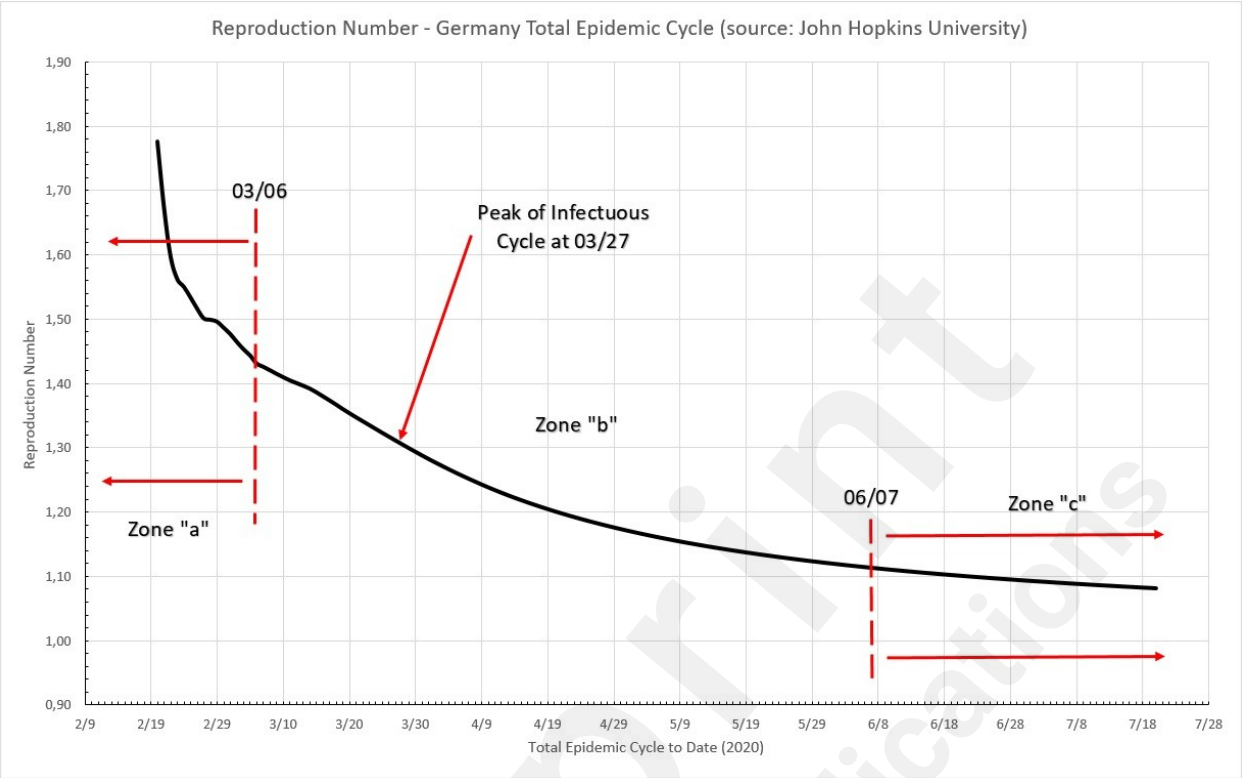

Figure 11 – Total epidemic cycle in Germany, using the number of infected people daily.

Sub-Notification

An arbitrary threshold line representing a 5% error was drawn in Figure 12. This limit tells that after the 50th day into the German critical cycle (the one between 5% of the peak value, before and after it), regardless the amount of sub notification, the error over the calculated Reproduction Number is no greater than 5%. At the other extreme, a 3x sub-notification basically does not induce errors larger than 5% over the Reproduction Number, in any time during the critical cycle. A maximum error of 16.84% is estimated for the worst case scenario here simulated, a 40x sub-notification, and the first day into the cycle. In overall, sub-notification appears to have no significant impact in Germany official infected numbers. Sub-notification also seems to have more impact in the very beginning of a given cycle, but turns itself irrelevant towards the end.

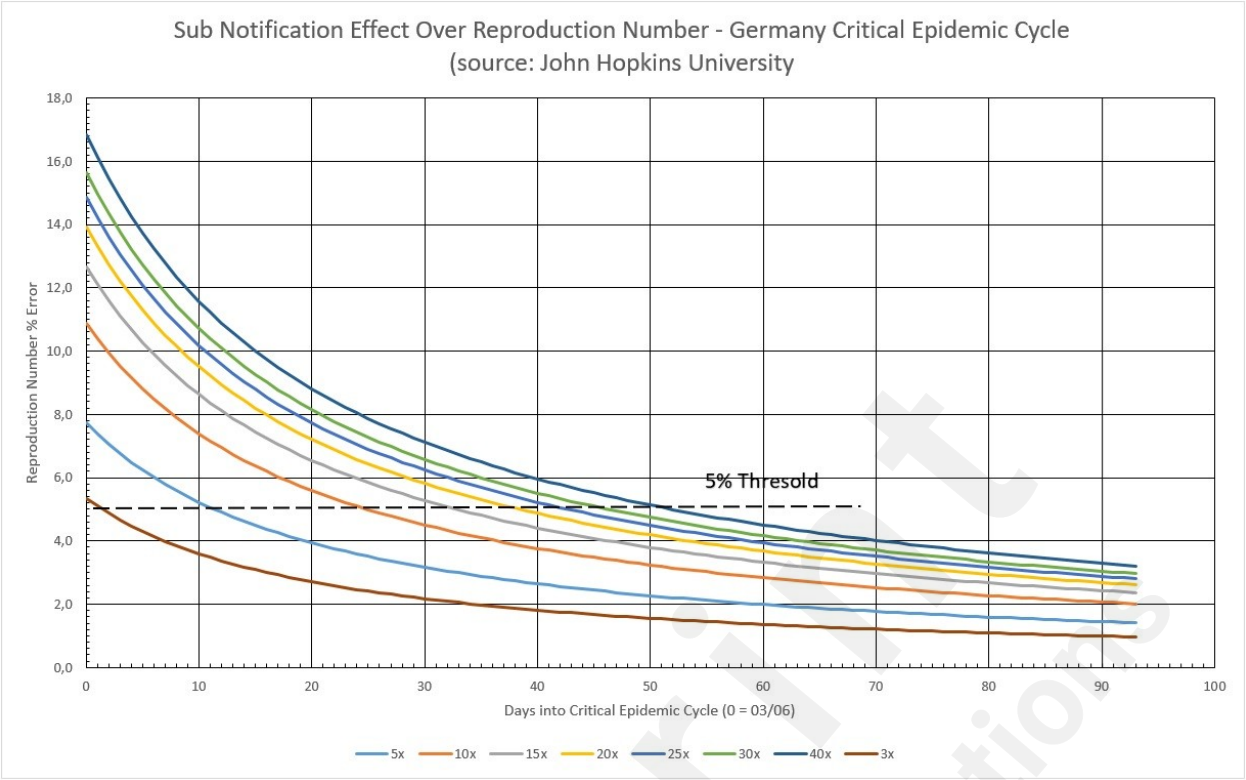

Figure 12 – Sub notification effect over Reproduction Number in Germany, during the critical epidemic cycle.

Table 3 - Errors associated with ignoring the existence of Sub Notification (SN) into the epidemic cycle.

SN	Max Error (%)	Min. Error (%)	Days Until ≤ 5%	Error (%) at Peak Day
3x	5.34	0.97	2	2.64
5x	7.73	1.41	12	3.85
10x	10.87	2.02	25	5.46
15x	12.66	2.37	33	6.39
20x	13.91	2.62	39	7.05
25x	14.87	2.81	43	7.55
30x	15.64	2.97	47	7.96
40x	16.84	3.21	52	8.60

Total Number of Infected

Data collected for Germany from February 15th to July 20th is plotted in Figure 13. The blue dots represent the daily registered infected cases submitted to MAMI, the red continuous line represents the Richard Growth Model curve, and drawn using parameters determined by the MAMI data.

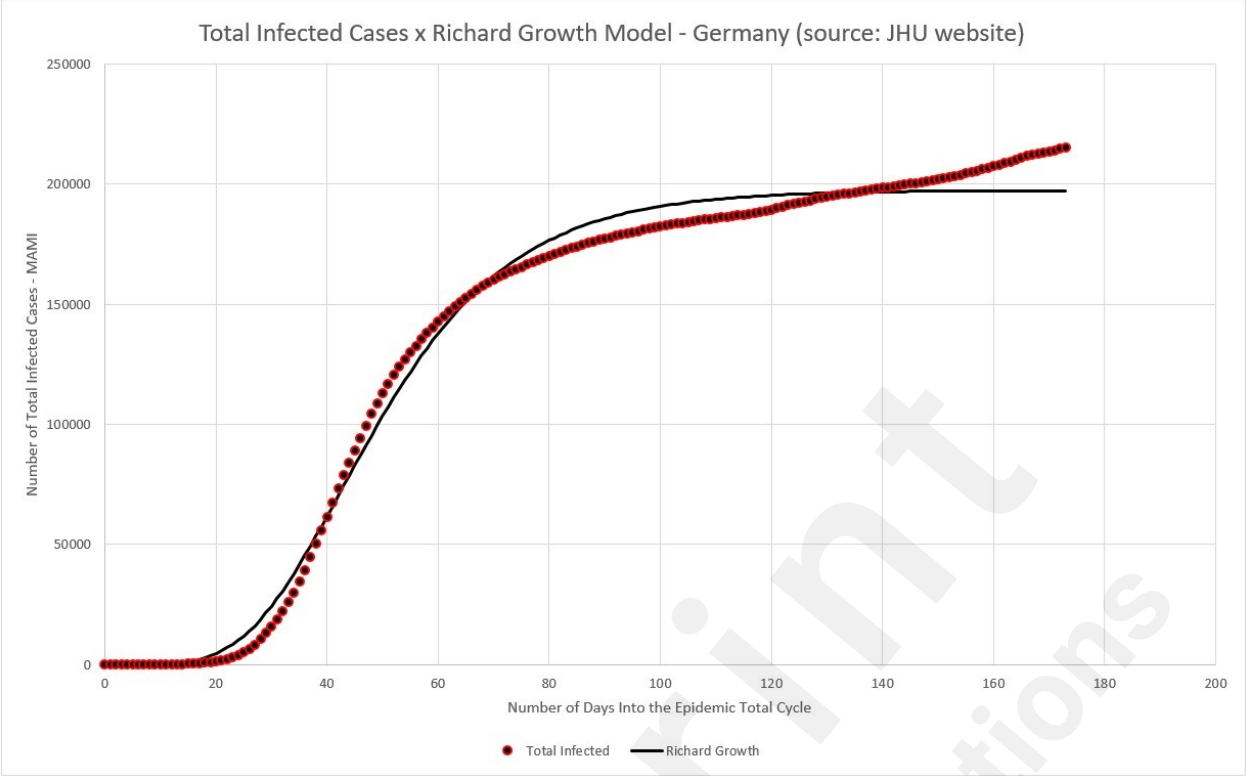

Figure 13 – Germany: total number of infected (MAMI) compared to Richard Growth Model prediction.

As discussed previously, the German critical epidemic cycle started at March the 6th. According to Table 5, the first case must be recorded 89 days before that, with X_3 indicating that the first case of the total epidemic cycle occurred around December, 8st 2019.

Table 4 – Curve-fitting data.

Curve-Fitting	
a	197372.97
b	-5.2260
c	0.0587
d	4.4208×10^{-4}

Table 5 – Epidemic parameter determined using curve-fitting data from Table 4

Epidemic Parameters	
X_1	197373
X_2	5,87%
X_3	89
r^2	0.9958

Impact of Incubation Period

In this topic we approach the model of formation of an infected persons inventory for the three countries considered. Simulations were made for incubation cycles of 3, 5, 7, 9 and 11 days. Inventories were calculated according to the formula presented in (12) and plotted together with the MAMI of detected cases. Figure 14 presents the sub notification study for Germany.

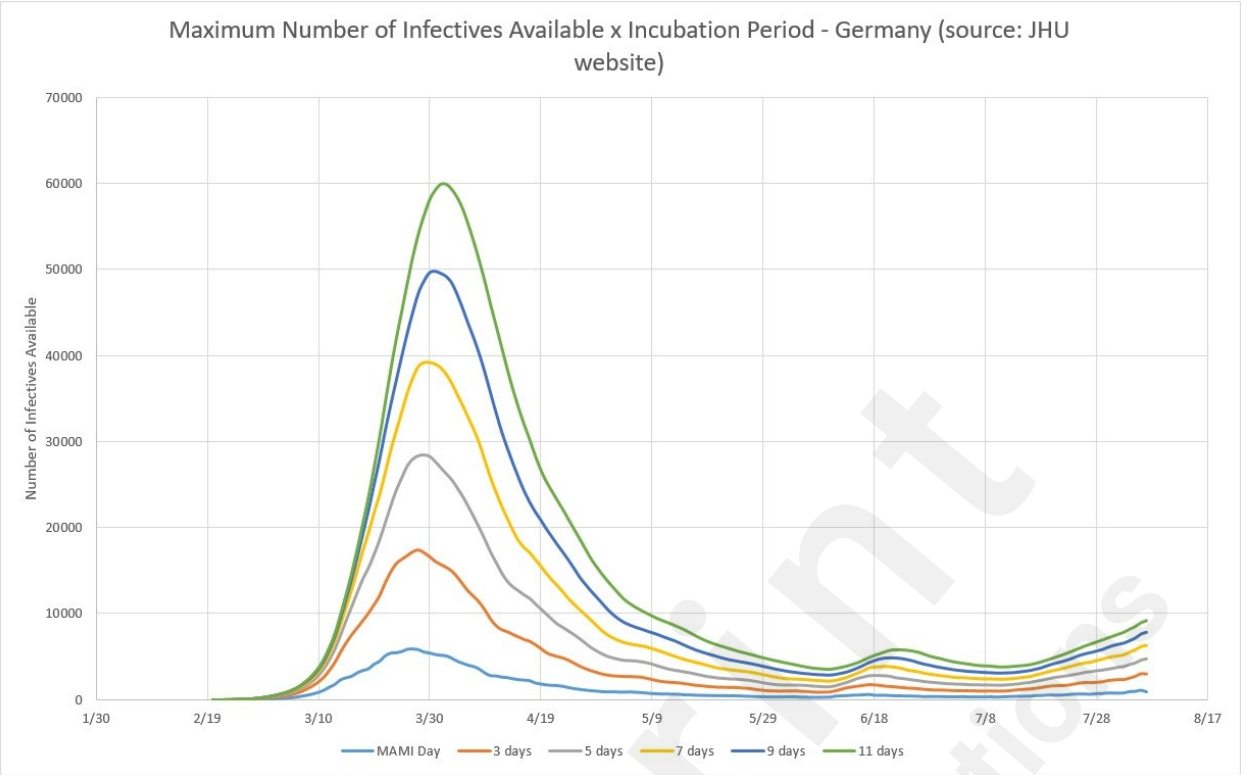

Figure 14 – Germany: Infected Persons Inventories for 3, 5, 7, 9, and 11 days of incubation, compared to MAMI.

Italy

Reproduction Numbers

It can be seem in Figure 15 that three distinct zones are formed. Zone “a” is in the beginning of the cycle and the Reproduction Number varies from 1.78 to 1.44 from one day to the next, once again this probably is just the reflection of large initial variation in number, but this zone is limited to no more than 5% of the MAMI peak value. It is easy to notice that the figures bear small influence in the overall disease behavior. Zone “b” describes the transmission during the critical disease cycle (from February 25th to June 15th). This is the most lethal period of the epidemic cycle and it is considered over once a 5% peak level is reached again. The remaining time, Zone “c”, is the residual cycle. In absolute values the Reproduction Number for the critical period starts with a 1.44 value and drops continuously towards 1.12.

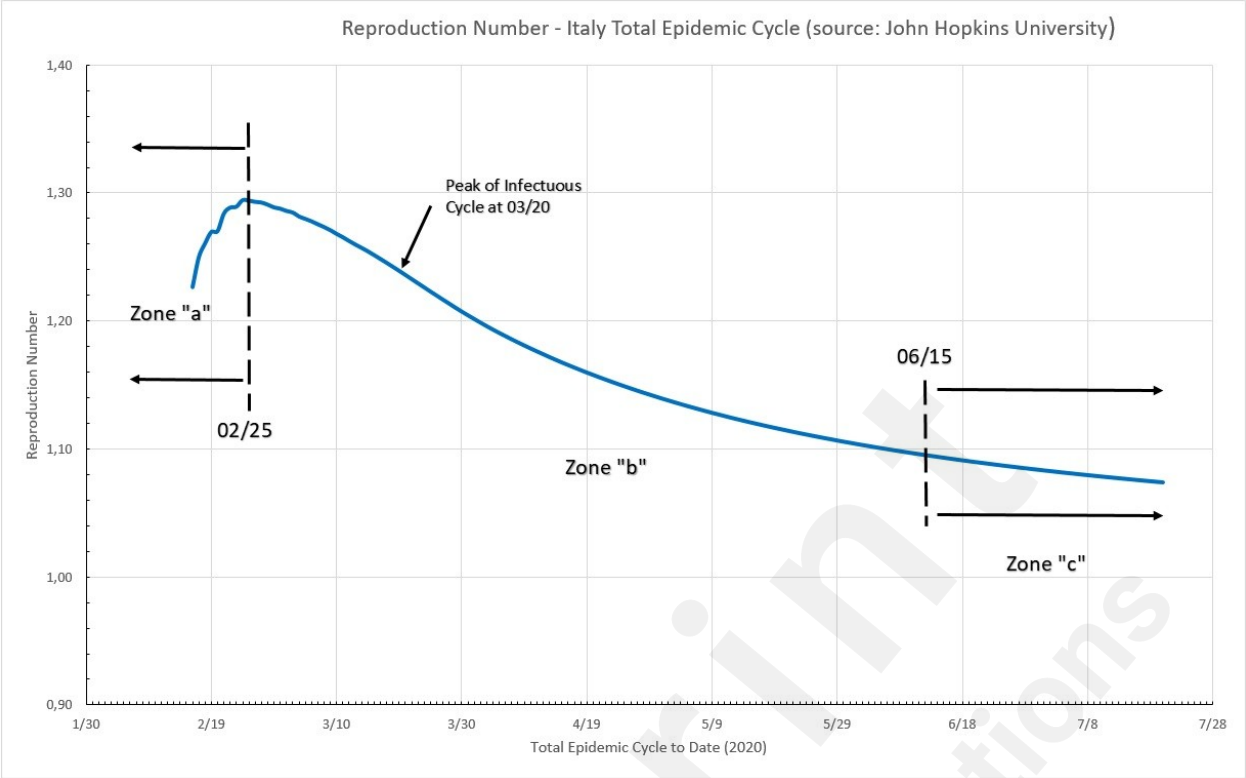

Figure 15 - Total epidemic cycle in Italy, using the number of infected people daily.

Sub notification

Italy sub notification case is presented in Figure 16. The 5% limit tells that after the 44th day into the Italian critical cycle, regardless the amount of sub notification, the error over the calculated Reproduction Number is no greater than 5%. At the other extreme, a 3x sub notification basically does not induce errors larger than 5% over the Reproduction Number, in any time during the critical cycle and 5x barely disturbs it. A maximum error of 12.34% is estimated for the worst case scenario here simulated, a 40x sub notification, and the first day into the cycle. In overall, sub notification appears to have no significant impact in Italy, as in the previous two cases, official infected numbers. Sub notification also have more impact in the very beginning of a given cycle, but turns itself irrelevant towards the end of it.

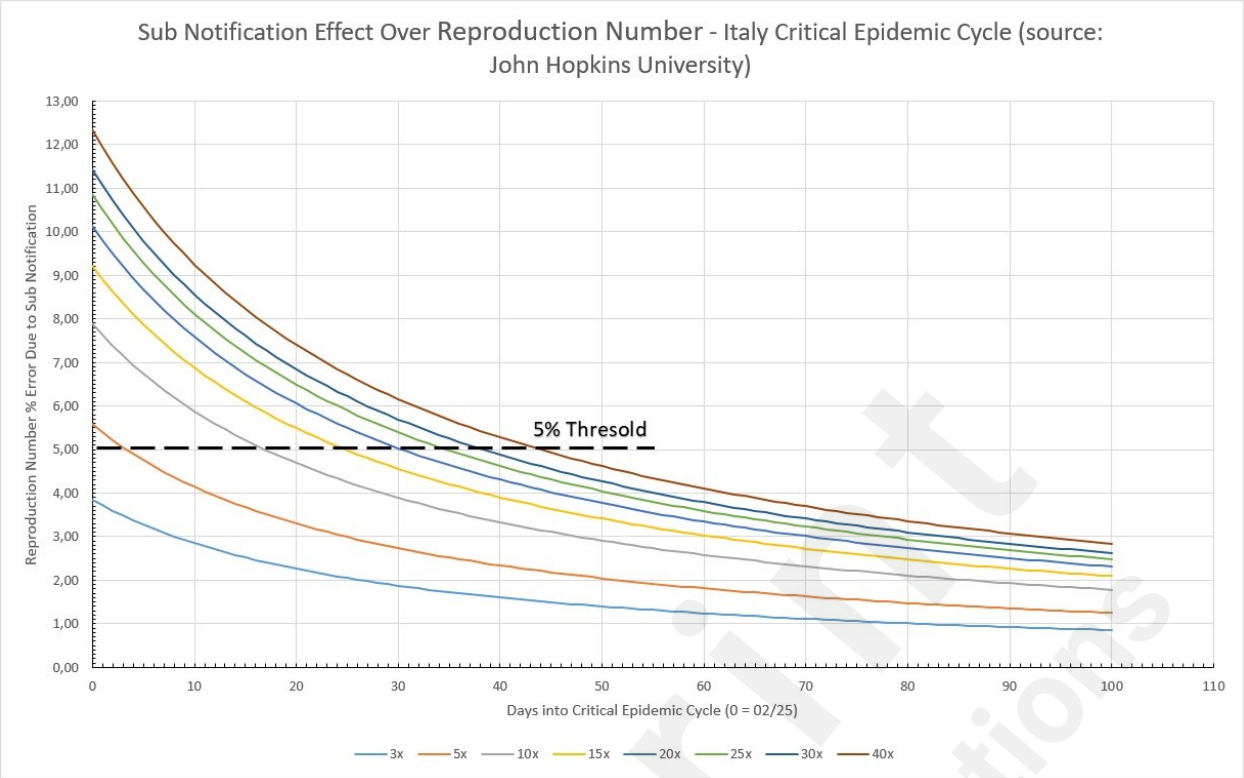

Figure 16 – Sub notification effect over Reproduction Number in Italy, during the critical epidemic cycle.

Table 6 - Errors associated with ignoring the existence of Sub Notification into the epidemic cycle - Italy.

Sub Notif.	Max Error (%)	Min. Error (%)	Days Until ≤ 5%	Error (%) at Peak Day
3x	3.85	0.85	--	2.09
5x	5.59	1.25	4	3.05
10x	7.89	1.78	17	4.33
15x	9.22	2.09	25	5.07
20x	10.15	2.31	31	5.60
25x	10.86	2.48	35	6.00
30x	11.44	2.62	39	6.33
40x	12.34	2.84	44	6.85

Total Number of Infected

Data collected for Italy from February 15th to July 20th is plotted in Figure 17. The blue dots represent the daily registered infected cases submitted to MAMI, the red continuous line represents the Richard Growth Model curve, and drawn using parameters determined by the MAMI data.

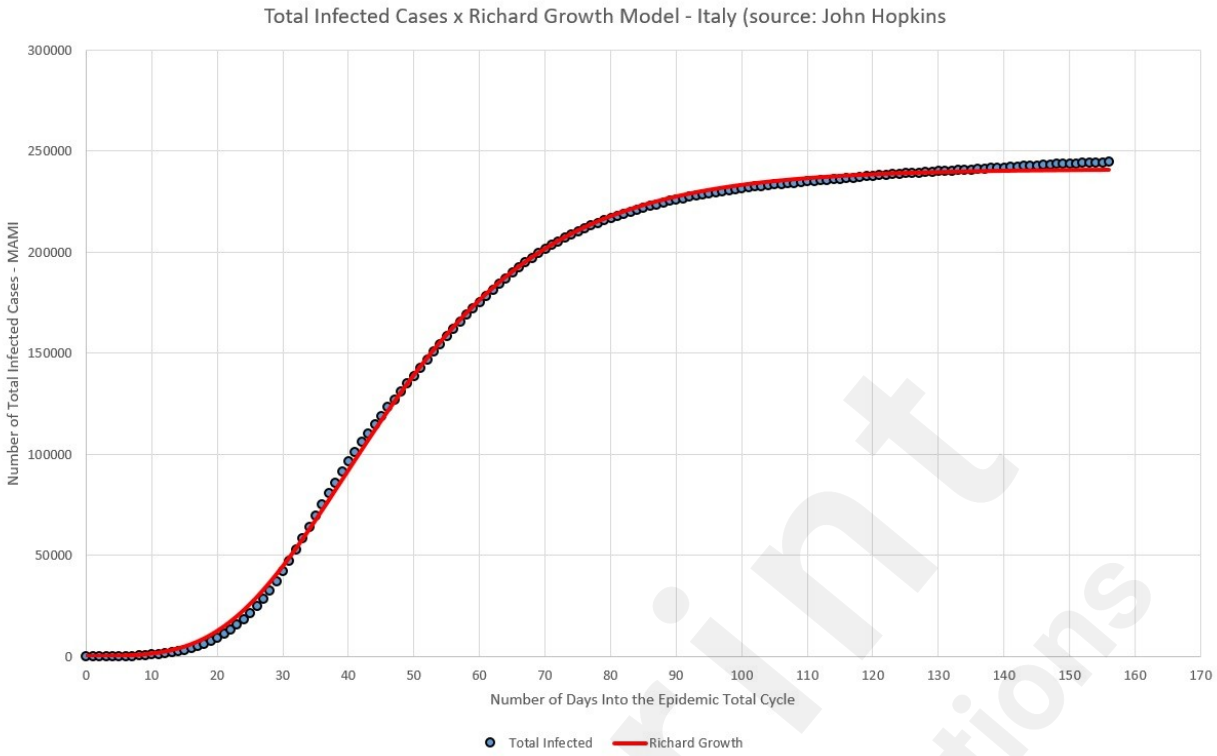

Figure 17 – Italy – total number of infected (MAMI) compared to Richard Growth Model prediction.

The Italian critical epidemic cycle started at February the 25th. According to Table 8, the first case must be recorded 86 days before that, with X_3 indicating that the first case of the total epidemic cycle occurred around December, 1st 2019.

Table 7 – Curve-fitting data.

Curve-Fitting	
a	241148.81
b	-4.8623
c	0.0562
d	8.4600×10^{-4}

Table 8 – Epidemic parameter determined using curve-fitting data from Table 7.

Epidemic Parameters	
X_1	241149
X_2	5,62%
X_3	86
r^2	0.9995

Impact of Incubation Period

Using the same reasoning used for Germany, Figure 18 presents the inventories of infected persons for Italy.

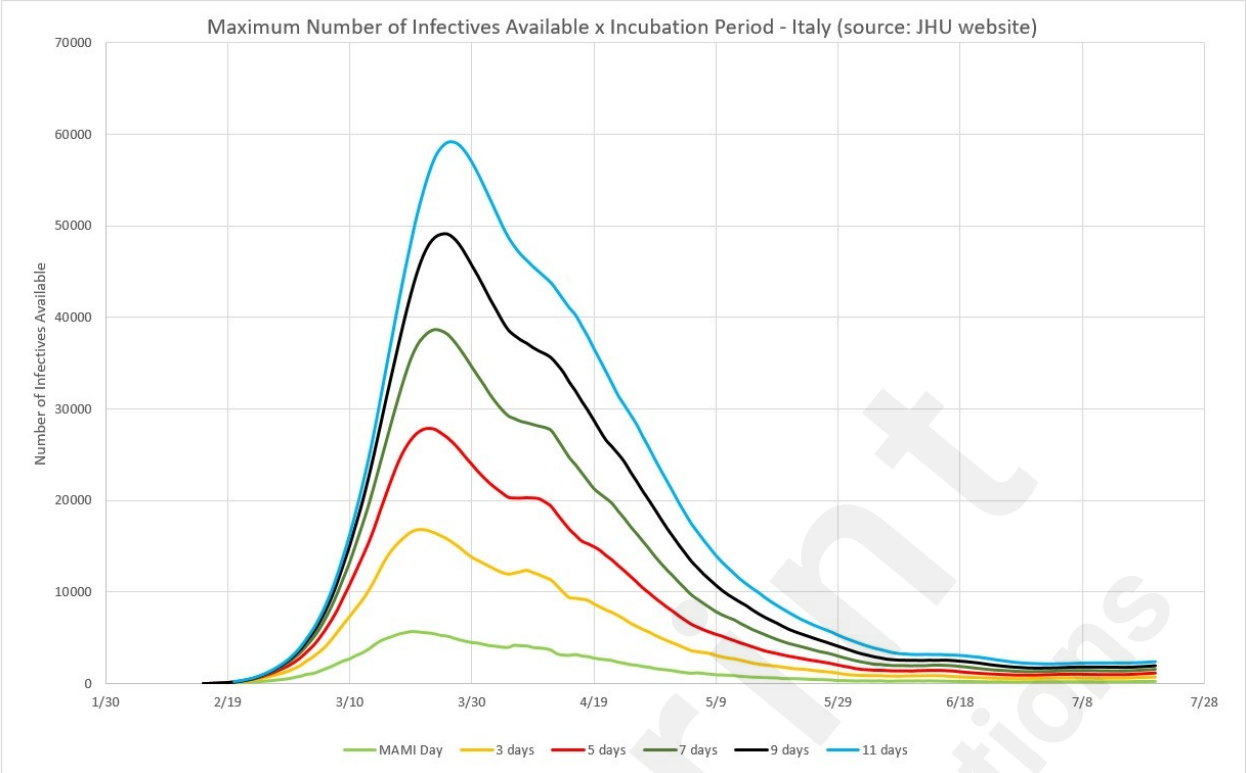

Figure 18 – Italy: Infected Persons Inventories for 3, 5, 7, 9, and 11 days of incubation, compared to MAMI.

Sweden

Reproduction Numbers

It can be seem in Figure 19 that two distinct zones are formed, once Sweden is considered, by the 5% criteria an “ongoing” epidemic cycle, although in the present date, close to the end. Zone “a” is in the beginning of the cycle and the Reproduction Number varies from circa 1.33 to 1.16 from one day to the next, once again this probably is just the reflection of large initial variation in number, but this zone is limited to no more than 5% of the MAMI peak value. It is easy to notice that the figures bear small influence in the overall disease behavior. Zone “b” describes the transmission during the critical disease cycle (from March 4th onward). This is the most lethal period of the epidemic cycle and it is considered over once a below 5% peak level is reached again. In absolute values the Reproduction Number for the critical period starts with a 1.16 value and drops continuously towards 1.07.

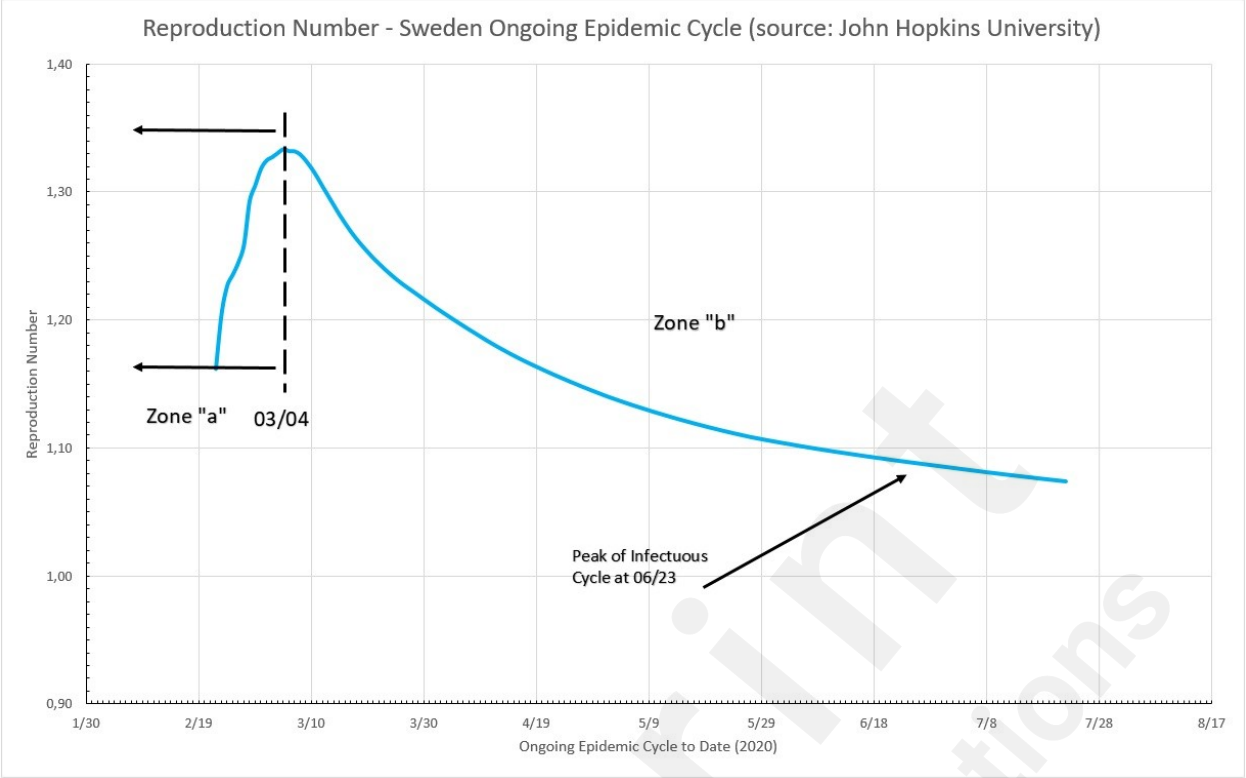

Figure 19 - Epidemic cycle in Sweden, using the number of infected people daily.

Sub Notification

Sweden sub notification effect is presented in Figure 20. The calculated limit tells that after the 54th day into the Swedish critical cycle, regardless the amount of sub notification, the error over the calculated Reproduction Number is no greater than 5%. On the other extreme, a 3x sub notification basically does not induce errors larger than 5% over the Reproduction Number, after the fourth day during the critical cycle. A maximum error of 18.53% is estimated for the worst case scenario here simulated, a 40x sub notification, and the first day into the cycle. In overall, sub notification appears to have no significant impact in Sweden. Sub notification also have more impact in the very beginning of a given cycle, but turns itself irrelevant towards the end of it.

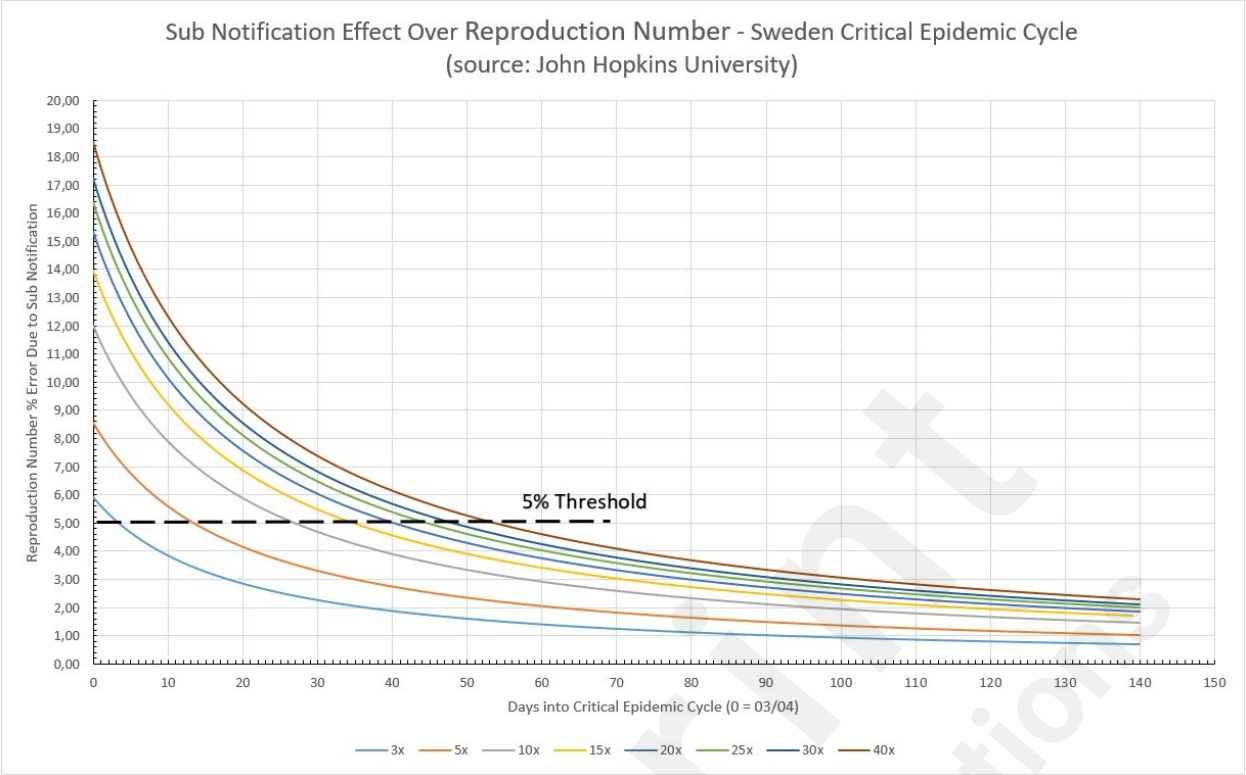

Figure 20 – Sub notification effect over Reproduction Number in Sweden, during the critical epidemic cycle.

Table 9 - Errors associated with ignoring the existence of Sub Notification into the epidemic cycle in Sweden.

SN	Max Error (%)	Min. Error (%)*	Days Until ≤ 5%	Error (%) at Peak Day
3x	5.92	0.69	4	0.85
5x	8.55	1.01	14	1.24
10x	12.01	1.45	27	1.77
15x	13.97	1.70	35	2.08
20x	15.33	1.88	41	2.30
25x	16.37	2.02	45	2.46
30x	17.22	2.13	49	2.60
40x	18.53	2.31	54	2.82

Total Number of Infected

Data collected for Sweden from February 15th to July 20th is plotted in Figure 21. The blue dots represent the daily registered infected cases submitted to MAMI, the red continuous line represents the Richard Growth Model curve, and drawn using parameters determined by the MAMI data.

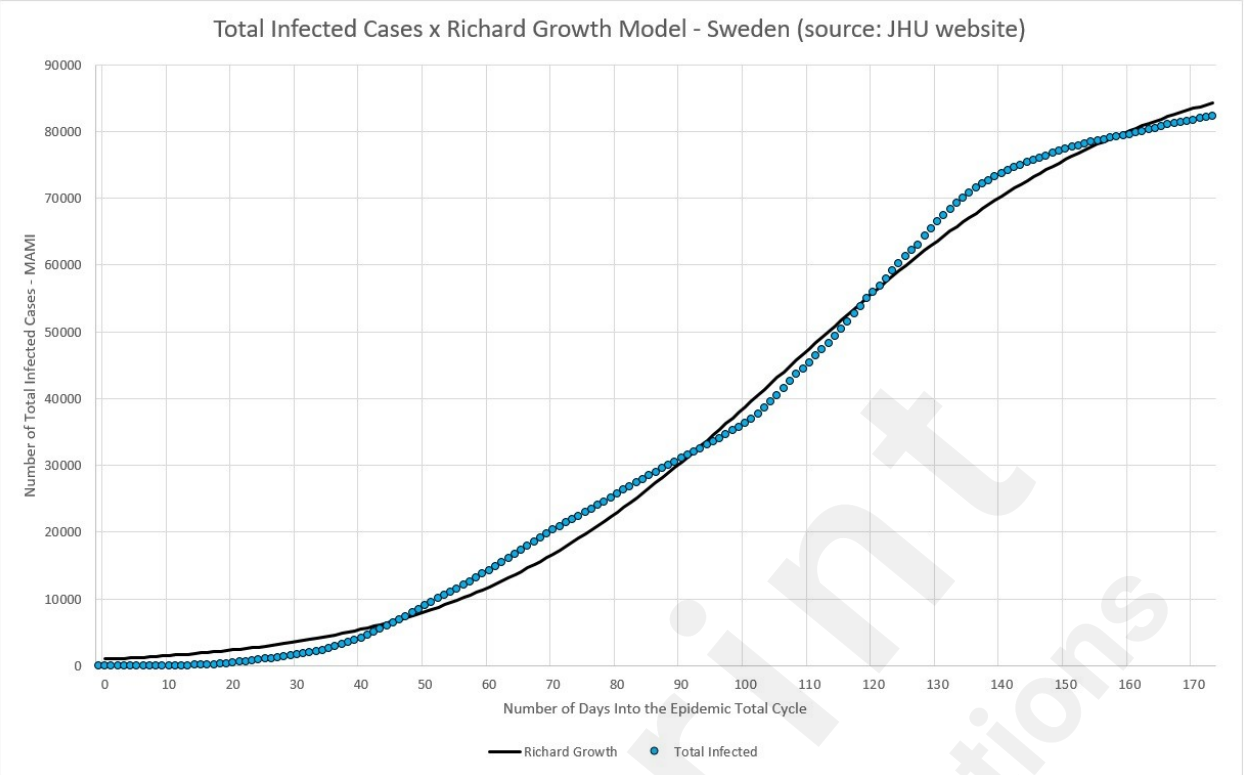

Figure 21 – Sweden – total number of infected (MAMI) compared to Richard Growth Model prediction.

Previously it was shown that the Swedish critical epidemic cycle started at March the 4th. According to Table 11, the first case must be recorded 98 days before that, with X_3 indicating that the first case of the total epidemic cycle occurred around November 27th 2019.

Table 10 – Curve-fitting data.

Curve-Fitting	
a	92538,59
b	3.4050
c	0.0348
d	7.5514×10^{-1}

Table 11 – Epidemic parameter determined using curve-fitting data from Table 10.

Epidemic Parameters	
X_1	92539
X_2	3,48%
X_3	98
r^2	0.9958

Impact of Incubation Period

Accordingly, Figure 22 presents the predicted inventories of infected persons for Sweden.

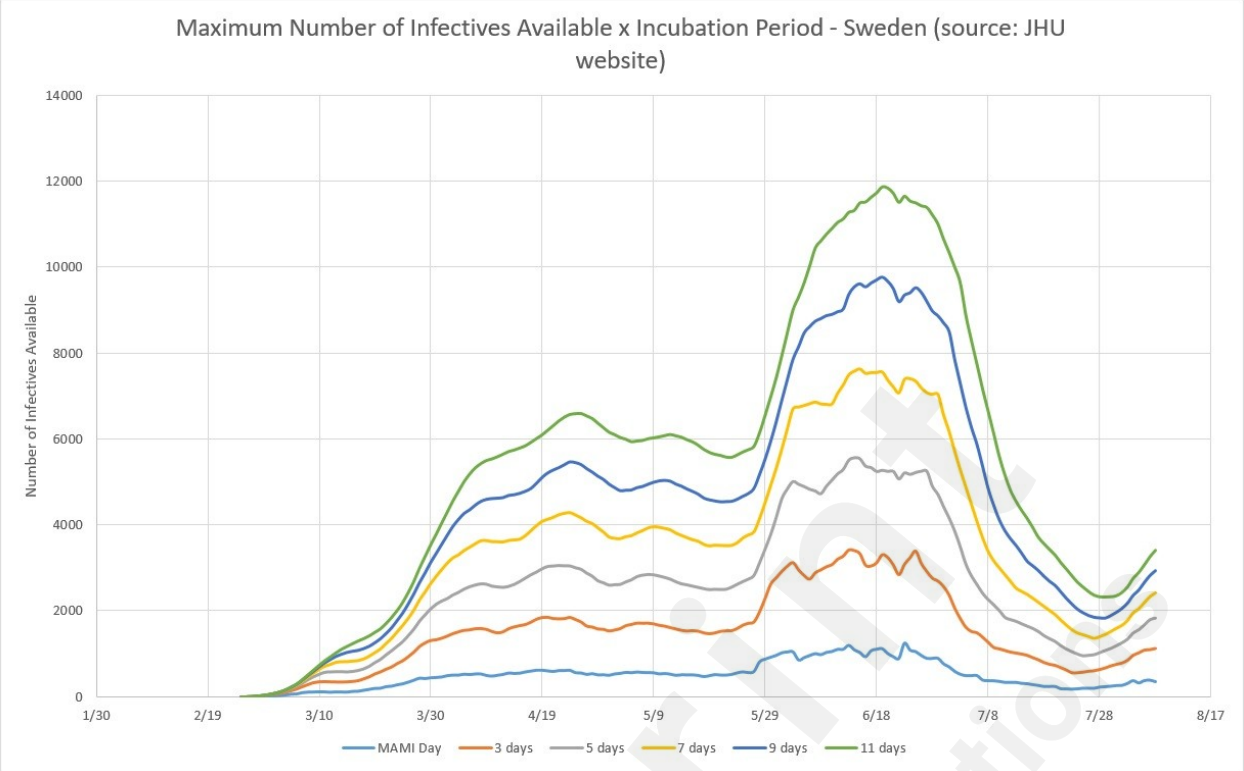

Figure 22 - Sweden: Infected Persons Inventories for 3, 5, 7, 9, and 11 days of incubation, compared to MAMI.

One cannot take the assumptions used to derive formula (12) as deterministic, considering that it describes a perfect “production” system. However, there is no biological system that behaves in such perfect and deterministic way. Therefore, the data shown in Figures 9, 13, and 17 are not conclusive by themselves, given the imperfections of the contamination paths, or the considered “production system”, should be taken into account. In other words, the efficiency of the transmission system must be evaluated, as it is done in the Discussion session.

Discussion

Most Lethal Cycle of Epidemics Control Performance

Using the definition of MLCE, a comparison of the three studied countries was performed. As parameters, it were applied an interval within the 5% limits and the non-dimensional time calculated by dividing the day numbers by the total MLCE duration, for each country. For the Reproduction Number, all the values were divided by the largest value found in the MLCE interval. All these transformations allow to estimate how efficient was the disease spreading control used in each country. In order to enrich the comparative analysis, Figure 23 presents the data from the three countries studied here and also from the UK, South Korea and the State of New York. Additional details on this and others comparisons can be found in [13]. Sweden and New York State were considered as still having an open MLCE by the time of the data analysis, therefore the end of the cycle considered was the day of the data collection (July, 22nd, 2020).

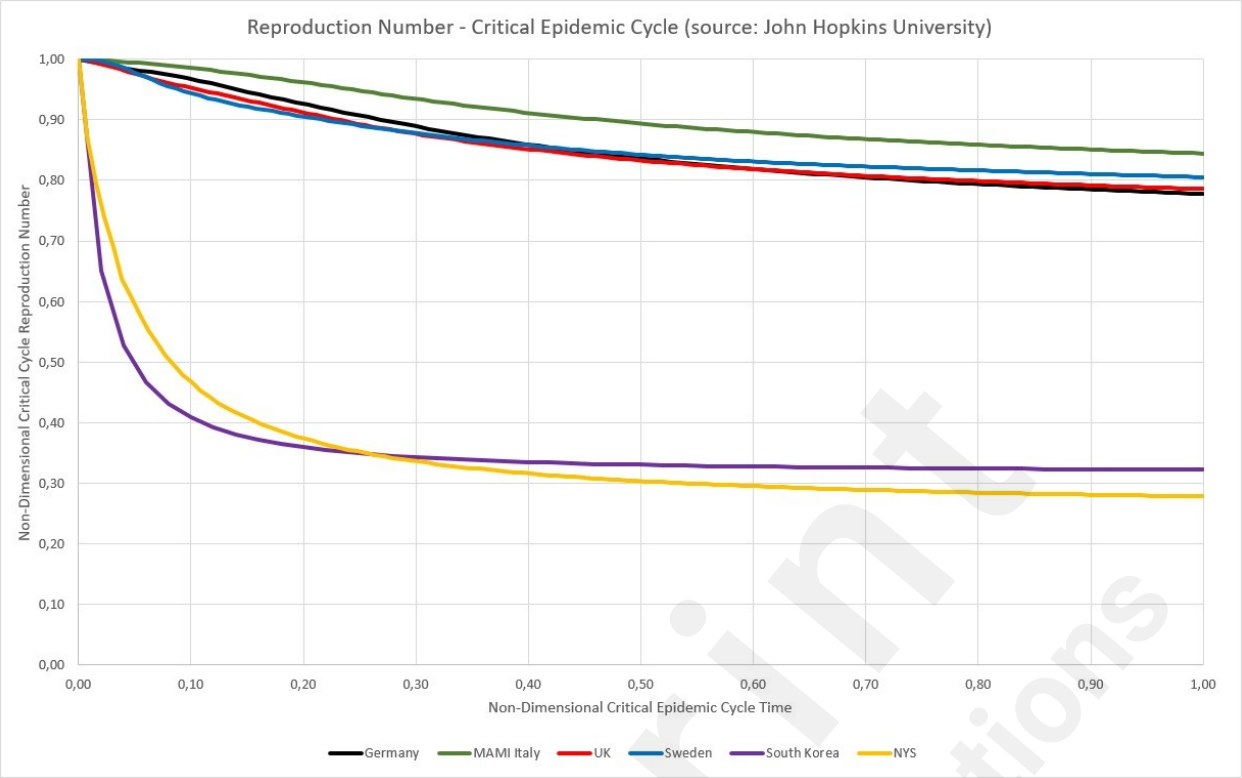

Figure 23 – Non-dimensional critical epidemic cycle for Germany, Sweden, UK and Italy.

Figure 23 shows that Italy was, relatively, the most unsuccessful place in reducing Reproduction Numbers, although not for a large margin. Germany and the UK have the same performance and kept R_t falling slowly but steadily. South Korea and New York State achieved a large drop in the early stages of the critical cycle, but after that, R_t became basically constant.

Efficiency of the Infection System

According to the experimental data obtained, the efficiency, or the capacity of spreading itself, of the biological system here described - the Sars-CoV-2 - has a Power function form, as shown in Figure 19. Although the three countries here analyzed present very different epidemic cycles, the percentage of people infected compared to the incubation period varies very little. This reflects, probably, that the incubation period is in fact a constant value. Figure 24 shows that, for example, for a 5-day incubation period, the percentage of people who were exposed to the virus and displayed symptoms severe enough to prompt them to look for medical care was around 20%. At the other extreme, if the virus had a 11-day incubation period, the numbers of actual cases registered would have indicated a 10% rate of infection in the general population.

This curve, although restricted to only these three countries, covers nations with quite different NPI policies, population sizes, and land masses. It shows that, according to registered cases, Sars-CoV-2 affected proportionally a small segment of these populations and at the same proportions. The sub-notification effect does not interfere with this curve behavior, once unregistered cases only happen into the complementary percentage, usually without symptoms.

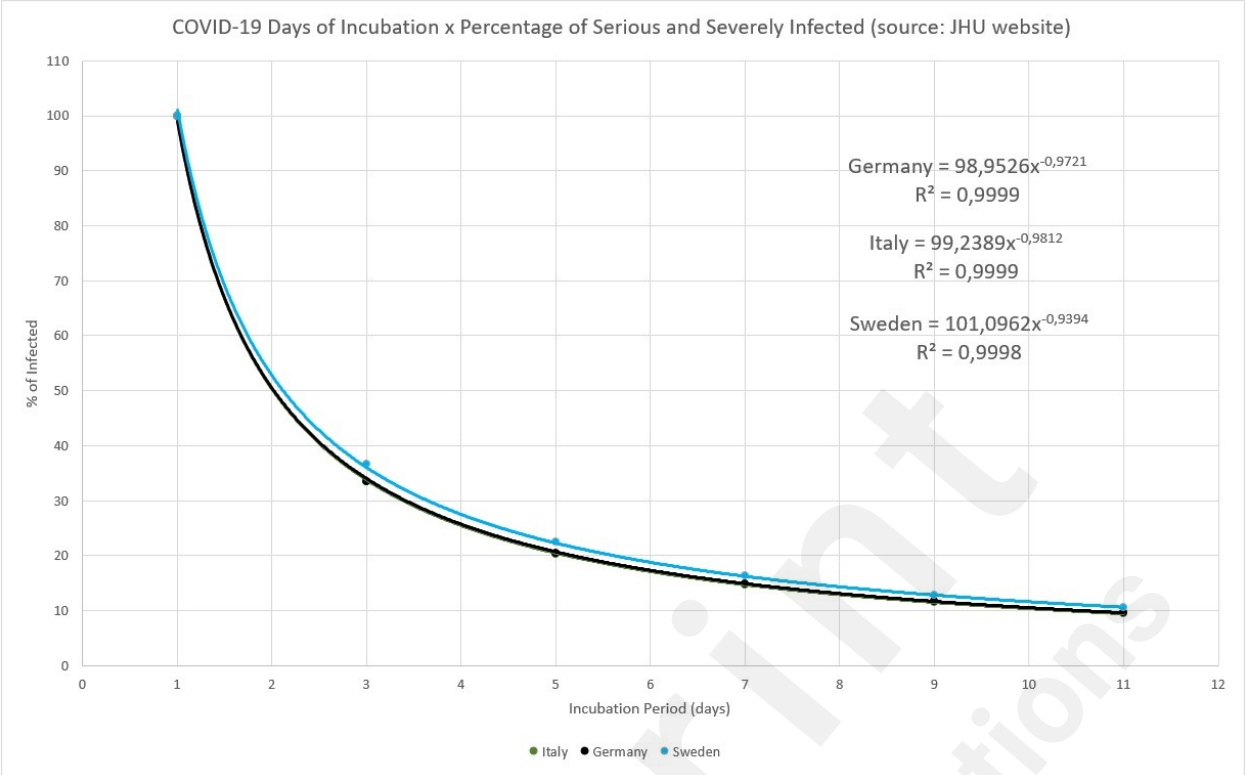

Figure 24 – COVID-19 Number of days of incubation versus percentage of serious and severe infected.

One conclusion is that, putting together formula (12) with the efficiency measurement in Figure 24, the reported rate of 80% of sub-notification [20], or 20% of people with more serious symptoms, represents 1/5 of the inventory of the infective persons. In other words, there is five times more persons in infective state than detected and reported by the MAMI figures, leading to a 5-day of incubation period. The next step is calculating the sub notification estimation, which then becomes straightforward: given the Incubation Period, how many times the registered amount should be multiplied to correctly express the estimated sub-notification? For example, for a 5-day incubation period in Germany, it is expected a sub-notification around 4 times the registered number of cases in any given day, if 100 were registered as infected, 400 were not. With this rationale it is possible to compare the sub notification factor with the incubation period for the three studied countries, as presented in Figure 25.

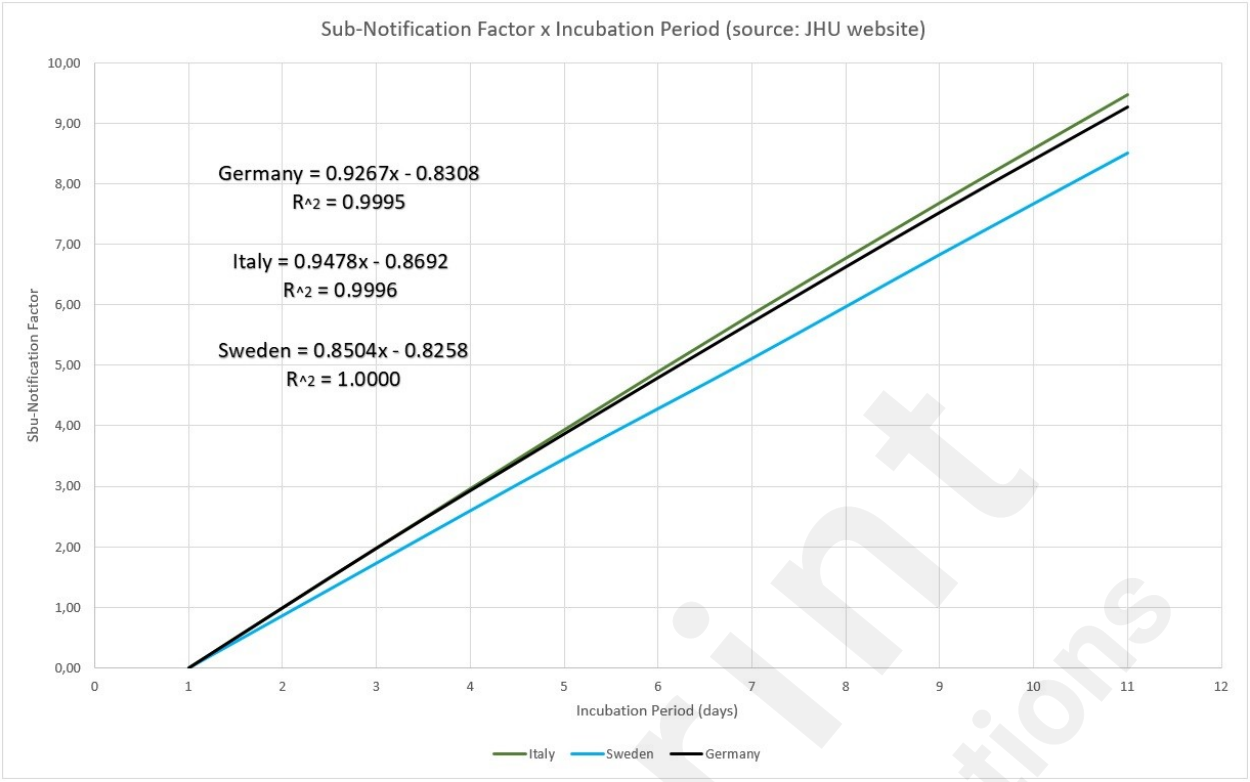

Figure 25 – Sub-notification factor for the studied countries.

General Findings

The early predictions on the progress of the local epidemic cycles of COVID-19 based on Gaussian distribution models and their derivatives, such as the Beta distribution, failed to obtain values close to reality, sometimes being very pessimistic, other too optimistic. Also, the nature of the data available for studies requires preliminary numerical treatment, since most of them present the number of daily deaths that occurred on the dates on which they were recorded by the health system and not on those that the deaths actually occurred. Moreover, countries with vast territories and populations should not be treated as a single case, but should be studied regionally, so that the evolution of the disease cycles can be clearly understood.

Through the observation of some early cycles, where a peak had already been reached, associated with a consistent reduction in the number of infections, it was possible to identify a triangular shape in these distributions. With the information on the approximate behavior of the variable in question (Reproduction Number) and the identification of a minimum and maximum, the use of the Triangular Distribution became clear. After applying this distribution over several local cycles, it was possible to identify similarities between pairs of cycles of localities and regions apparently without direct demographic correlation. Normalization allows you to use an already completed cycle to estimate the behavior of a cycle that is still evolving. The method using the similarity of cycles was able to estimate the end of the cycle up to 34 days before the end of the cycle, but requires that there exists a similar cycle. These similarities were confirmed by Kolmogorov-Smirnov tests applied to the data series (Appendix 1), demonstrating the hypothesis that the triangular distribution applies to these comparisons and, therefore, is applicable to the prediction of the dimensionless behavior of these cycles. Also, understanding the basic behavior of the local epidemic cycles also allowed to demonstrate the impact of sub-notification on calculations.

It is important to note that starting dates influence all the parameters that govern every statistical models used for characterizing the infection. The Logistic Model together with the

model based on the concept of inventory of infected persons can be used to obtain three parameters of the epidemic cycle: the number of total infected, the daily infection rate and the lag phase, which determined the actual probable onset of the epidemic for the studied countries – solving the problem of noise generation in other parameters by wrongly determined onset dates.

Hence, the experimental framework here proposed offers a set of simple and efficient methods for calculating not only the Reproduction Number, but also other variables that influence the epidemic cycles and supporting the decision-making process of health authorities, being an interesting tool especially for those places where mass testing is not available. Currently, when the occurrence of a "second wave" of infection by Sars-CoV-2 is identified, this framework is being applied again, in order to definitively demonstrate its efficacy and efficiency.

Bibliographic References

1. Pereira IG, Guerin JM, Silva Júnior AG, et al. Forecasting Covid-19 Dynamics in Brazil: A Data Driven Approach. Int J Environ Res Public Health. 2020;17(14):E5115. Published 2020 Jul 15. doi:10.3390/ijerph17145115

2. Musa SS, Zhao S, Wang MH, Habib AG, Mustapha UT, He D. Estimation of exponential growth rate and basic reproduction number of the coronavirus disease 2019 (COVID-19) in Africa. Infect Dis Poverty. 2020;9(1):96. Published 2020 Jul 16. doi:10.1186/s40249-020-00718-y

3. Hong HG, Li Y. Estimation of time-varying reproduction numbers underlying epidemiological processes: A new statistical tool for the COVID-19 pandemic. PLoS One. 2020;15(7):e0236464. doi:10.1371/journal.pone.0236464

4. Kogan NE, Clemente L, Liautaud P, et al. An Early Warning Approach to Monitor COVID-19 Activity with Multiple Digital Traces in Near Real-Time. Preprint. ArXiv. 2020;arXiv:2007.00756v2. Published 2020 Jul 1.

5. Hao X, Cheng S, Wu D, Wu T, Lin X, Wang C. Reconstruction of the full transmission dynamics of COVID-19 in Wuhan [published online ahead of print, 2020 Jul 16]. Nature. 2020;10.1038/s41586-020-2554-8. doi:10.1038/s41586-020-2554-8

6. Ogden NH, Fazil A, Arino J, et al. Modelling scenarios of the epidemic of COVID-19 in Canada. Can Commun Dis Rep. 2020;46(8):198-204. Published 2020 Jun 4. doi:10.14745/ccdr.v46i06a08

7. Fawad M, Mubarik S, Malik SS, Hao Y, Yu C, Ren J. Trend Dynamics of Severe Acute Respiratory Syndrome Coronavirus 2 (SARS-CoV-2) Transmission in 16 Cities of Hubei Province, China. Clin Epidemiol. 2020;12:699-709. Published 2020 Jul 2. doi:10.2147/CLEP.S254806

8. Zuo M, Khosa SK, Ahmad Z, Almaspoor Z. Comparison of COVID-19 Pandemic Dynamics in Asian Countries with Statistical Modeling. Comput Math Methods Med. 2020;2020:4296806. Published 2020 Jun 28. doi:10.1155/2020/4296806

9. Lin YF, Duan Q, Zhou Y, et al. Spread and Impact of COVID-19 in China: A Systematic Review and Synthesis of Predictions From Transmission-Dynamic Models. Front Med (Lausanne). 2020;7:321. Published 2020 Jun 18. doi:10.3389/fmed.2020.00321

10. Chaudhry RM, Hanif A, Chaudhary M, et al. Coronavirus Disease 2019 (COVID-19): Forecast of an Emerging Urgency in Pakistan. Cureus. 2020;12(5):e8346. Published 2020 May 28. doi:10.7759/cureus.8346

11. Park SW, Bolker BM, Champredon D, Earn DJD, Li M, Weitz JS, Grenfell BT, Dushoff J. 2020 Reconciling early-outbreak estimates of the basic reproductive number and its uncertainty: framework and applications to the novel coronavirus (SARS-CoV-2) outbreak. J. R. Soc. Interface 17: 20200144. http://dx.doi.org/10.1098/rsif.2020.0144

12. De Carvalho, EA, De Carvalho, RA. Identification of Patterns in Epidemic Cycles and Methods for Estimating Their Duration: COVID-19 Case Study. *MedRxiv* (2020). Published 2020 Jul 15. doi: https://doi.org/10.1101/2020.07.13.20153080

13. De Carvalho, E. A. De Carvalho, R. A. COVID-19: Time-Dependent Effective Reproduction Number and Sub-notification Effect Estimation Modeling. *MedRxiv* (2020). Published 2020 Jul 28. doi: https://doi.org/10.1101/2020.07.28.20164087

14. De Carvalho, R. A. De Carvalho, E. A. COVID-19: Estimation of the Actual Onset of Local Epidemic Cycles, Determination of Total Number of Infective, and Duration of the Incubation Period. *MedRxiv* (2020). Published 2020 Ago 23. doi: https://doi.org/10.1101/2020.08.23.20180356

15. Kotz, S. and J. Rene van Dorp (2004). “Beyond Beta - Other Continuous Families of Distributions with Bounded Support and Applications”. World Scientific Publishing Company, Singapore (2004).

16. Hilbe, J. M. Logistic Regression Models. Chapman & Hall/CRC Texts in Statistical Science, 1st Edition, 2017.

17. Bizzarri M, Di Traglia M, Giuliani A, Vestri A, Fedeli V, Prestininzi A. New statistical RI index allow to better track the dynamics of COVID-19 outbreak in Italy. Sci Rep. 2020 Dec 22;10(1):22365. doi: 10.1038/s41598-020-79039-x.

18. Gude-Sampedro F, Fernández-Merino C, Ferreiro L, Lado-Baleato Ó, Espasandín-Domínguez J, Hervada X, Cadarso CM, Valdés L. Development and validation of a prognostic model based on comorbidities to predict Covid-19 severity. A population-based study. Int J Epidemiol. 2020 Dec 8. doi: 10.1093/ije/dyaa209.

19. Nate Silver: https://projects.fivethirtyeight.com/2020-nba-player-projections/ accessed in 09/jul/2020.

20. World Health Organization (WHO). Similarities and Differences Between COVID-19 and Influenza. https://www.who.int/emergencies/diseases/novel-coronavirus-2019/question-and-answers-hub/q-a-detail/q-a-similarities-and-differences-covid-19-and-influenza . Accessed on 23th of July, 2020.

Supplementary Files

Figures

A6 – MoH (black) x TP website (red) data comparison after MAMI.

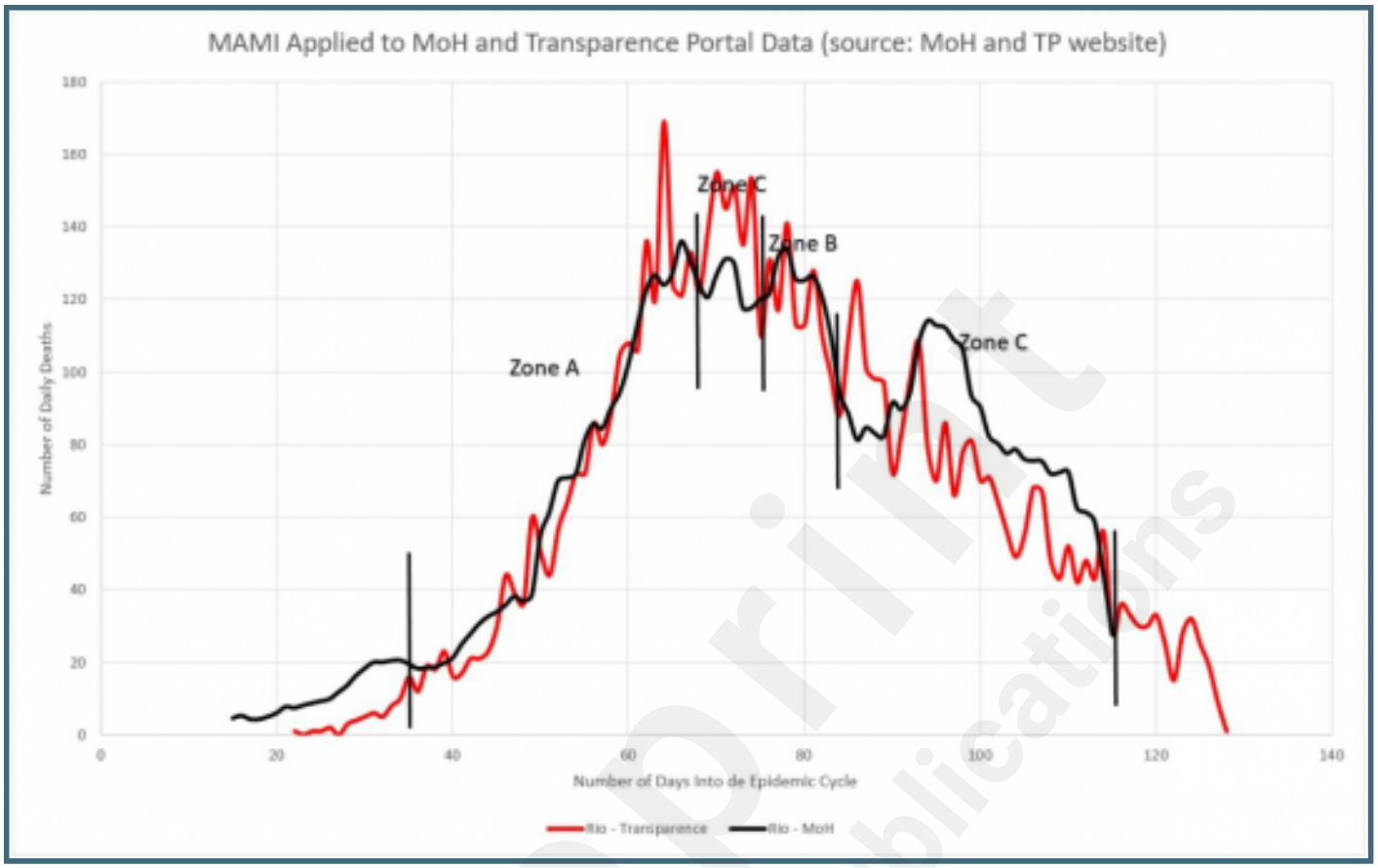

A5 – The Rio de Janeiro's cycle, "closed" by the time the analysis was done.

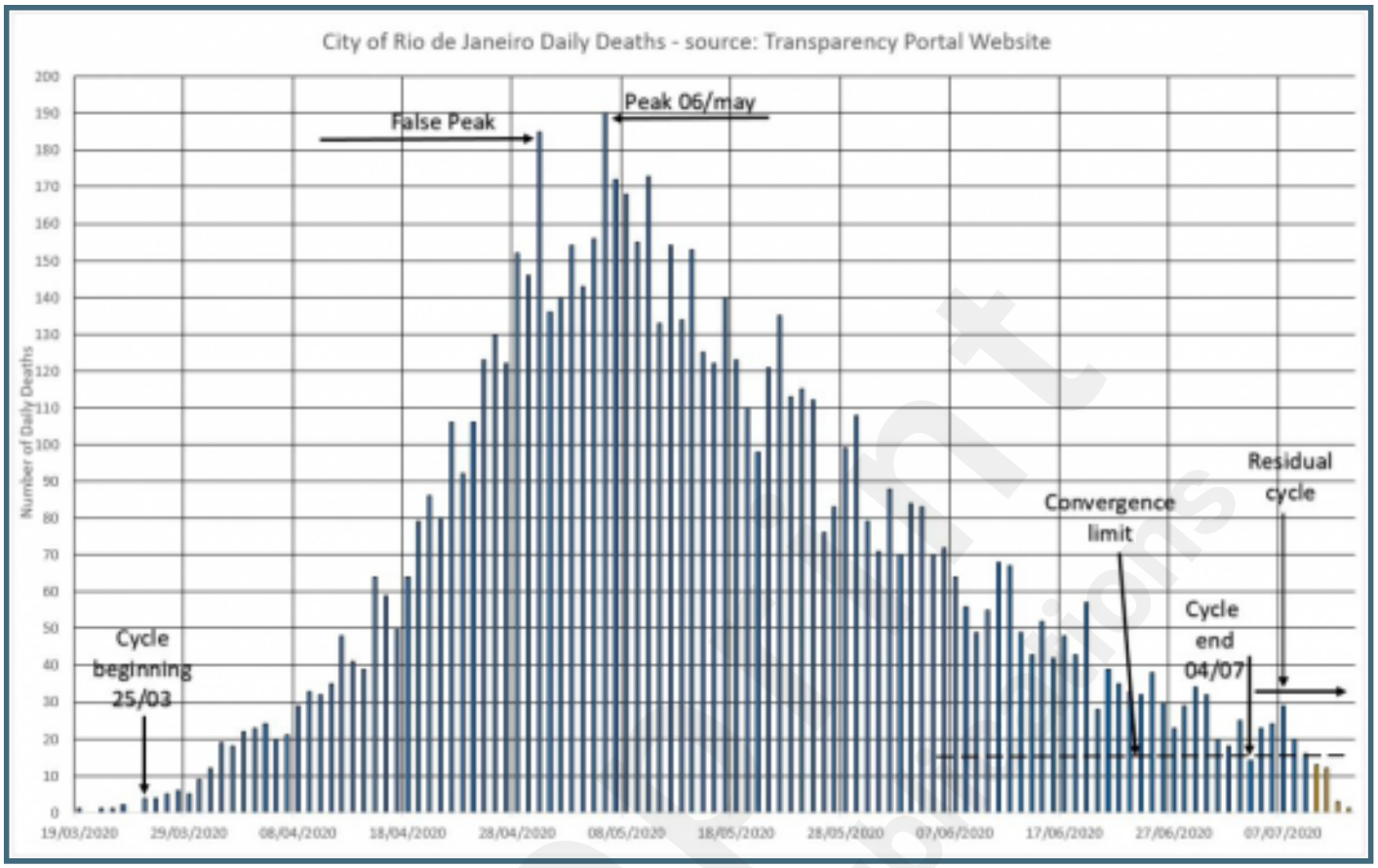

A4 – Data extrapolation for end of cycle estimation using data collected in July the 5th, 2020.

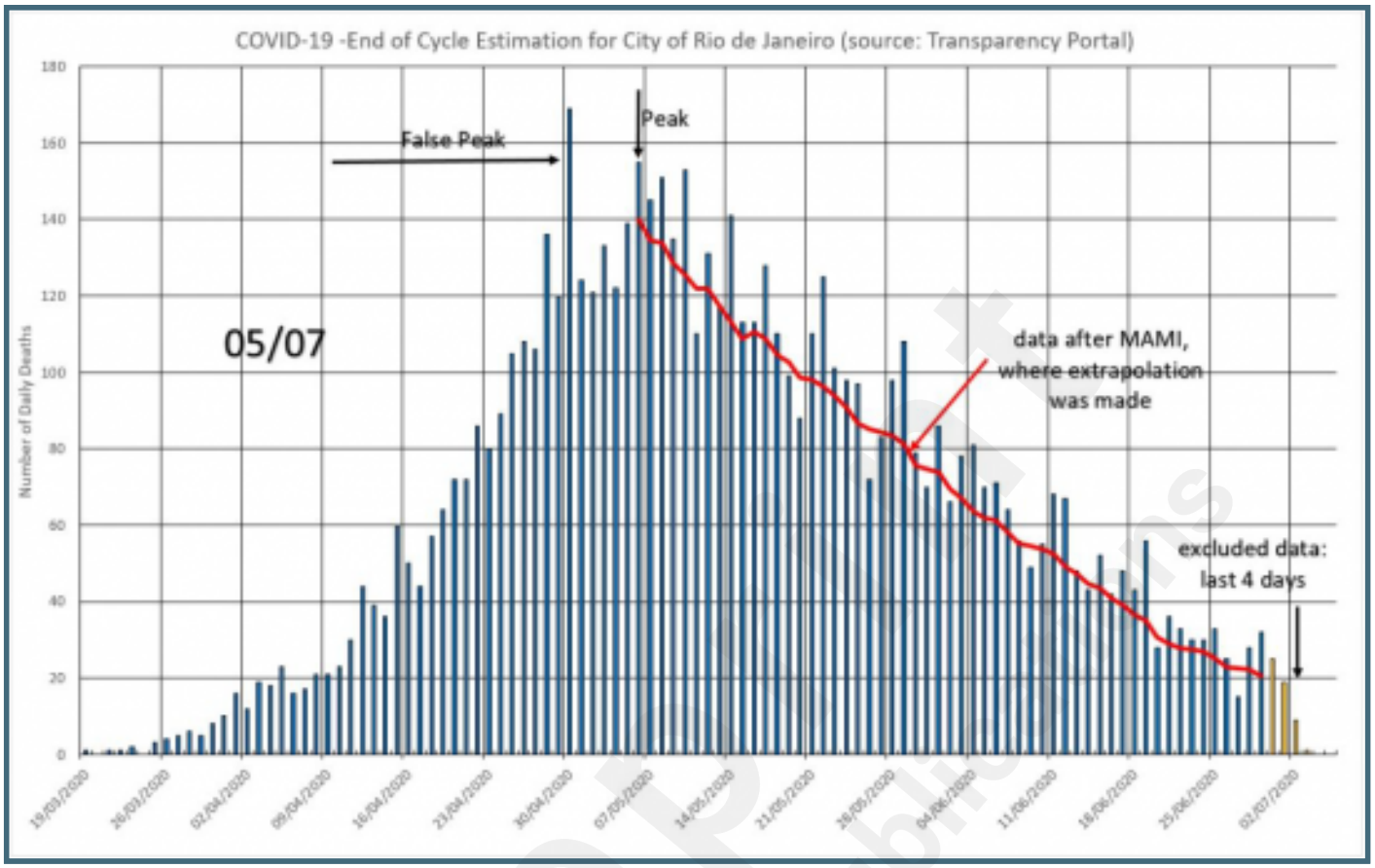

A3 – Several evaluations for the end of the cycle comparing the city of Rio de Janeiro and Italy.

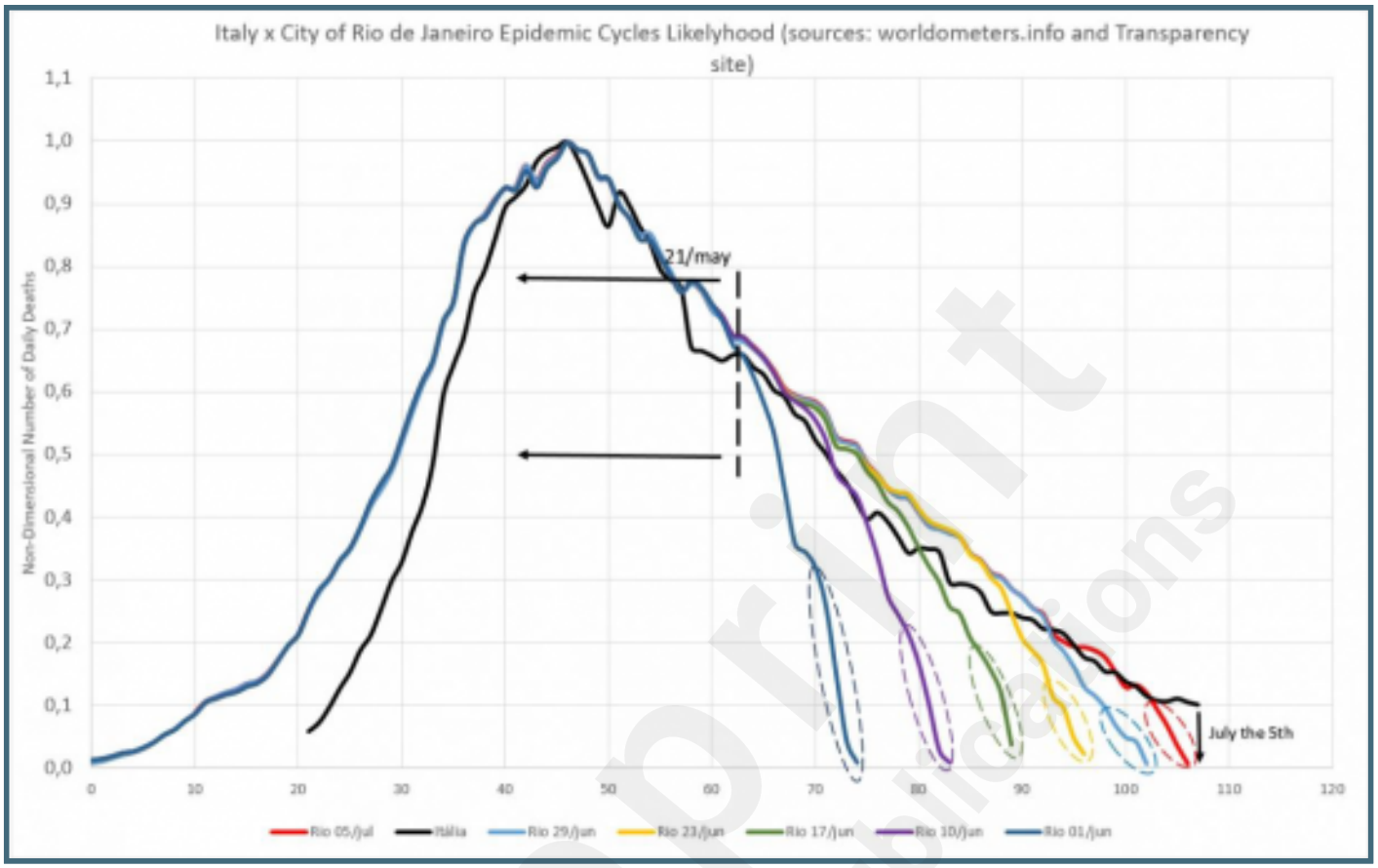

A2 - Daily death figures data for Brazil, in three days.

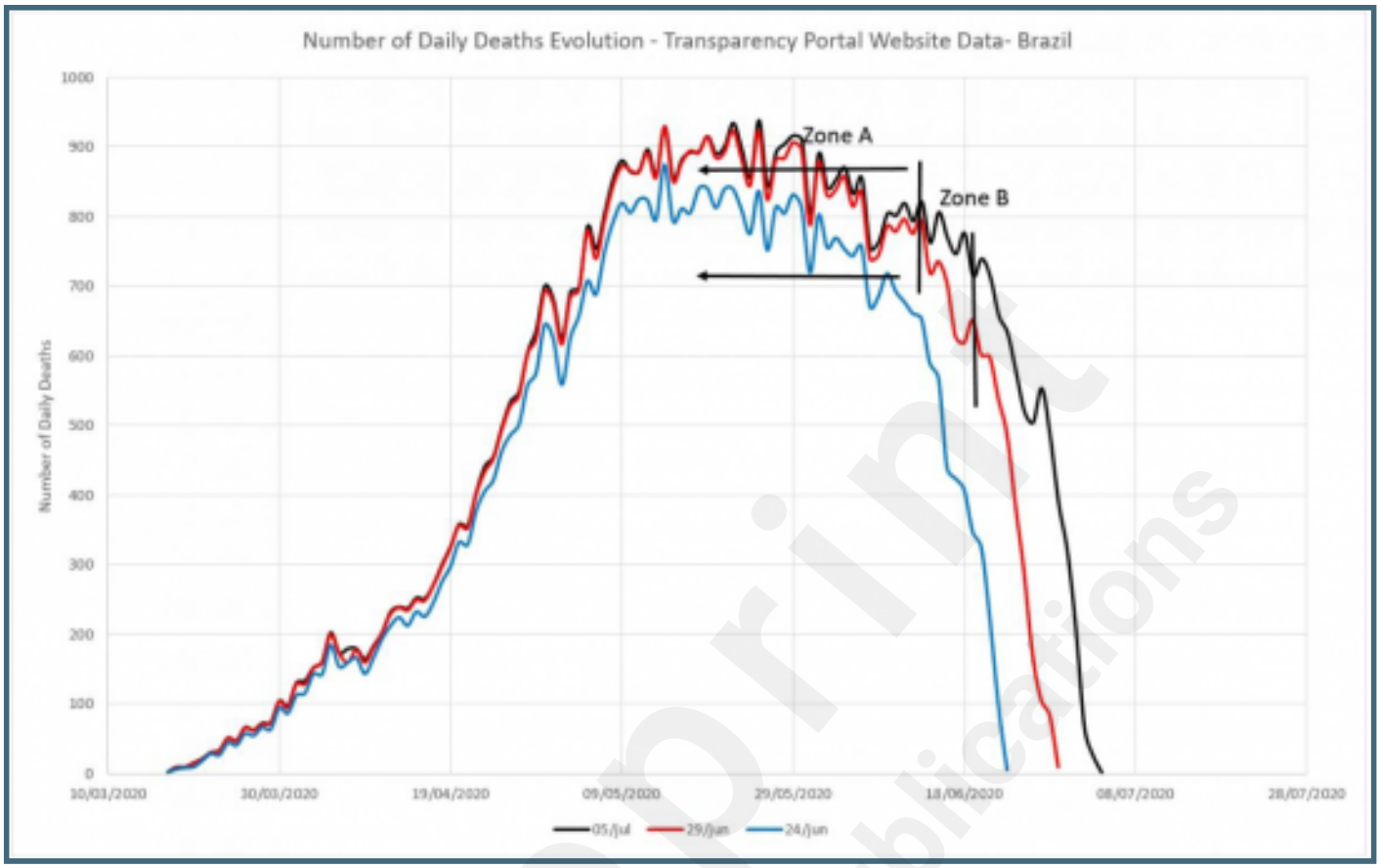

A1 – Daily death figures data for the City of Rio de Janeiro, in three days.

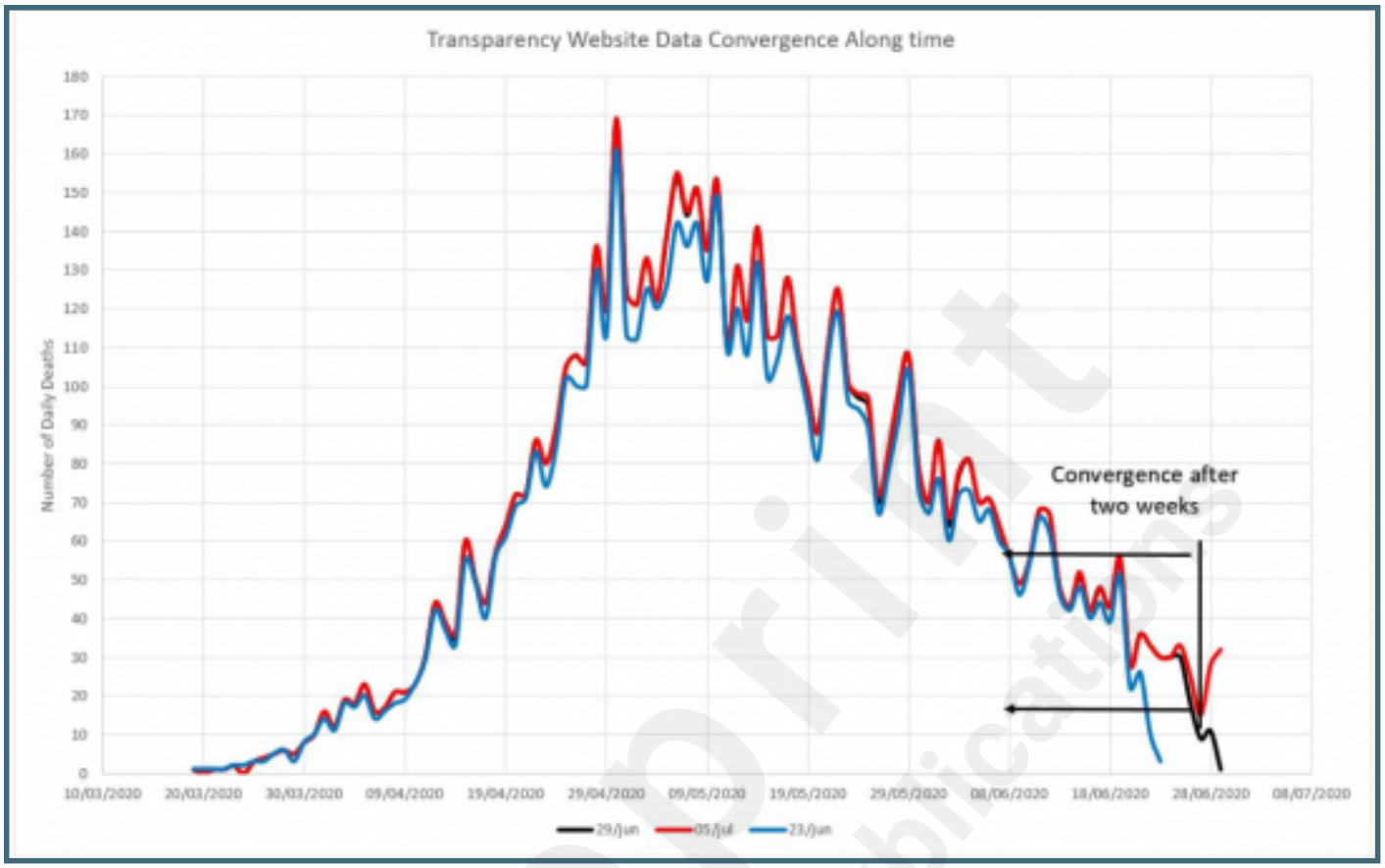

Sub notification effect over Reproduction Number in Italy, during the critical epidemic cycle.

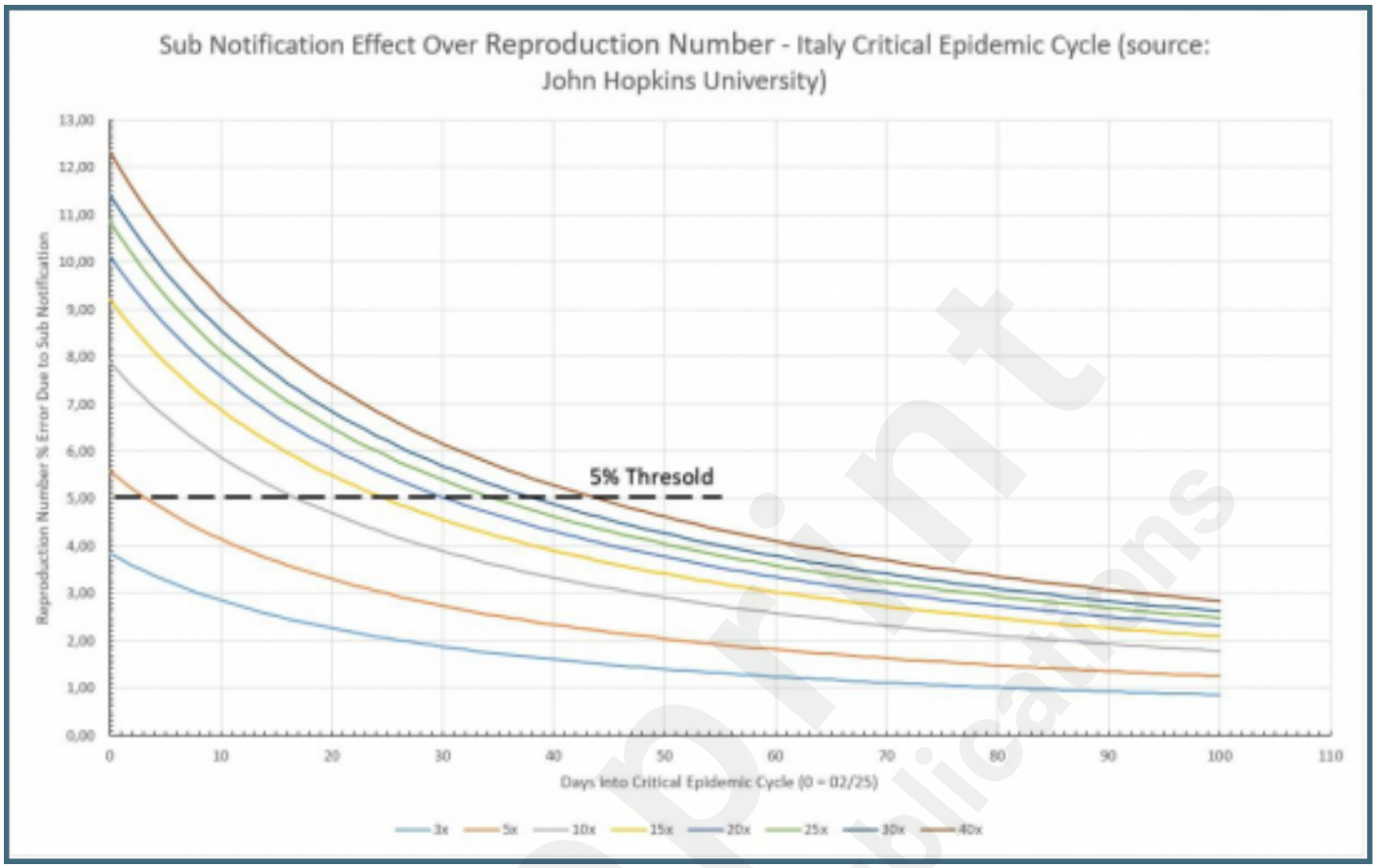

COVID-19 Number of days of incubation versus percentage of serious and severe infected.

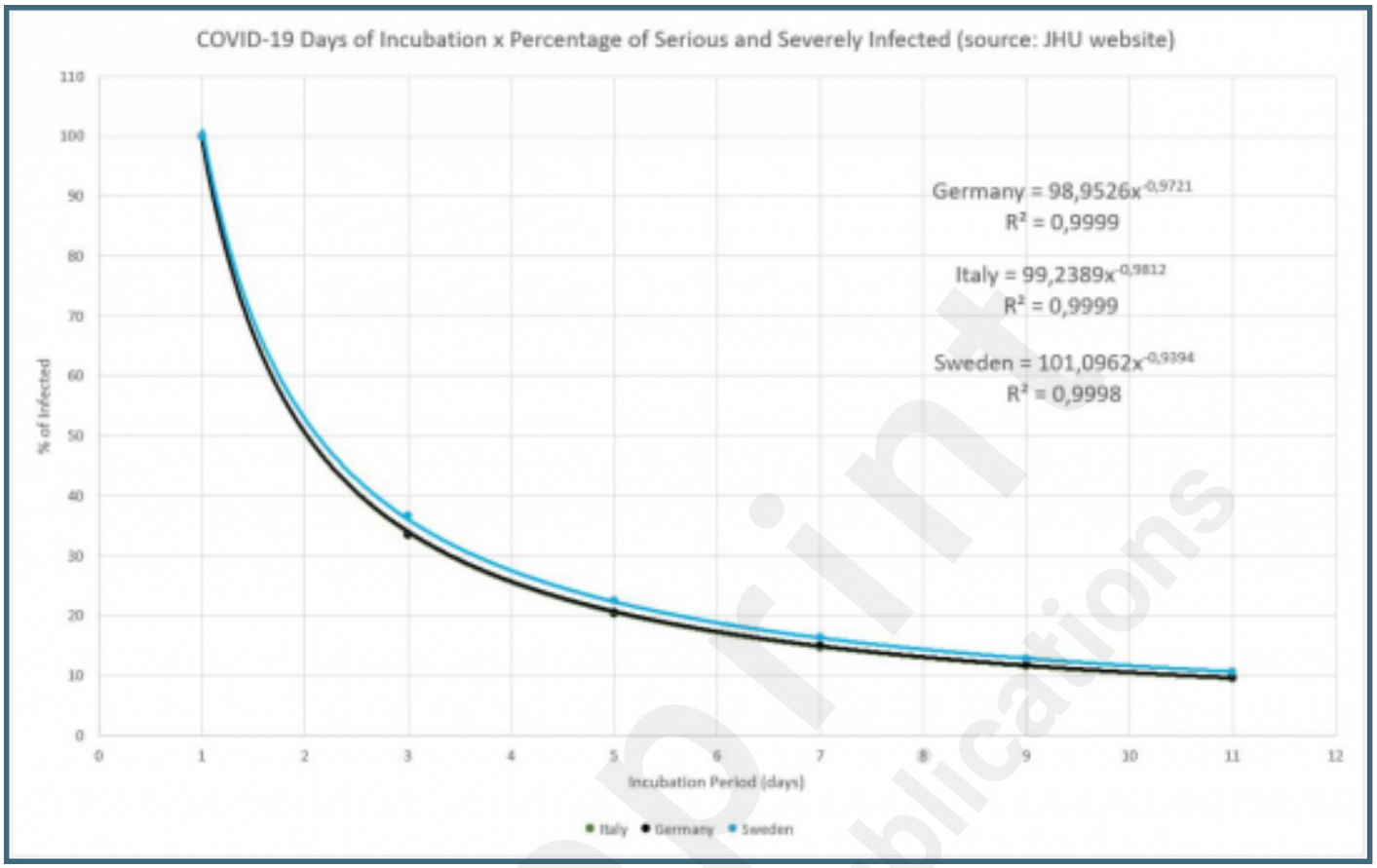

Non-dimensional critical epidemic cycle for Germany, Sweden, UK and Italy.

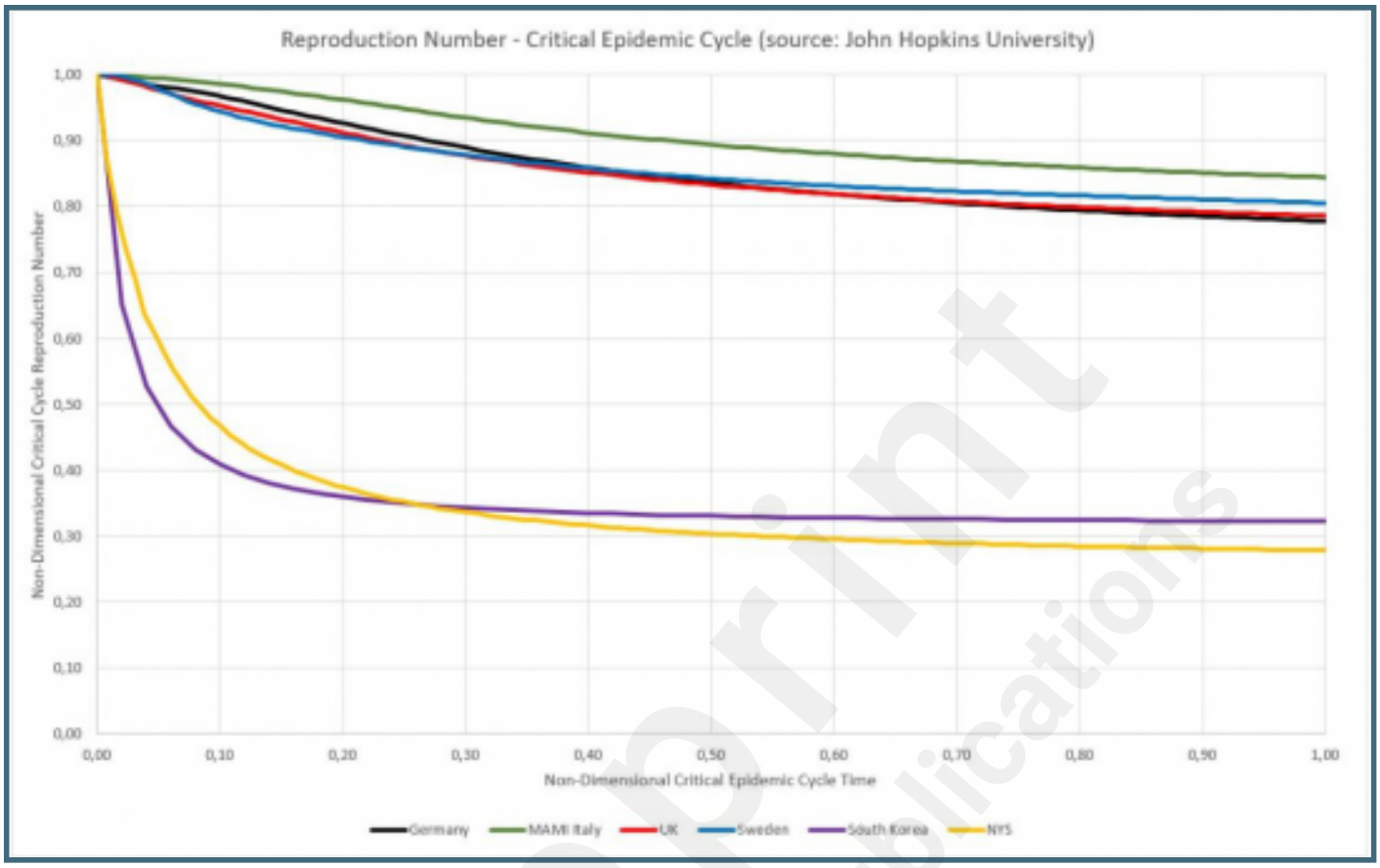

Sweden: Infected Persons Inventories for 3, 5, 7, 9, and 11 days of incubation, compared to MAMI.

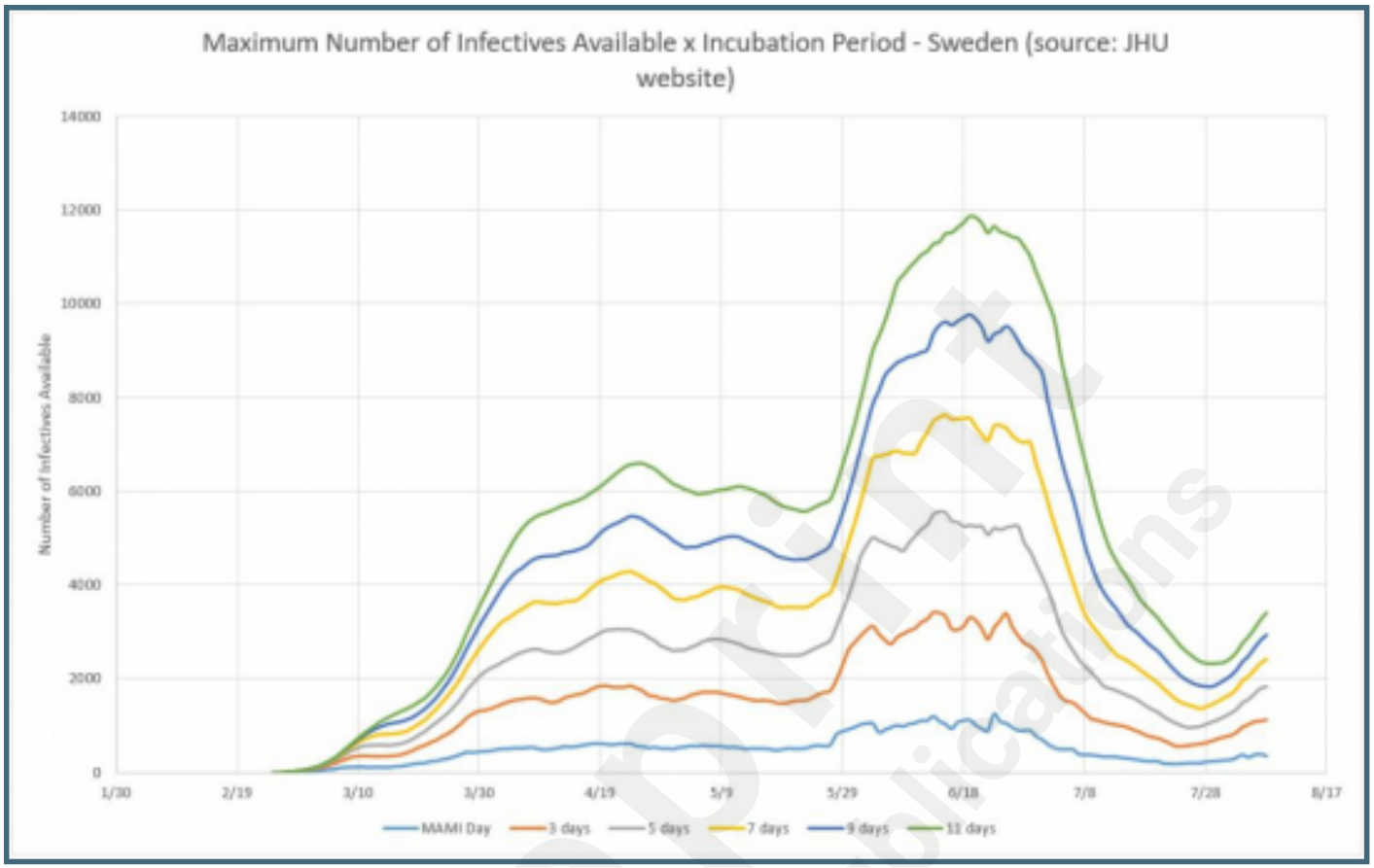

Sweden – total number of infected (MAMI) compared to Richard Growth Model prediction.

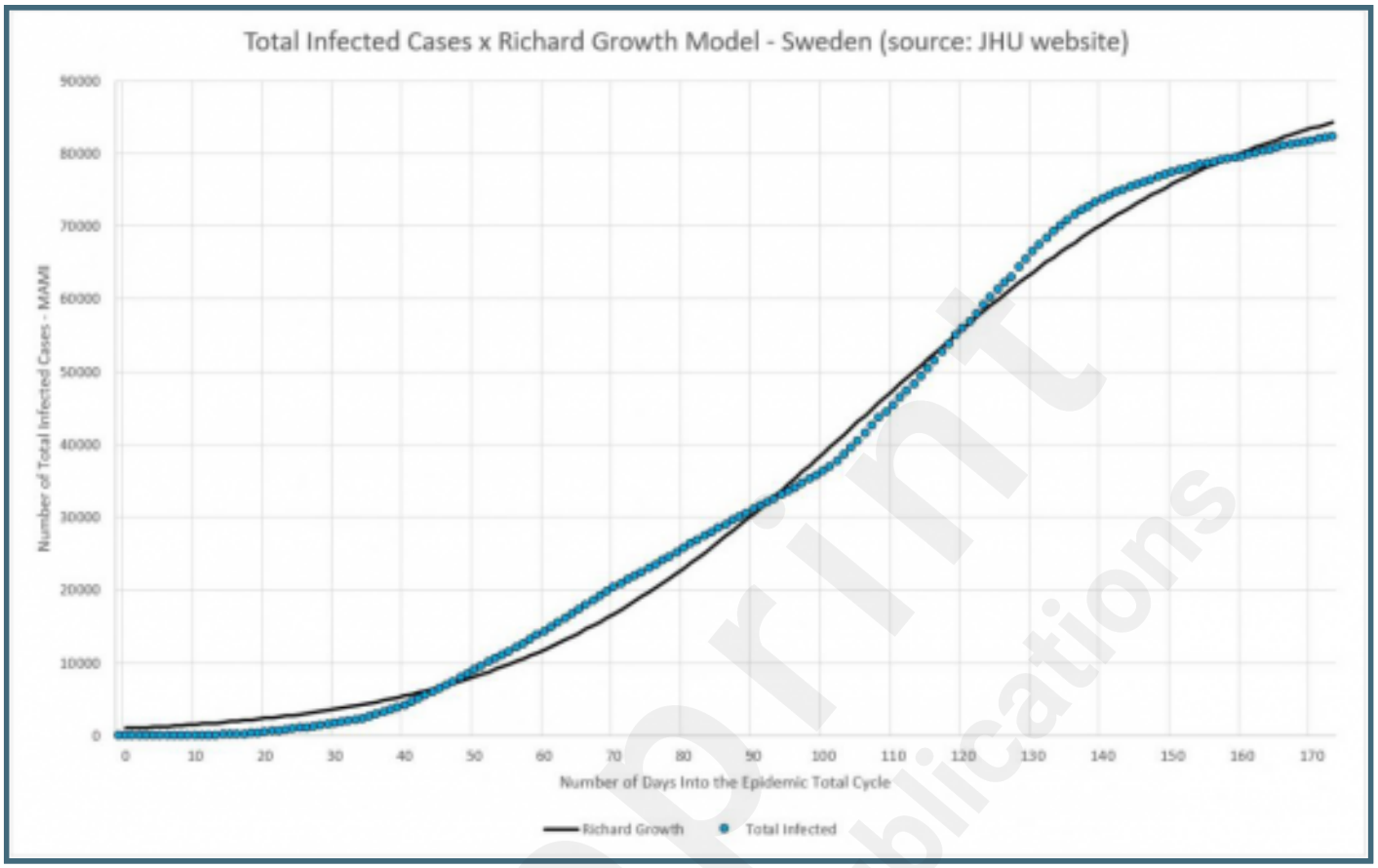

Sub notification effect over Reproduction Number in Sweden, during the critical epidemic cycle.

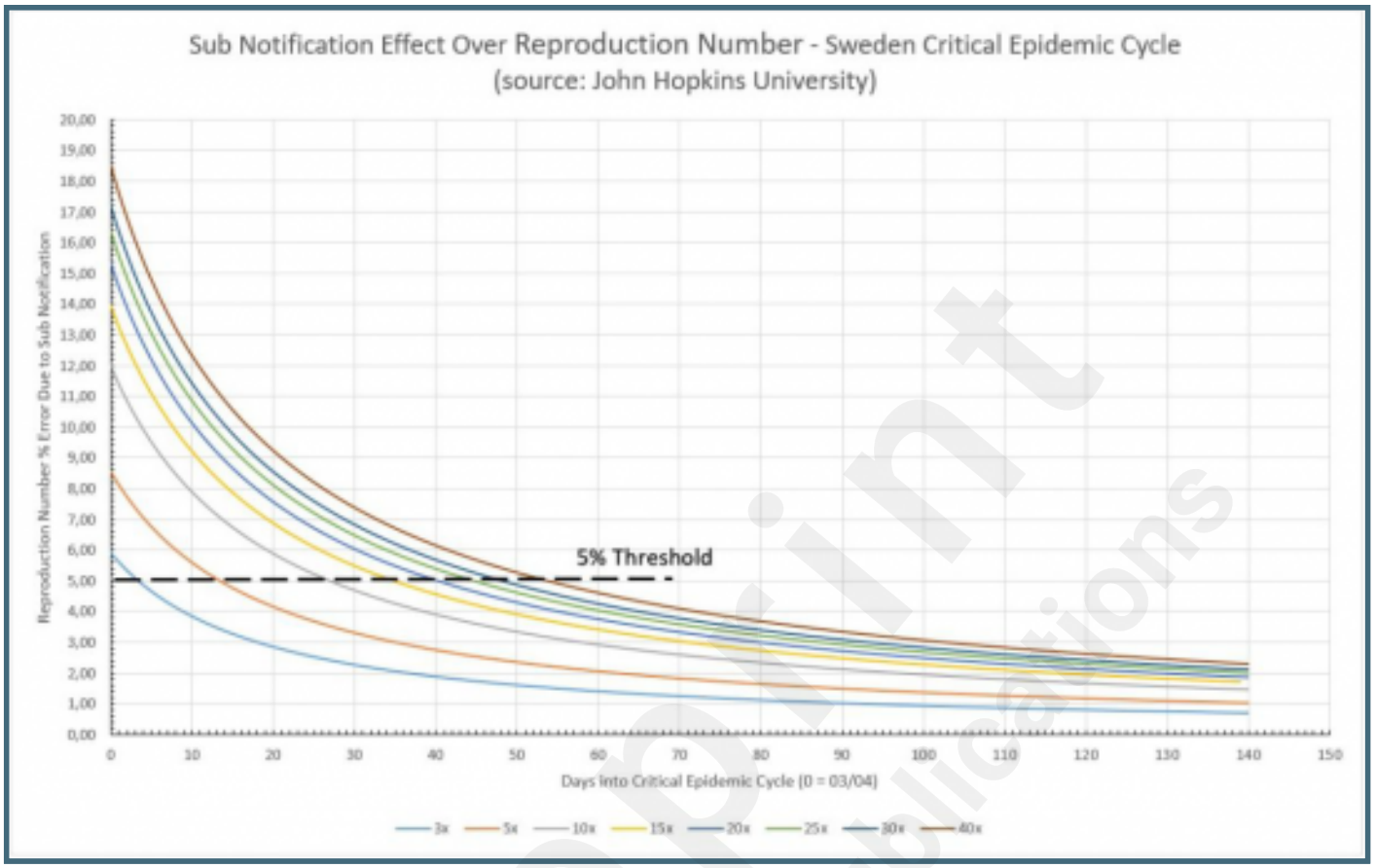

Epidemic cycle in Sweden, using the number of infected people daily.

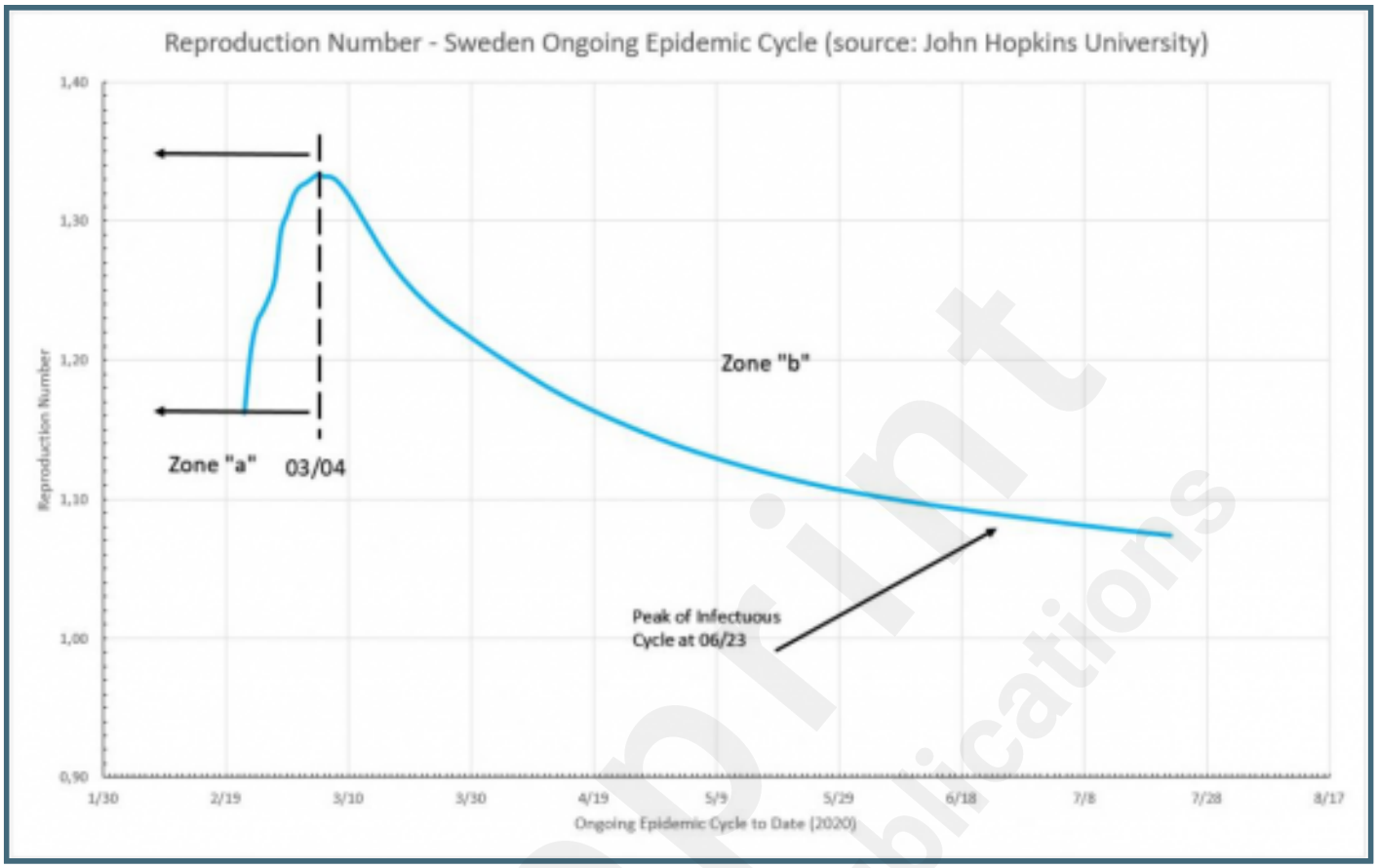

Italy: Infected Persons Inventories for 3, 5, 7, 9, and 11 days of incubation, compared to MAMI.

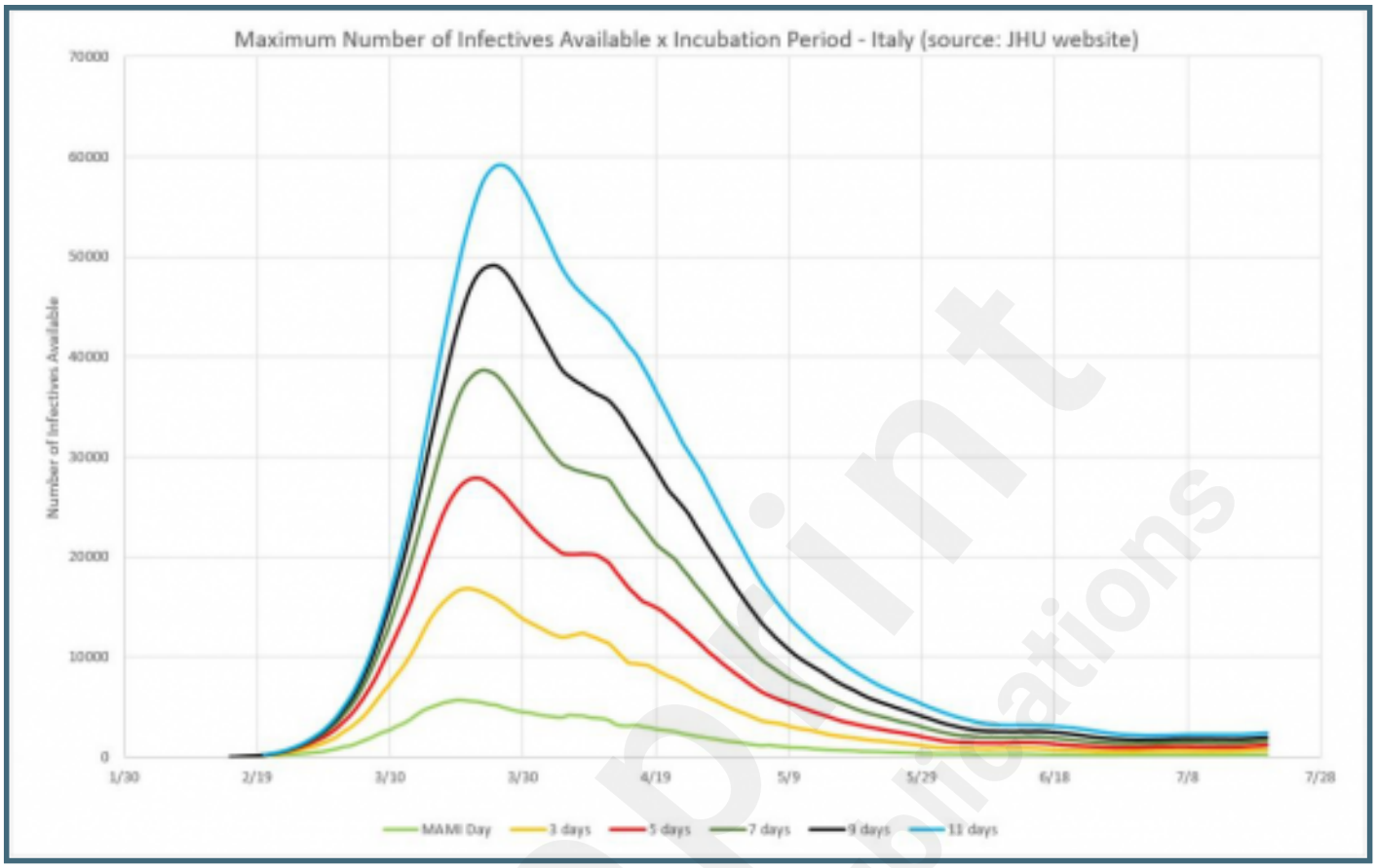

Sub-notification factor for the studied countries.

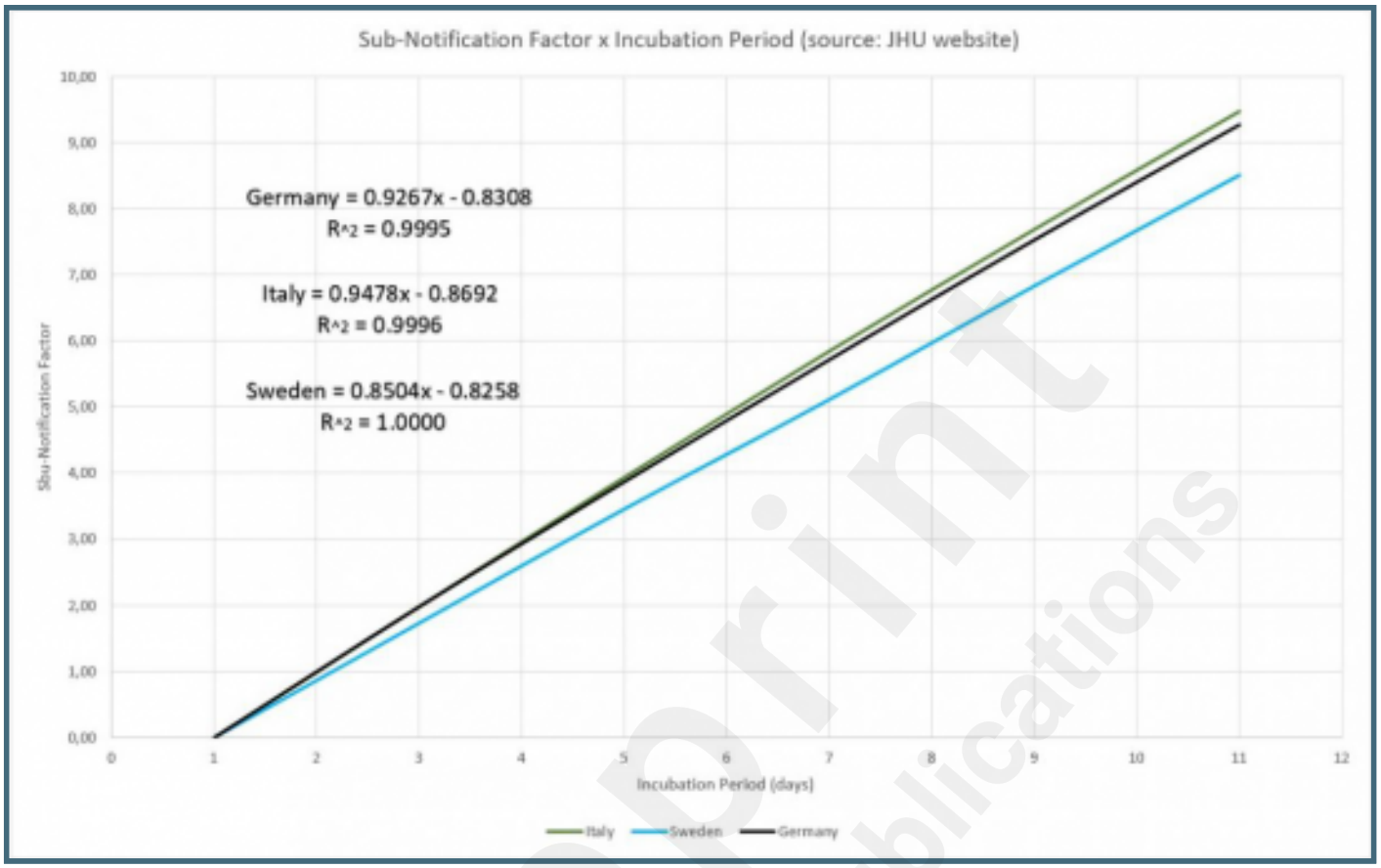

Italy – total number of infected (MAMI) compared to Richard Growth Model prediction.

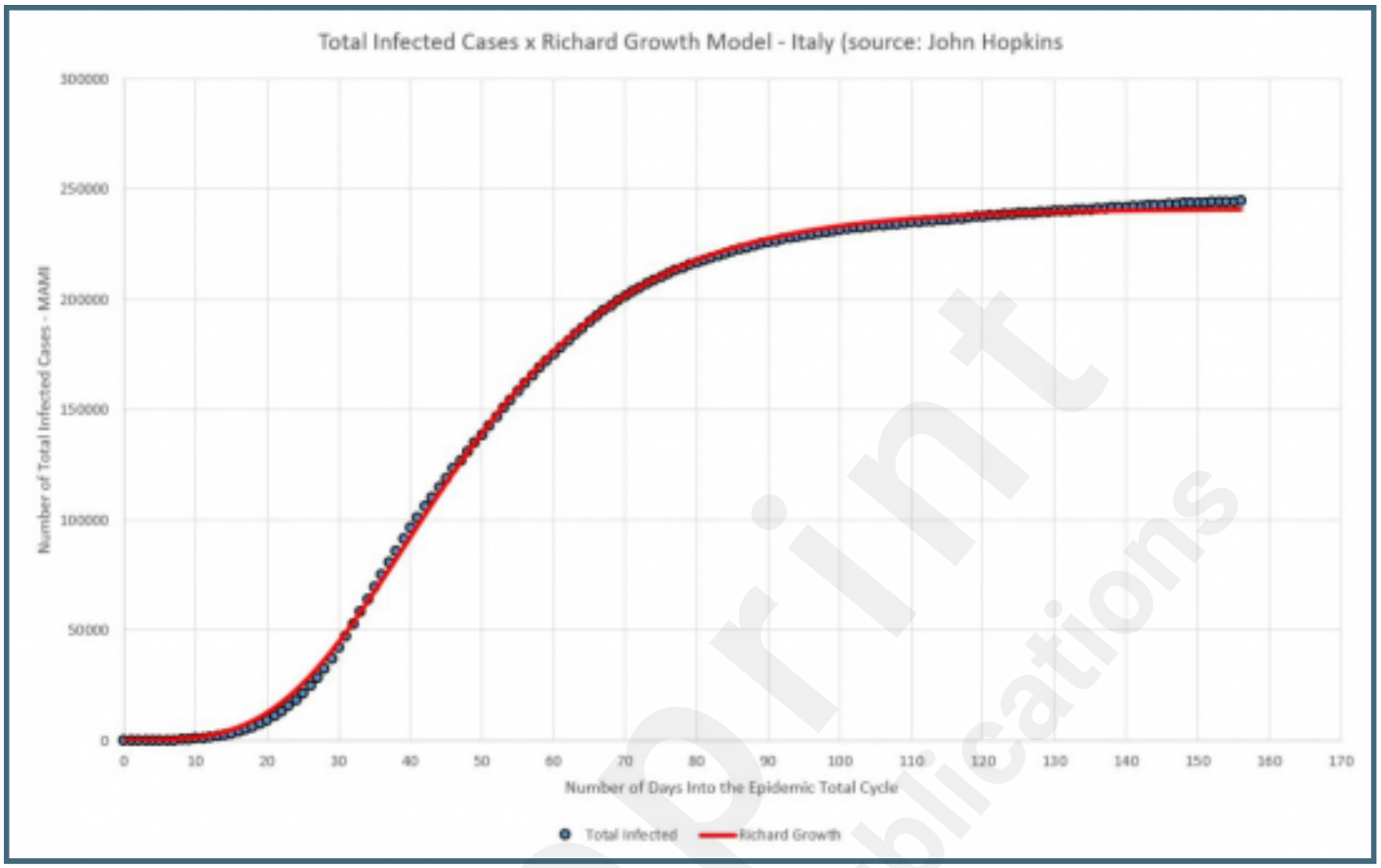

Total epidemic cycle in Italy, using the number of infected people daily.

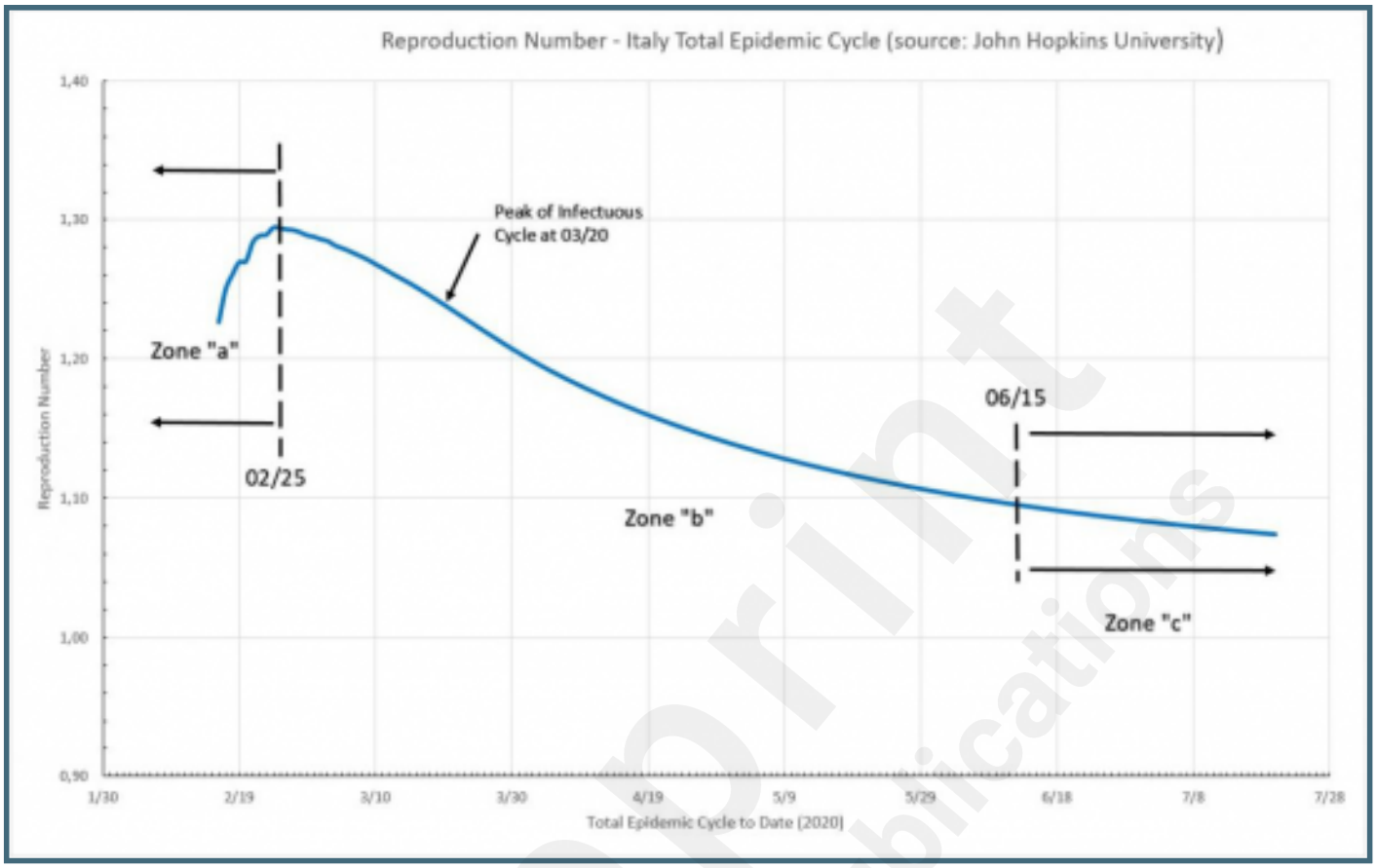

MAMI effect over Reproduction Numbers expressed for two different countries, South Korea and Italy. South Korea: the blue line is Rt obtained from MAMI applied to registered data, the red line is Rt determined for registered data. For Italy: the yellow line is Rt for registered data and the green line for MAMI applied to registered data.

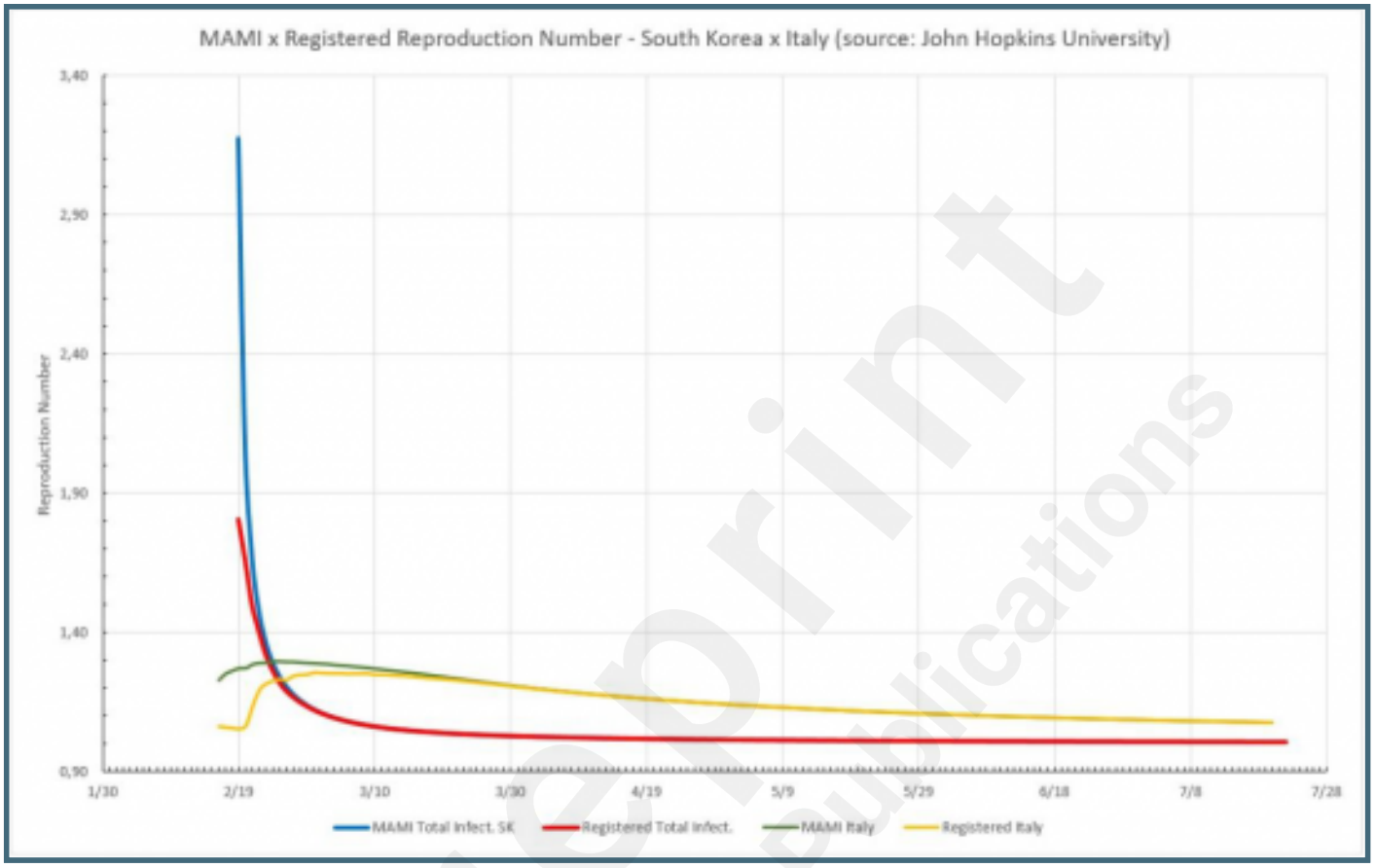

The Swedish Cycle.

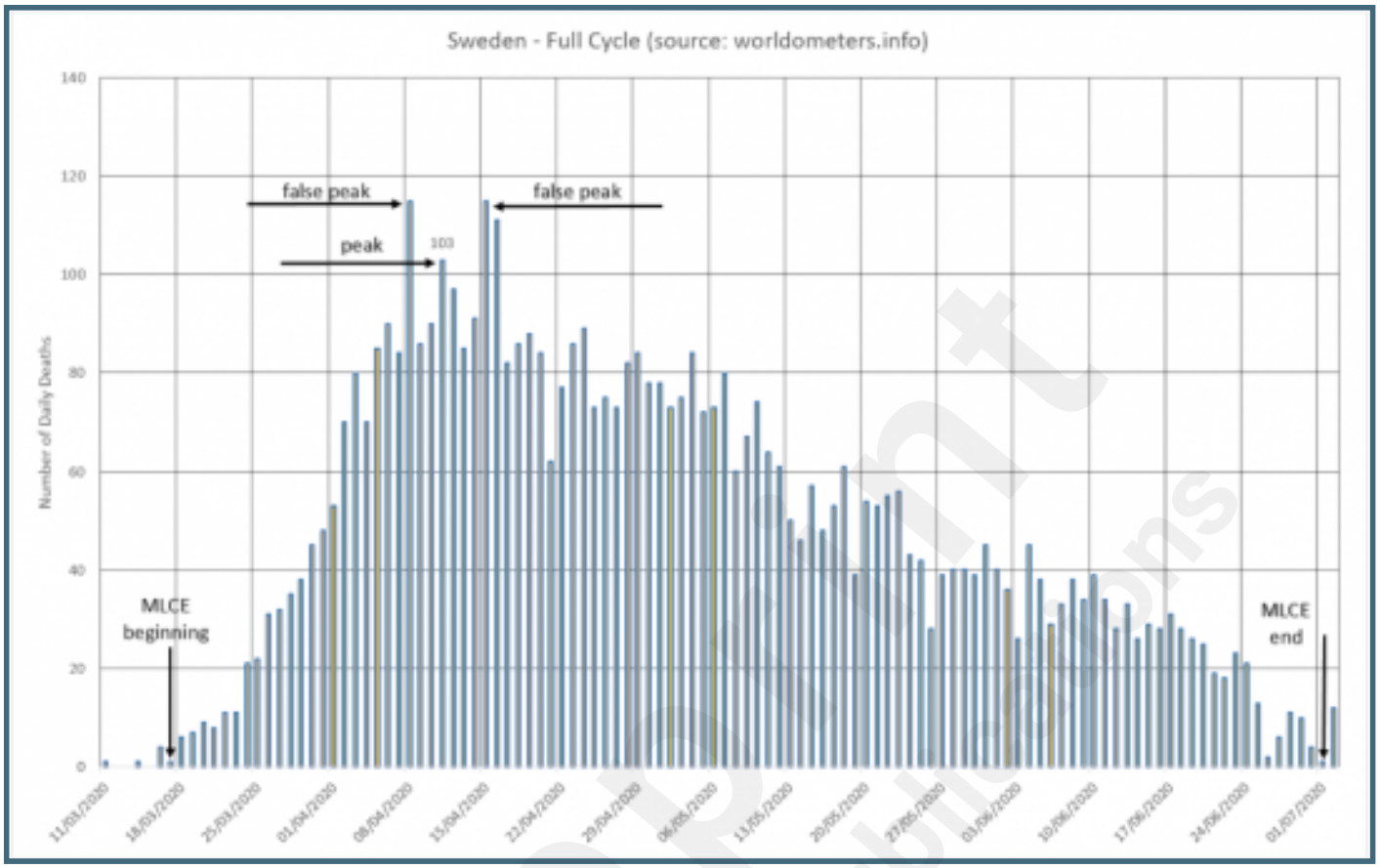

COVID-19 lethal cycles generic shape.

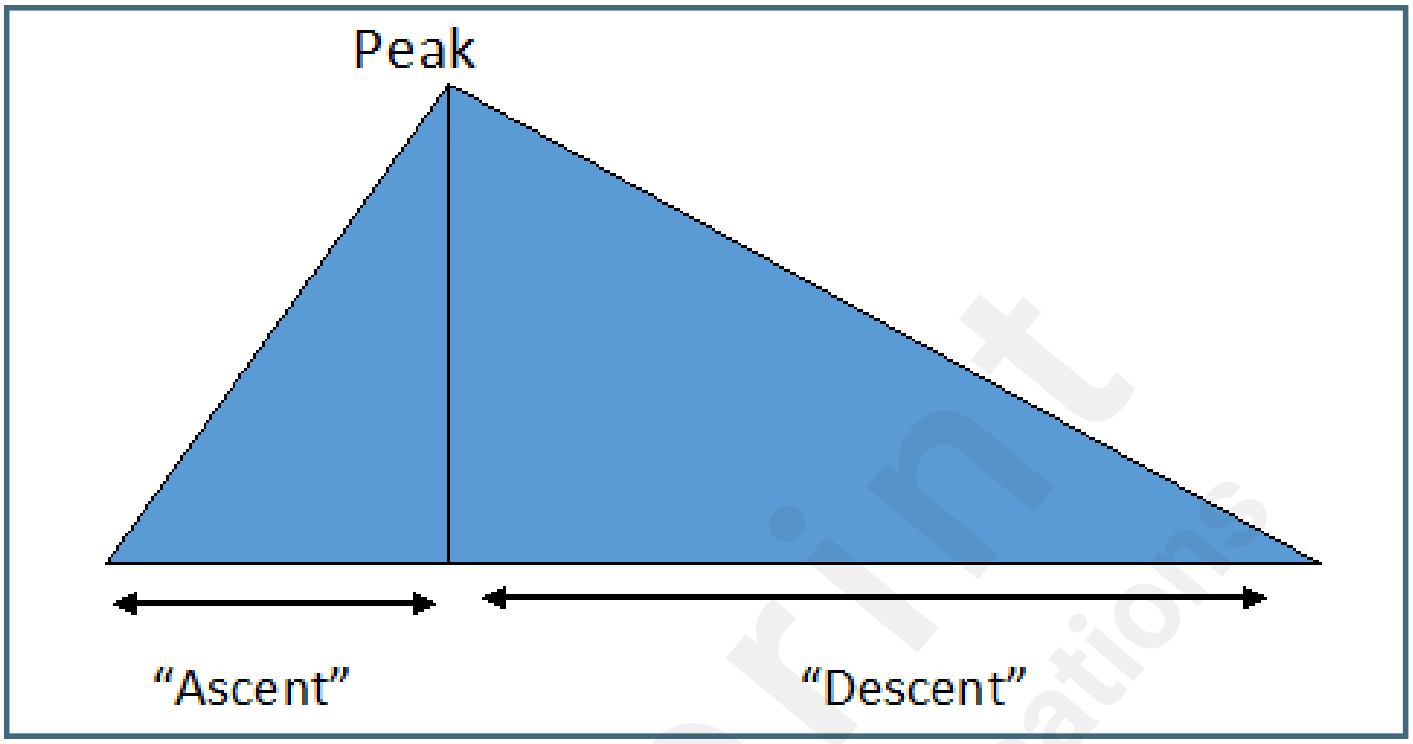

Sweden’s and USA’s epidemic cycles compared.

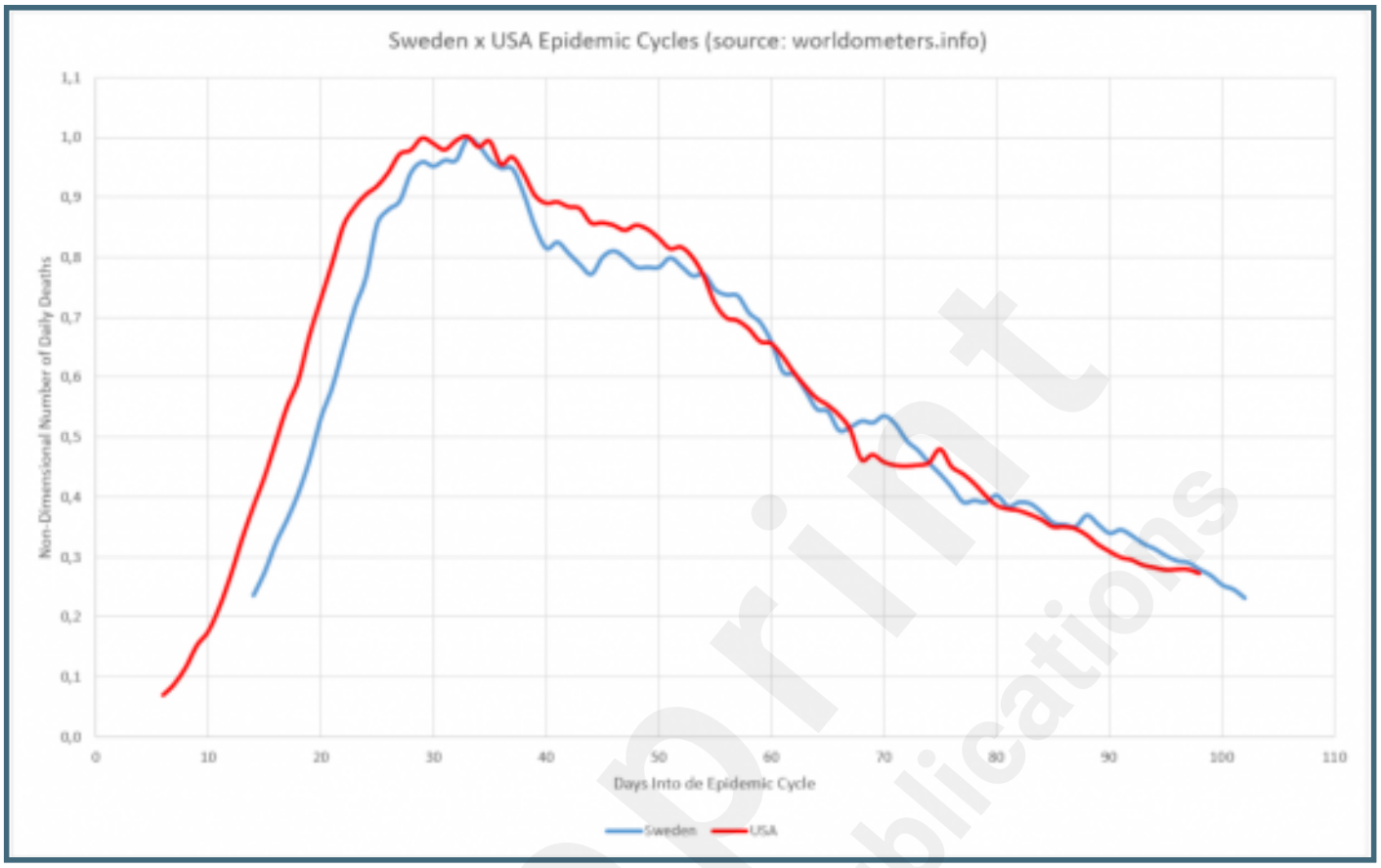

The German cycle.

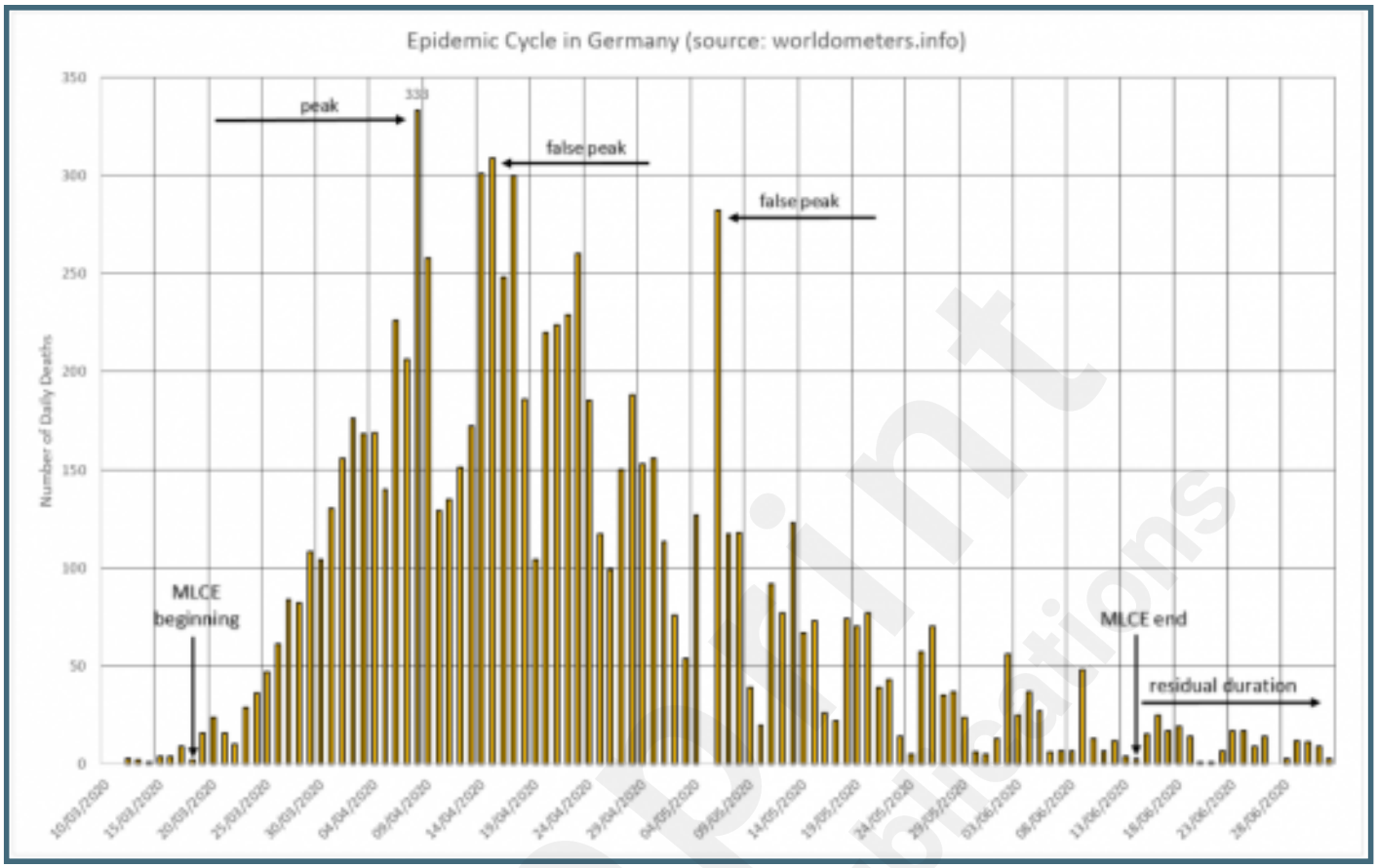

The Italian cycle.

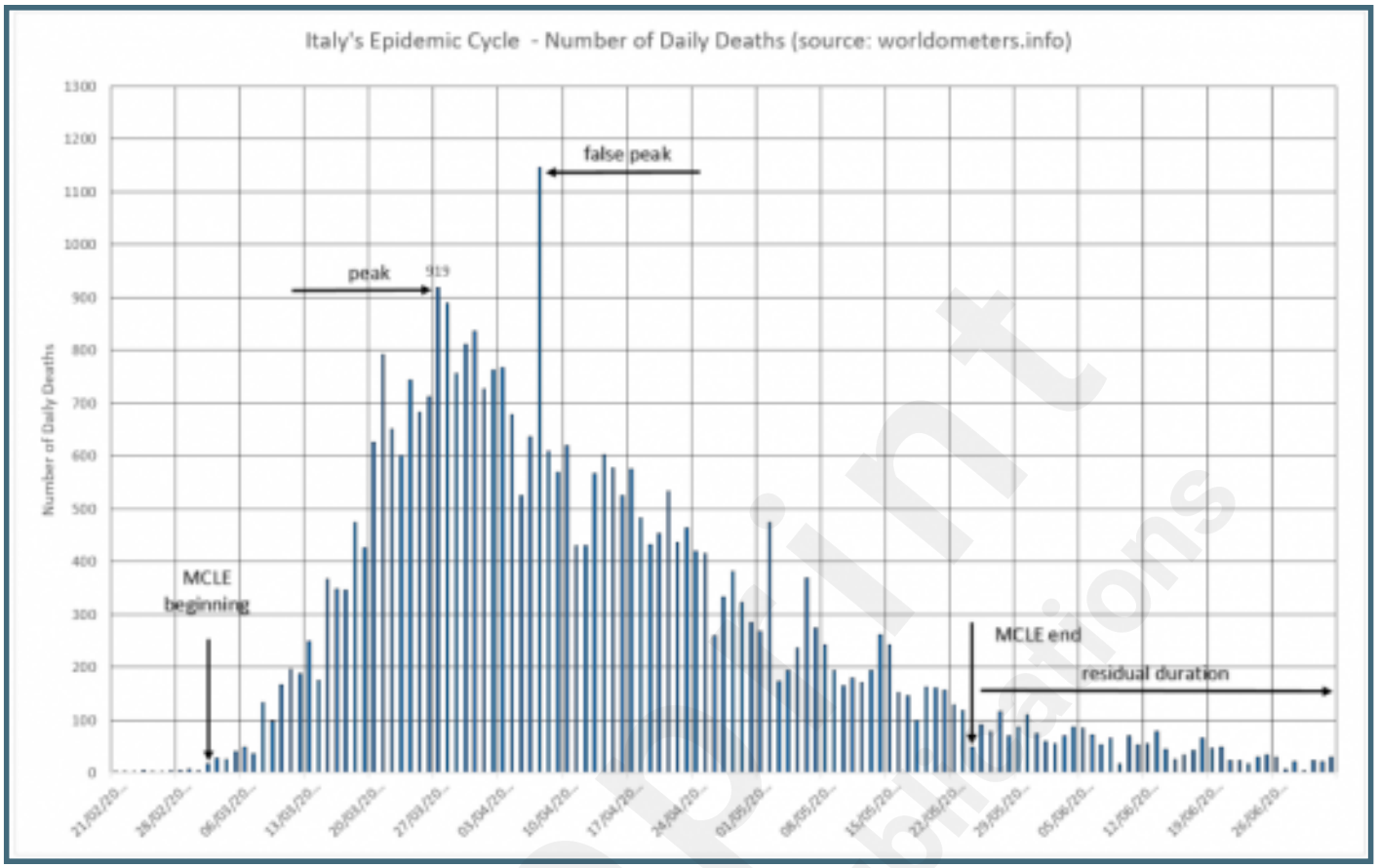

Germany: Infected Persons Inventories for 3, 5, 7, 9, and 11 days of incubation, compared to MAMI.

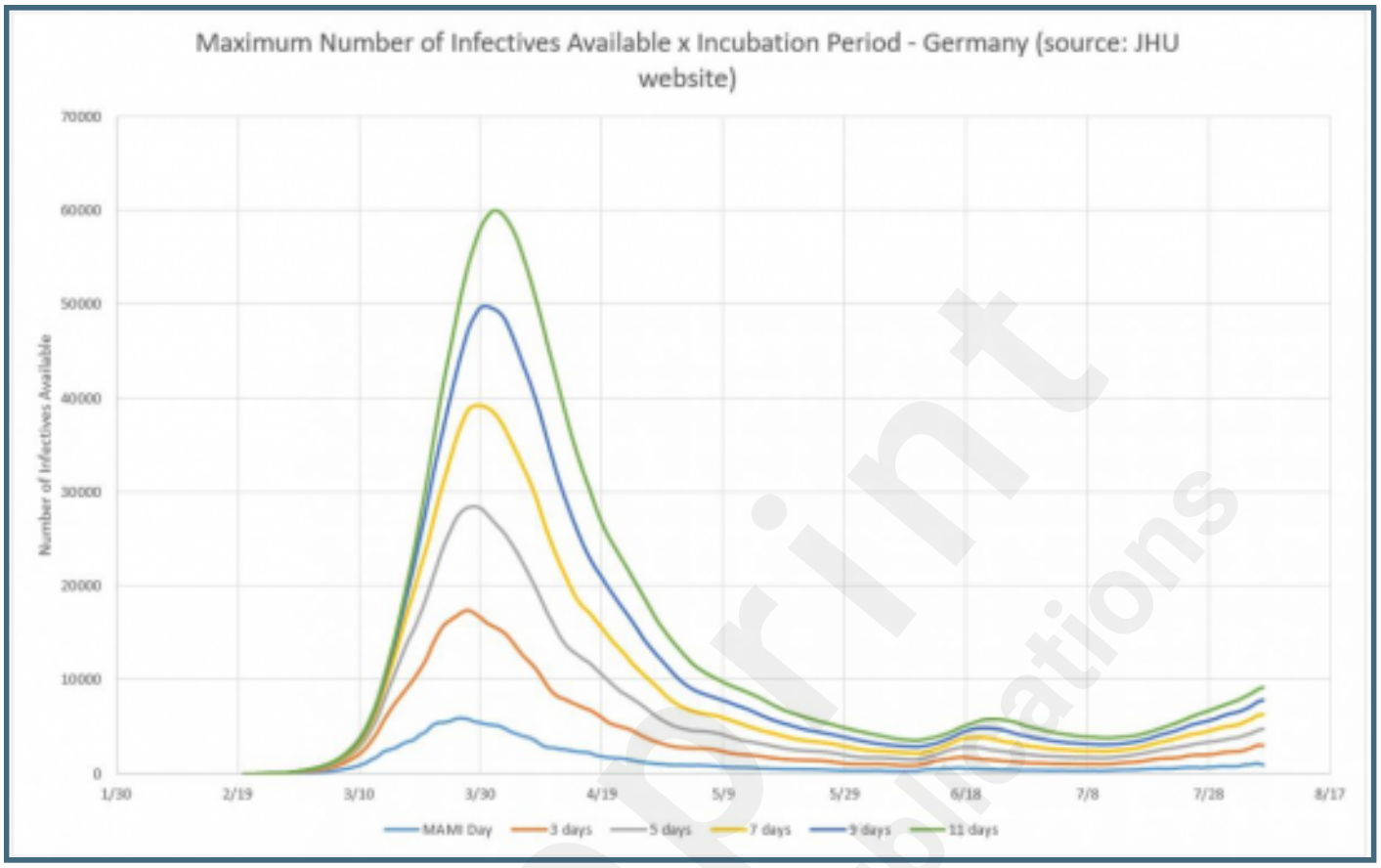

A7 – Number of daily deaths according to MoH (black line) and Transparency Portal (red).

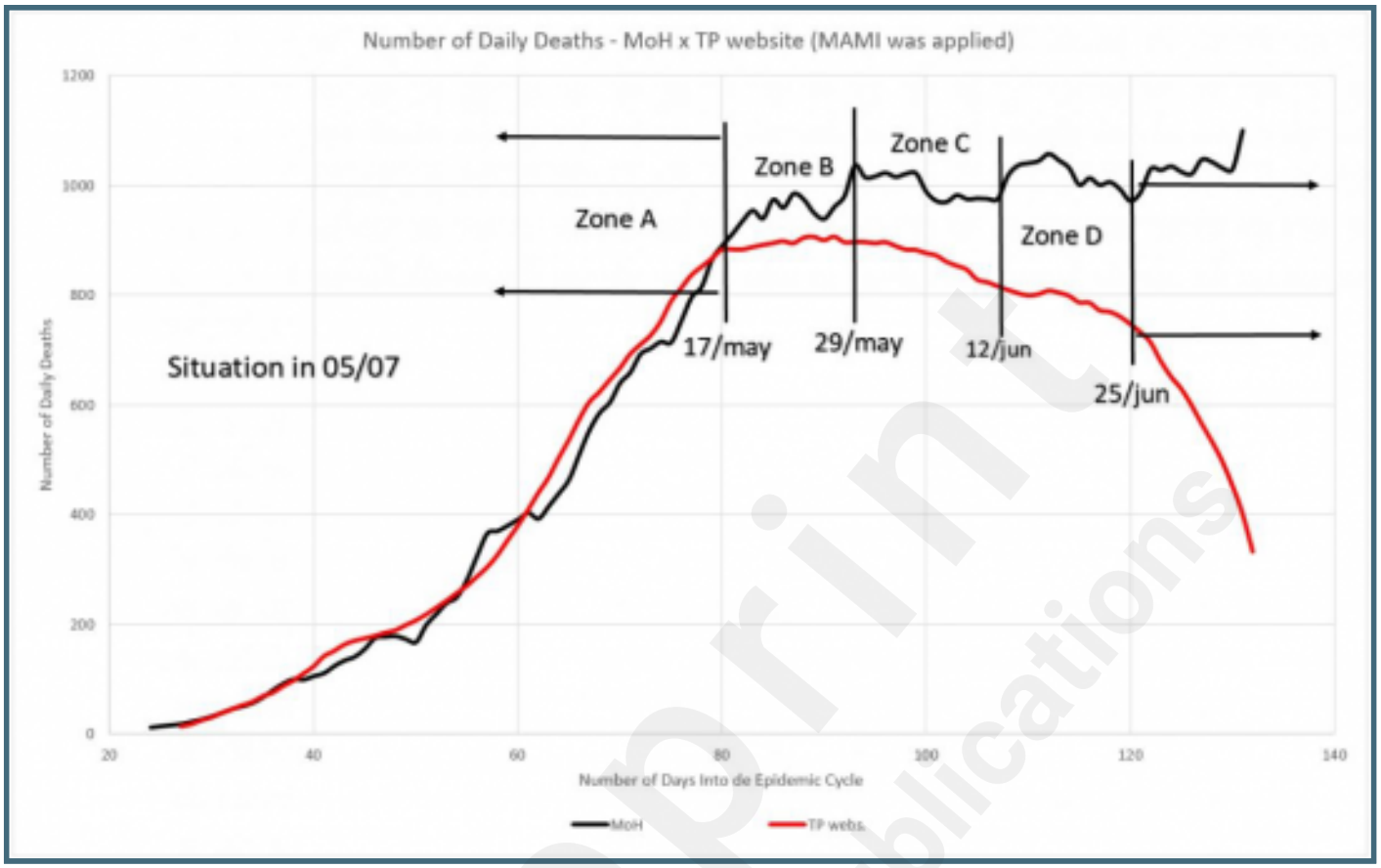

Number of COVID-19 cases reported for Germany. The black line represents the daily reported numbers, blue bars their MAMI, and the red line the total cases to date and uses the right hand axis as reference.

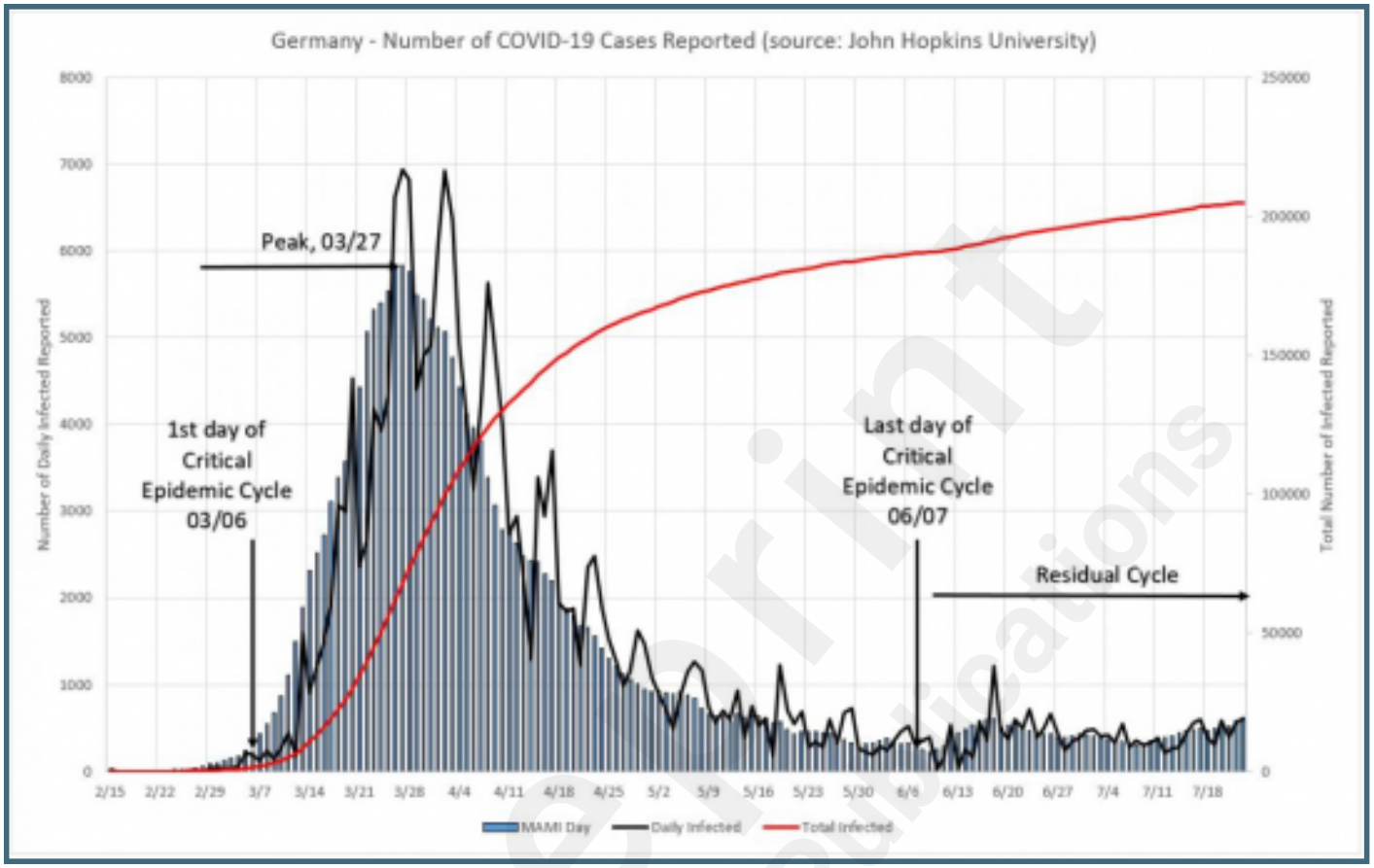

Number of COVID-19 cases reported for Italy. The black line represents the daily reported numbers, blue bars their MAMI, and red line the total cases to date and uses the right hand axis as reference.

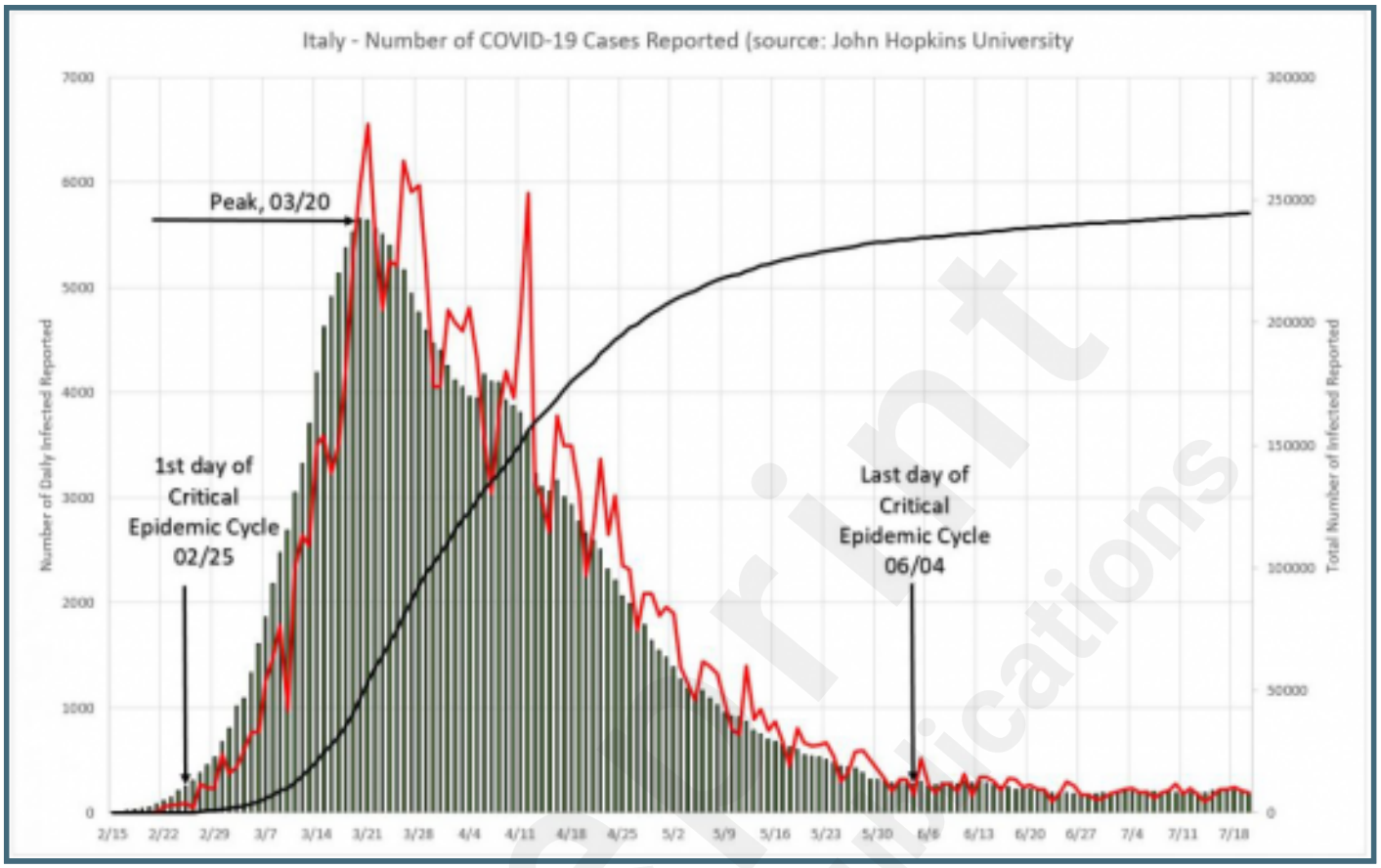

Number of COVID-19 cases reported for Sweden. The black line represents the daily reported numbers, blue bars their MAMI, and red line the total cases to date and uses the right hand axis as reference.

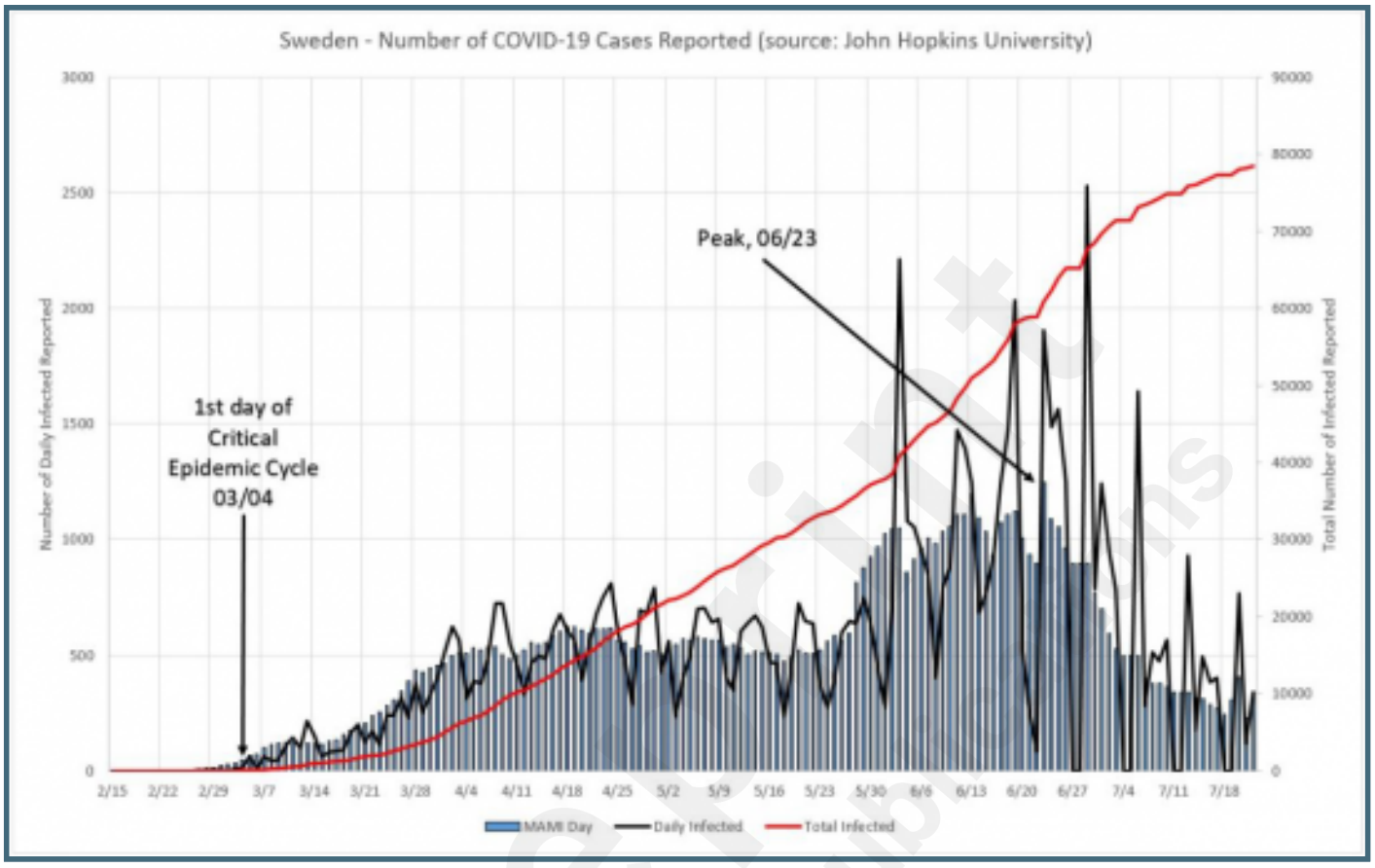

Behaviors of (1 + b) and Rt factors, for the first 20 days in the German epidemic cycle.

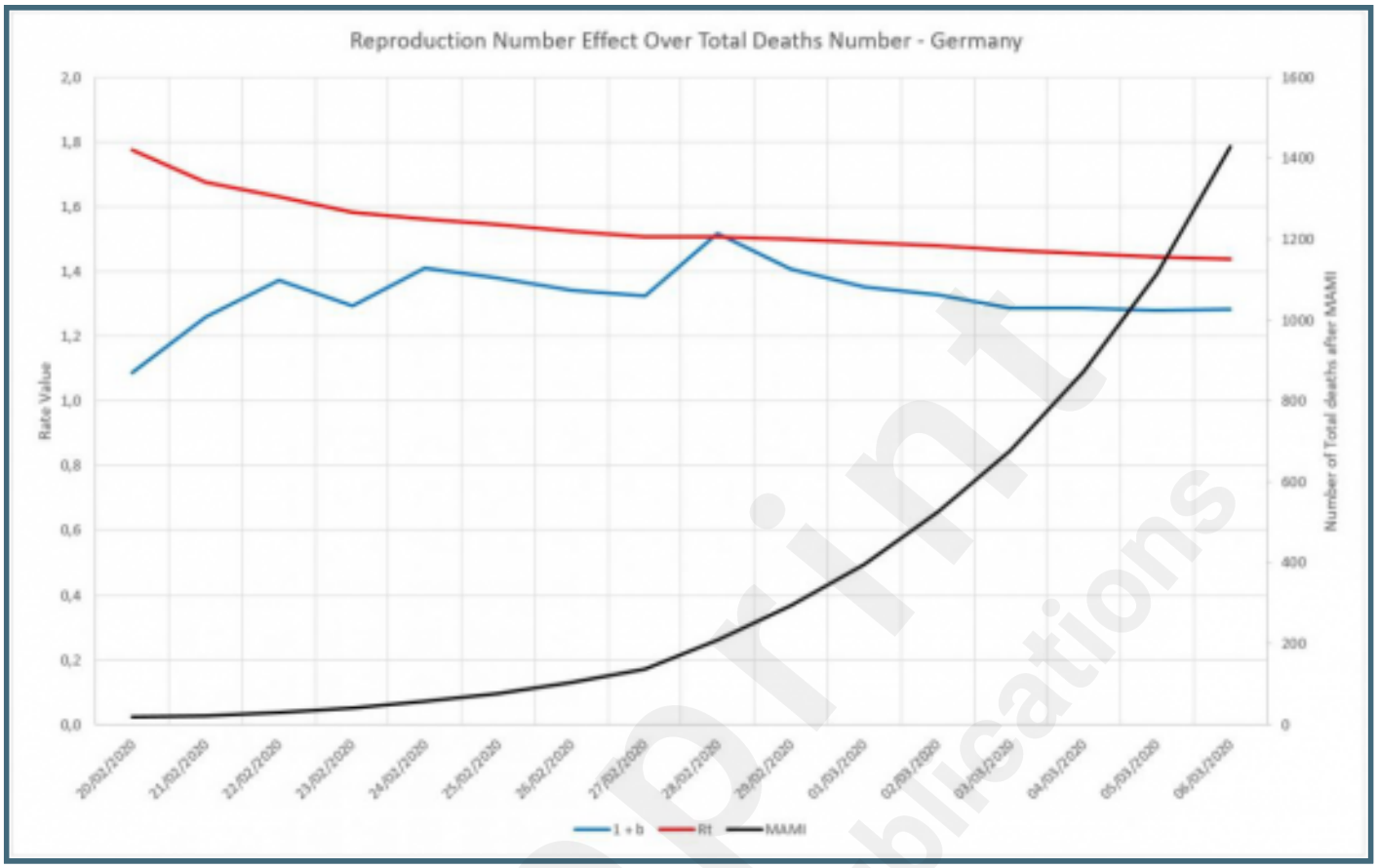

Total epidemic cycle in Germany, using the number of infected people daily.

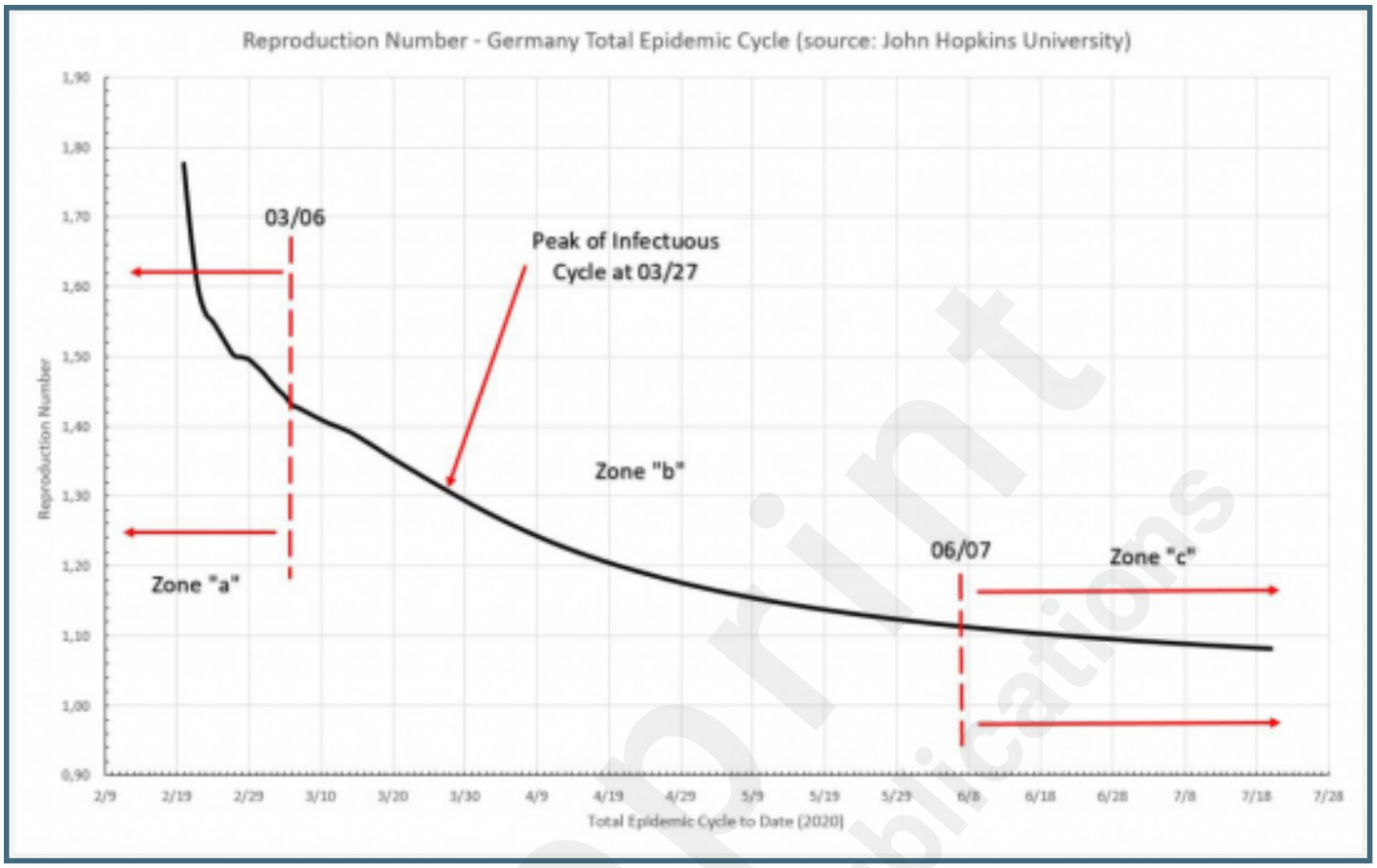

Sub notification effect over Reproduction Number in Germany, during the critical epidemic cycle.

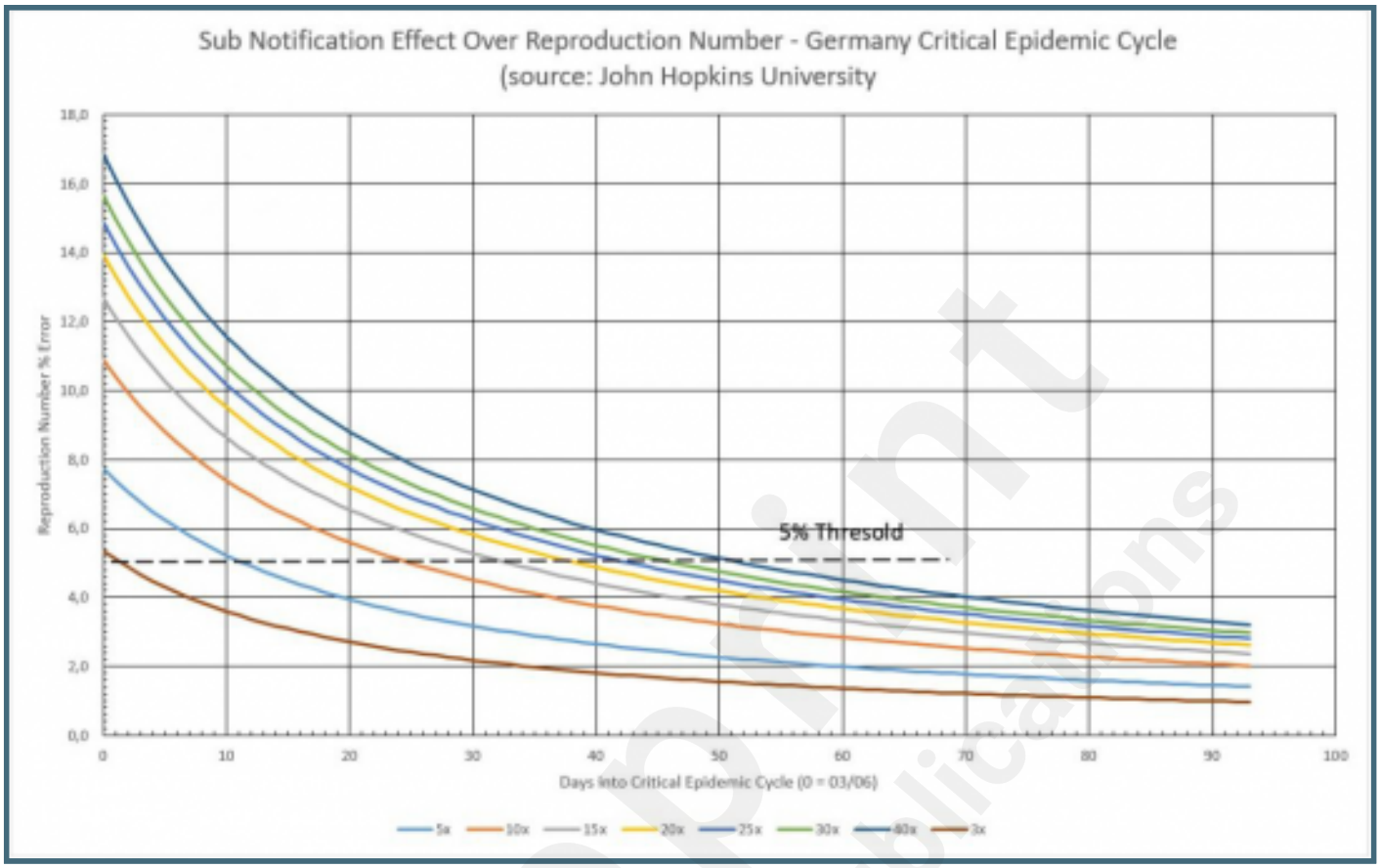

Germany: total number of infected (MAMI) compared to Richard Growth Model prediction.

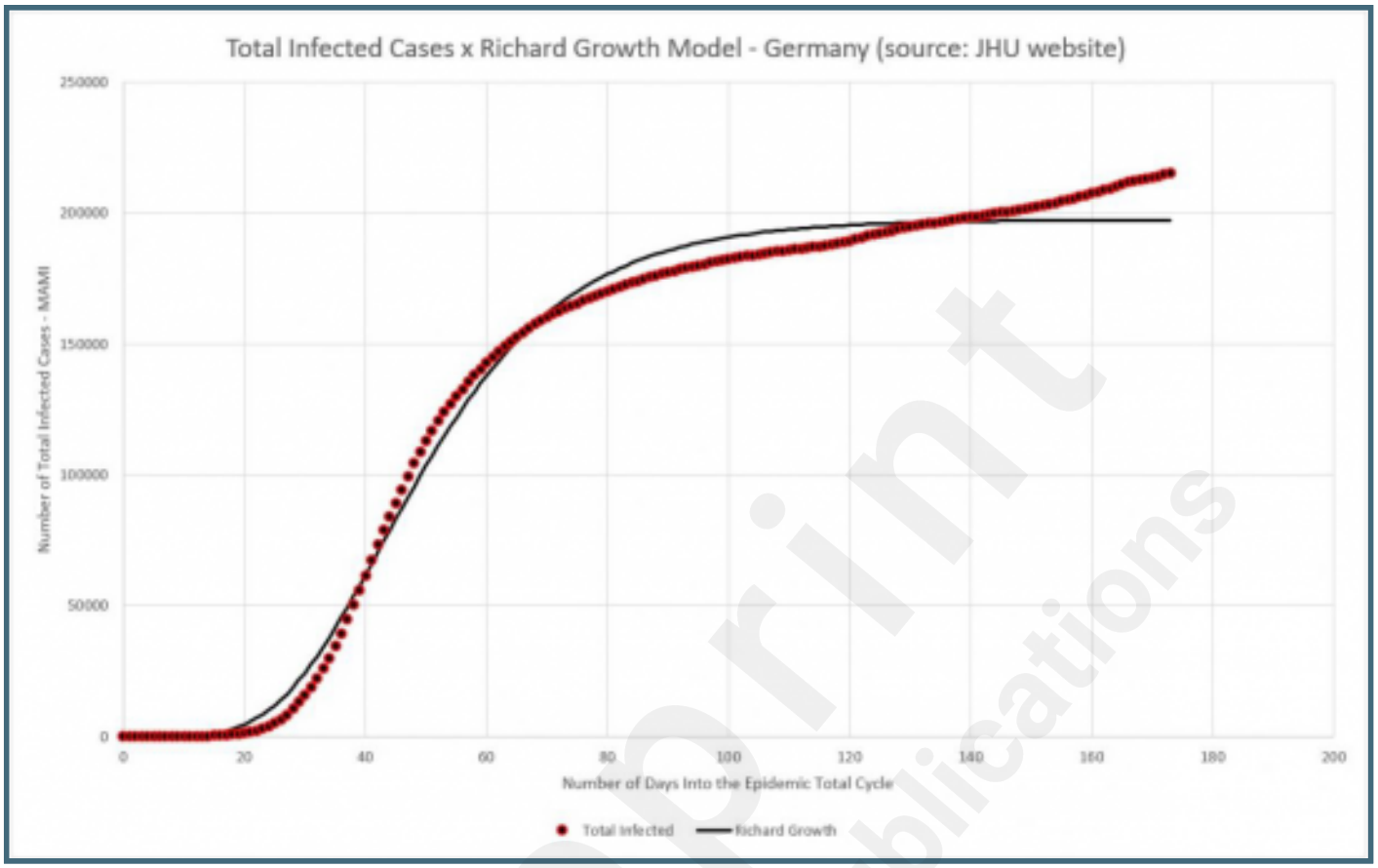

Multimedia Appendixes

Data and calculations for the studied local cycles.
URL: https://asset.jmir.pub/assets/4b6237c95e1b8191b7c815e91469ed79.xlsx

Data and calculations for Rt and Sub notification.
URL: https://asset.jmir.pub/assets/5cb03aee66d9420f7e654947dfc1bc86.xlsx

Data and calculations for the Logistic Model and the Inventory Model.
URL: https://asset.jmir.pub/assets/2baf935a5e50ccf69338bfd605146a65.xlsx

Extra case study: Brazil.
URL: https://asset.jmir.pub/assets/9ac735dfc8321b5542bd438f2730eee3.docx

Related publication(s) - for reviewers eyes onlies

Original paper with marked modifications.
URL: https://asset.jmir.pub/assets/40fd92df3e8f1e1930af6ca4f4b16491.pdf